Geological Survey of Norway
NO-7491 Trondheim, Norway
Tel.: 47 73 90 40 00
Telefax 47 73 92 16 20

REPORT

Report no.: 2005.039 | ISSN 0800-3416 | Grading: Open

Title:
Norwegian kyanite quartzites - potential resources of high purity quartz?

Authors:
Axel Müller, Jan Egil Wanvik, Andreas Kronz

Client:
NGU

County:
Østlandet, Trøndelag, Nordland

Commune:
Elverum, Mo in Rana, Narvik,…

Map-sheet name (M=1:250.000)
Hamar, Torsby, Ålesund, Narvik, Saltdal

Map-sheet no. and -name (M=1:50.000)
Elverum, Kynna, Snota, ….

Deposit name and grid-reference:

Number of pages: 70 Price (NOK): 405,00
Map enclosures: 0

Fieldwork carried out:	Date of report:	Project no.:	Person responsible:
Sommer 2004	01.12.2005	270400	Are Korneliussen

Summary:

This study represents an evaluation of Norwegian kyanite quartzite occurrences as potential deposits of high purity quartz raw material. Kyanite quartzites are rare fine-grained quartzites with 70 to 85 vol.% quartz and >15 vol.% kyanite (Al_2SiO_5) which occur in Proterozoic supracrustal rock units. Kyanite quartzites form stratiform lens-shaped bodies, which can extend several kilometers.

Kyanite quartzites from Gullsteinberget, Knøsberget, Kjeksberget, Sormbrua, Tverrådalen, Juovvačorrú and Nasafjell have been investigated. Trace elements in quartz from these rocks has been analysed by LA-ICP-MS. Major and trace element concentrations of whole rock were determined by X-ray fluorescence spectrometry (XRF). Crystal textures, crystal intergrowth and crystal size distribution of quartz in kyanite quartzites has been studied by optical microscopy, scanning electron microscope cathodoluminescence (SEM-CL) and backscattered electron imaging.

Trace element concentrations in quartz of the kyanite quartzites are low. Quartz contains 5 – 30 ppm Al, 0.2 – 16 ppm Ti, <1 ppm Li, <1 ppm B and <2 ppm Fe. Due to the low trace element concentrations, the quartz in the investigated kyanite quartzites can be considered as "high purity quartz" (Al <25 ppm and Ti <10 ppm). The concentrations are in the same range of concentrations of high purity quartz products, which are mined and produced in Norway and elsewhere.

Advantages of Norwegian kyanite quartzite deposits from the economic perspective are: (1) low concentrations of trace elements in quartz, (2) quartz is almost free of fluid inclusions, (3) size and exposure of kyanite quartzite bodies allows open pit mining in most of the areas. (4) kyanite separates can be used for alumina production and (5) kyanite quartzites may be also attractive dimension stones.

Disadvantages are: (1) Intergrowths of quartz with kyanite and mica, (2) the heterogeneous distribution of kyanite and mica in the rock, (3) the small average crystal size of quartz (100 – 600 µm), (4) the enrichment of impurities along grain boundaries, (5) common mineral micro inclusions in quartz of rutile, apatite, zircon, titanite, pyrite, and other Fe-Ti oxides and sulfides.

Taken all advantages and disadvantages of the investigated Norwegian kyanite quartzites in account, these rocks can be considered as potential resources of high purity quartz. The most attractive deposits from the economic view is the Gullsteinberget deposit in Solør. However, this pilot study provides only a few preliminary results of spot checks. For resource evaluation a much more extensive study of the Norwegian kyanite quartzites has to be carried out.

Keywords: industrial minerals	kyanite quartzite	quartz
kyanite	LA-ICP-MS	

Contents

Figures

Tables

APPENDIX

1. Introduction

Quartz is becoming a strategic mineral being the raw material for high purity silica glass, silicon and ferrosilicon production for the high tech industry. Traditionally, Norway is one of the most important producers of silicon in the world. The demands of quality and supply of the raw material quartz are increasing. For that reason, an evaluation of potential quartz deposits in Norway is performed currently by the Norwegian Geological Survey (Norges geologiske undersøkelse - NGU).

The trace element content of quartz is its most important quality criterion. Typical trace elements are Al, Ti, H, K, Na, Li, B, Fe, P and Ge, whereby Al and Ti are commonly the most abundant impurities in quartz. The lower the concentration of these elements in the quartz the higher is the price of quartz raw material on the world market which varies between 15 and 2000 U$ per tonne. The trace element signature of quartz depends mainly on the *P-T* conditions and the chemistry of the fluid/melt from which the quartz crystallised. But subsequent metamorphic overprint and alteration may cause the internal redistribution, uptake and/or expulsion of trace elements and lattice defects (silicon and oxygen vacancies, broken bonds).

Quartz-rich pegmatites, hydrothermal quartz veins, quartz sands, sandstones and quartzites are rocks which are world-wide mined for quartz raw material. Kyanite quartzites are rare fine-grained quartzites with 70 to 85 vol.% quartz and >15 vol.% kyanite (Al_2SiO_5) which occur in supracrustal units of the Proterozoic crystalline in Norway. Kyanite quartzites form stratiform lens-shaped bodies, which can extend several kilometers. Kyanite causes the characteristic turquoise color of the rock which makes the rock attractive for dimension stone production, too (Fig. 1). Common minor and accessory minerals are pyrophyllite ($AlSi_2O_5OH$), muscovite ($KAl_2(AlSi_3O_{10})(F,OH)$), rutile ($TiO_2$), pyrite ($FeS_2$) and zicon ($ZrSiO_4$). Kyanite quartzites can contain up to 5 vol.% muscovite and/or pyrophyllite. Kyanite quartzites are laminated in cm-scale where quartz-rich layers alternate with kyanite-rich and mica-rich layers. A characteristic feature is the absence of feldspar.

Traditionally, kyanite quartzite has been mined for kyanite. Kyanite is the raw material for high-alumina refractories forming the inner lining of furnaces and high-temperature vessels widely used in the production of metals, ceramics, glass and cement. Examples of presently mined kyanite deposits are located at Willis Mountain and East Ridge, Virginia USA (Kyanite Mining Cooperation 2005). These deposits contain several tens of millions of tons of open-pit ores with >25 vol.% kyanite in the rock. Between 1985 and 1992 the kyanite quartzite deposit of Hålsjöberg in Värmland in Sweden was mined mainly for kyanite but also for dimension stone production. The dimension stone has the commercial name “Caribbean Blue” due to the turquoise colour of the rock.

In 2003 a pilot study of trace element concentrations in quartz of the kyanite quartzite from Nasafjell in northern Norway was performed at the NGU in Trondheim (Wanvik, 2003). The analytical results done by laser ablation inductively coupled plasma mass spectrometry (LA-ICP-MS) show that quartz from the Nasafjell kyanite quartzite has low concentrations of Al, Ti and Li in comparison to quartz products of other Norwegian deposits. Therefore, kyanite quartzites could be a new type of high purity quartz deposit if the low trace elements observed in the sample from Nasafjell is a typical characteristic of quartz in Norwegian kyanite quartzites.

The aim of the study is to verify on a broader scale if the low trace element concentrations found in the Nasafjell kyanite quartzite is a common feature of these rocks. Kyanite quartzites from Solør, Surnadal, Skjomen and Nasafjell in Norway (Fig. 2) and from Hålsjöberg in Värmland in Sweden and from Rio Levele in Mozambique have been sampled. In addition, quartzite and kyanite-bearing metaarkose which occur close to the Surnadal kyanite quartzite has been investigated. Trace elements in quartz from these samples has been analysed by LA-ICP-MS at the NGU applying the analyses procedure of Flem et al. (2002). Major and trace element concentrations of whole rock were determined by X-ray fluorescence spectrometry (XRF). Crystal textures, crystal intergrowth and crystal size distribution of quartz in kyanite quartzites has been studied by optical microscopy. Scanning electron microscope cathodoluminescence (SEM-CL) has been applied in order to reveal the internal growth and alteration pattern of quartz crystals. The results give information about the crystallisation history of the kyanite quartzites. This information will help to better understand the processes which are responsible for the low concentration of trace elements in quartz.

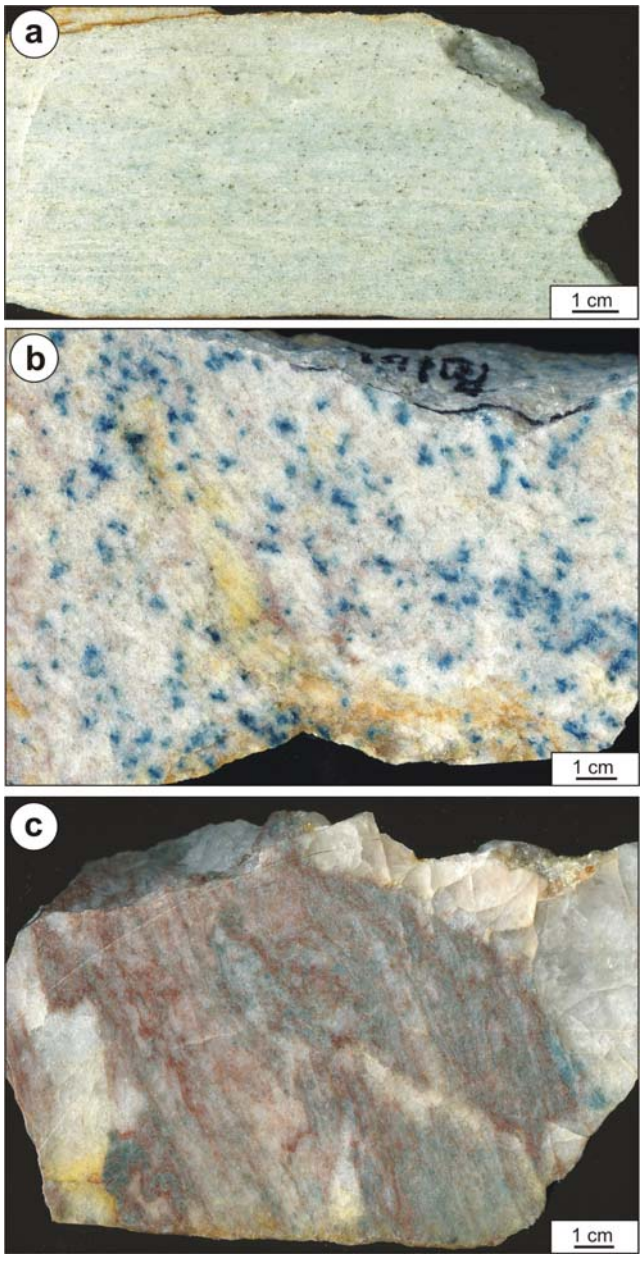

Figure 1. *Hand specimen scans of Norwegian kyanite quartzites. a – Typical fine-grained kyanite quartzite of the Gullsteinberget deposit in Solør with slight turquoise coloration caused by kyanite. Black dots are pyrite. b - Kyanite quartzite from Sormbrua in Solør with blue nests of kyanite, wavellite and lazulite. c – Kyanite quartzite from Sormbrua in Solør containing a kyanite- and rutile-rich layer.*

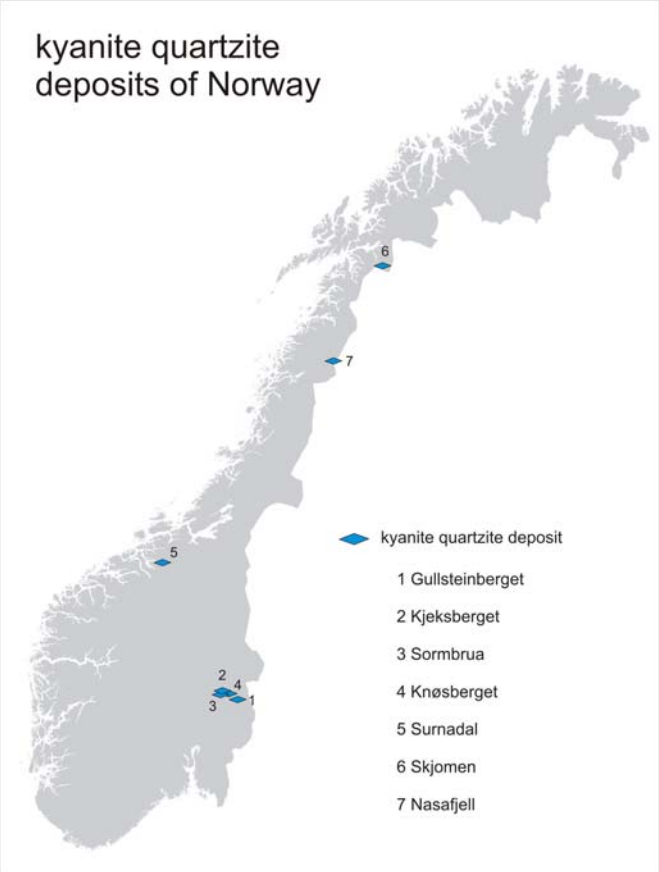

Figure 2. *Locations of investigated kyanite quartzite occurrences in Norway.*

2. Methods

2.1. X-ray fluorescence spectrometry (XRF)

Major and trace element concentrations of kyanite quartzites and regional related quartzites and metaarkoses were determined by X-ray fluorescence spectrometry (XRF) using Phillips PW1480 spectrometer equipped with a Sc/W X-ray tube at NGU Trondheim. Ca. 3 g sample material milled to ~40 µm are fused at 1030°C for 10 min. Loss on ignition (LOI) is determined gravimetrically and it is used as an approximate measure of volatiles such as H_2O and CO_2. 0.6 g of the sample material used for major element determination is then fused in a Pt-crucible with lithium tetra borate ($Li_2B_4O_7$) at 1120°C yielding a homogeneous, optically flat glass disc. Major element analysis is carried out on fused glass discs for Na, Mg, Al, Si, P, K, Ca, Ti, Mn and Fe. The total Fe concentration is calculated as Fe_2O_3. Accuracy and limits of detection of major elements are listed in Table 1.

Table 1. *Accuracy and limits of detection for XRF whole rock analyses of major element.*

oxide	SiO_2	Al_2O_3	Fe_2O_3	TiO_2	MgO	CaO	Na_2O	K_2O	MnO	P_2O_5
$K_{element}$*	0.073	0.039	0.03	0.006	0.038	0.008	0.056	0.007	0.006	0.014
limits of detection (wt.%)	0.1	0.1	0.01	0.01	0.01	0.01	0.1	0.01	0.01	0.01

*Accuracy = $K_{element} \cdot \sqrt{(\text{concentration in sample} + 0.1)}$ [%]

For trace elements, pressed powder pellets using binding agent wax Hoechst C are analysed for Rb, Sr, Y, Zr, Nb, Ba, Pb, Th, U, Sc, V, Cr, Co, Ni, Cu, Zn, Ga, Mo, As, Sb, Sn, Ce, Nd, La, W, Cs, Ta, Pr, Hf, S, Cl and F. Accuracy and limits of detection of trace elements are listed in Table 2.

Table 2. *Accuracy and limits of detection (LOD) for XRF whole rock analyses of trace elements.*

element	Ba	Sb	Sn	Ga	Zn	Cu	Ni	Yb	Co	Ce	Nd	La	W	Cs	Ta	Pr	Mo
$K_{element}$*	1.6	0.75	0.73	0.52	0.86	1.3	0.68	0.8	0.46	1.1	1.0	0.52	0.8	1.13	0.79	0.72	0.64
LOD (ppm)	10	10	10	10	5	10	5	15	5	10	10	10	10	10	10	10	5

element	Nb	Zr	Y	Sr	Rb	U	Th	Pb	Cr	V	As	Sc	Hf	S	Cl	S
$K_{element}$*)	0.35	0.48	0.28	0.42	0.37	0.48	0.49	0.86	3.5	1.3	0.47	0.51	0.55	0.33	0.08	0.15
LOD (ppm)	5	5	5	5	5	10	5	10	10	10	5	10	10	1000	1000	1000

*Accuracy = $K_{element} \cdot \sqrt{(\text{concentration in sample} + 10)}$ [ppm]

2.2. Optical microscopy

Microscopic photographs were obtained from thin sections using AXIOPLAN 2e IMAGING ZEISS optical microscope equipped with an AXIOCAM ZEISS digital camera. Crystal size measurements were carried out on scaled image A4-prints of microphotographs taken using a magnification of 250x. In this way it was possible to keep track of which crystals had been measured. Maximum length and orthogonal width were measured of 200 crystals for each sample. The crystal size was determined by the average of the maximum length and orthogonal width of the crystal. Sizes of 200 crystals were plotted logarithmic in a crystal size distribution (CSD) diagram for each sample (Figs. 3, 21). The CSD diagram illustrates the crystal frequency for a certain range of crystal size. The example in Fig. 3 shows two possible patterns of CSD in order to understand the difference between the maximum of CSD and the average crystal size. Example 1 has a crystal size maximum at 150 µm (=0.15 mm) and the average crystal size of all 200 crystals is ca. 230 µm. Example 2 has two crystal size maxima at 150 mm and at 900 mm and the average crystal size is ca. 580 µm.

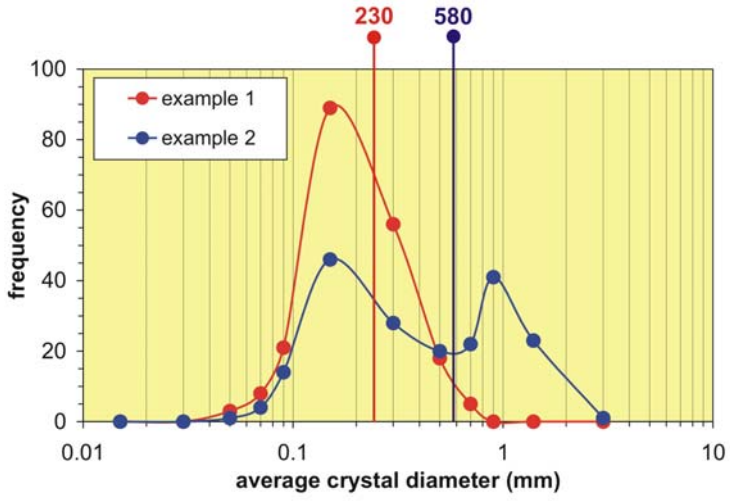

Figure 3. *Theoretical examples of the crystal size distribution (CSD) of quartz in a quartz-bearing rock. Each example implies 200 measurements of crystal size. The vertical lines mark the average crystal sizes, which do not correspond the maxima of CSD.*

2.3. Scanning electron microscope cathodoluminescence (SEM-CL)

Scanning electron microscope cathodoluminescence (SEM-CL) images were obtained from polished thin sections coated with carbon using the LEO 1450VP analytical SEM with an attached CENTAURUS BS BIALKALI type cathodoluminescence (CL) detector. The applied acceleration voltage and current at sample surface was 20 kV and ~3 nA, respectively. Due to the general low CL intensity of quartz, thin sections were coated with a very thin layer of carbon (10 to 15 Å) using the POLARON RANGE CC7650 Carbon Coater. The coating time was chosen to 2 s instead of 5 s usual applied for SEM investigations. The BIALKALI tube has a CL response range from 300 (violet) to 650 nm (red) (Fig. 4). It peaks in the violet spectrum range around 400 nm. The CL images were collected from one scan of 43 s photo speed and a processing resolution of 1024 by 768 pixels and 256 grey levels. The brightness and contrast of the collected CL images were improved with the PhotoShop software.

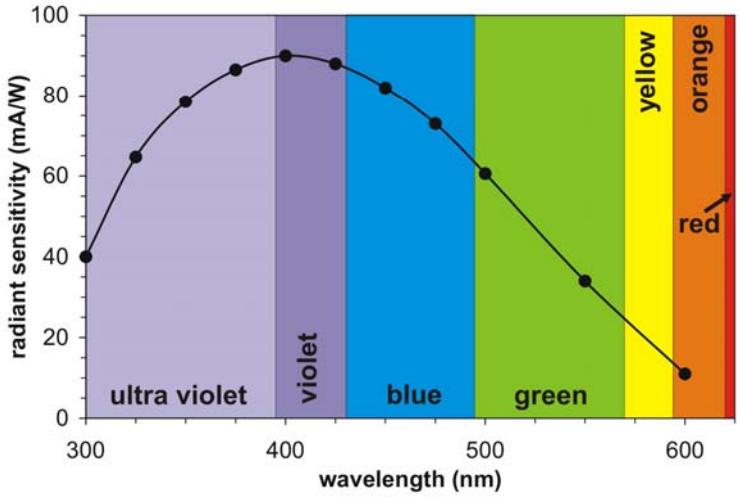

Figure 4. *Spectral sensitivity characteristics of the CENTAURUS BS BIALKALI cathodoluminescence detector. The detector has the highest sensitivity at 400 nm which corresponds to violet luminescence colours. The detector has very little response towards orange and red luminescence (590 to 760 nm).*

2.4. Laser ablation inductively coupled mass spectrometry (LA-ICP-MS)

A double focusing sector field inductively coupled mass spectrometer (ICP-MS; Finnigan MAT, model-ELEMENT) was used for the determination of concentrations of Li, Be, B, Mn, Ge, Rb, Sr, Ba, Pb, Na, Mg, Al, P, K, Ca, Ti, Mn and Fe in quartz from kyanite quartzites. Flem et al. (2002) give detailed description of the measurement procedure applied in the laboratory of NGU. Operating conditions of the ICP-MS are listed in Table 3. The laser used for ablation was a Finnigan MAT, UV laser probe operating at 266 nm. The laser was run with a pulse width of 3 ns (Q-switched), a shot frequency of 20 shots s-1, pulse energy of 0.7-0.8 mJ and 30 µm spot size on rasters not larger than 180 x 250 µm.

Table 3. *Operating parameter of the ICP-MS and key method parameters.*

plasma conditions	
plasma power	1075 W
auxiliary gas flow	0.89 l/min
sample gas flow	1.1 – 1.2 l/min
cone	high performance Ni
CD-1 guard electrode	yes
data collection	
scan type	E-scan
no. of scans	15

The existence of spectroscopic interferences required the use of variable mass resolutions. Li, Be, B, Mn, Ge, Rb, Sr, Ba and Pb were analysed at low mass resulotion ($m/\Delta m \approx 3500$), but Al, Na, Ca, P, Cl, Mg, Ti and Fe required medium mass resolution ($m/\Delta m = 300$) and K high mass resolution ($m/\Delta m > 8000$). The isotope ^{29}Si, was used as internal standard at low mass resolution, and ^{30}Si at medium and high mass resolution.

External calibration was done by using four silicate glass reference materials produced by the National Institute of Standards and Technology (NIST SRM 610, NIST SRM 612, NIST SRM 614, NIST SRM 616). In addition, the standard reference material 1830, soda-lime float glass (0.1 wt.% Al_2O_3) from NIST, the high purity silica BCS 313/1 reference sample from the Bureau of Analysed Samples, UK, the certified reference material "pure substance No. 1" silicon dioxide SiO_2 from the Federal Institute for Material Research and Testing, Berlin, Germany and the Qz-Tu synthetic pure quartz monocrystal provided by Andreas Kronz from the Geowissenschaftliches Zentrum Göttingen (GZG), Germany, were used.

Each measurement consists of 15 scans of each isotope, with a measurement time varying from 1 s per scan of K in high resolution to 0.02 s per scan of, e.g. Mn in low resolution. An Ar-blank was run before each standard and sample measurement. The background signal was subtracted from the instrumental response of the standard before normalisation against the internal standard. This was done to avoid memory effects between samples. A weighted linear regression model including several measurements of the different standard was used for calculation of the calibration curve for each element.

10 successive measurements on the Qz-Tu were used to estimate the limits of detections (LOD). LOD are based on 3 times standard deviation (3σ) of the 10 measurements divided by the sensitivity S. Typical detection limits are given in Table 4.

Table 4. *Typical limits of detection (LOD) are based on 10 measurements on the Qz-Tu synthetic quartz monocrystal. Concentrations of Qz-Tu represent the average of three measurements applying the LA-ICP-MS the measurement procedure of Flem et al. (2002) at NGU.*

isotope	^{7}Li	^{9}Be	^{11}B	^{24}Mg	^{27}Al	^{31}P	^{39}K	^{44}Ca	^{47}Ti	^{55}Mn	^{56}Fe	^{74}Ge	^{85}Rb	^{88}Sr	^{138}Ba	^{208}Pb
LOD (ppm)	1	0.4	1	5	10	5	3	60	0.09	0.3	1	0.5	0.4	0.15	0.04	0.01
Qz-Tu (ppm)	1.832	<0.25	0.382	66.6	8.03	33.17	3.61	<16.42	<0.1	2.544	<3.97	<0.54	0.224	<0.20	0.022	0.016

2.5. Electron probe micro analysis (EPMA) of kyanite

The electron probe microanalyses of kyanite were obtained using a JEOL 8900 RL electron microprobe at the Geowissenschaftliches Zentrum Göttingen, Germany. The analyses were carried out using an accelerating voltage of 20 kV and beam currents of 20 nA. The beam size was 5 µm. Representative detection limits (3σ of single background measurement) for minor and trace elements in kyanite were 51 ppm for Ti, 63 for Fe, 48 for V, 132 for Na, 54 for Mg, 45 for Ca, 69 for Mn, 51 for Cr and 57 for K.

3. Geological settings of kyanite quartzites

3.1. Solør

Four major occurrences of kyanite quartzites were sampled in the Solør area: 1) Gullsteinberget, 2) Knøsberget, 3) Sormbrua and 4) Kjeksberget (Fig. 5). The four deposits are 15 to 35 km SW of Elverum hosted in Middle to Upper Proterozoic fine- to medium-grained granitic gneisses of the Solør Complex (Fig. 6). The granitic gneisses are assumed to have ages of 1.6 to 1.8 Ga. (Nordgulen 1999). The Knøsberget, Sormbrua and Kjeksberget deposits are situated in a dome-like gneiss structure, close (5 to 10 km) to the rocks of the NNW-SSE striking units of the "Oslofield" in the west. The units of the "Oslofield" comprises here metarhyolites, metatuffs and monzodioritic augengneiss. The Gullsteinberget deposit is situated about 10 km ESE of the dome-like gneiss structure. All four deposits are in close relationship with metagabbros and fine-grained amphibolites (hyperites) occurring commonly in the granitic gneisses of the Solør Complex.

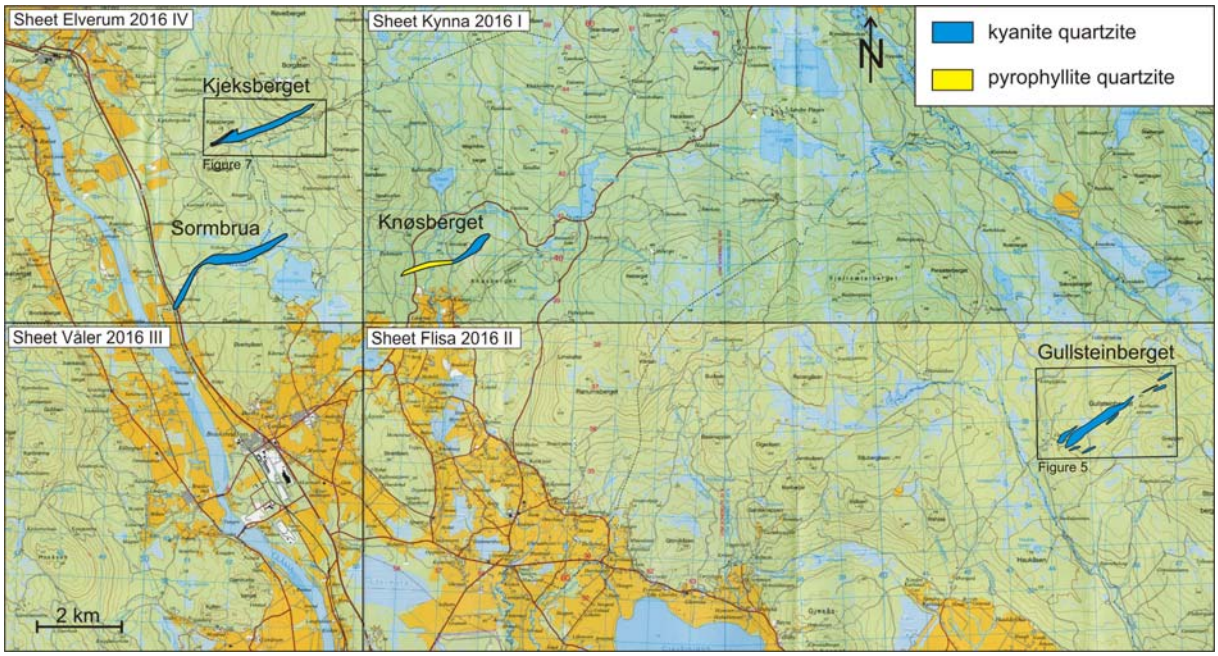

Figure 5. *Locations of the kyanite quartzite deposits of Solør.*

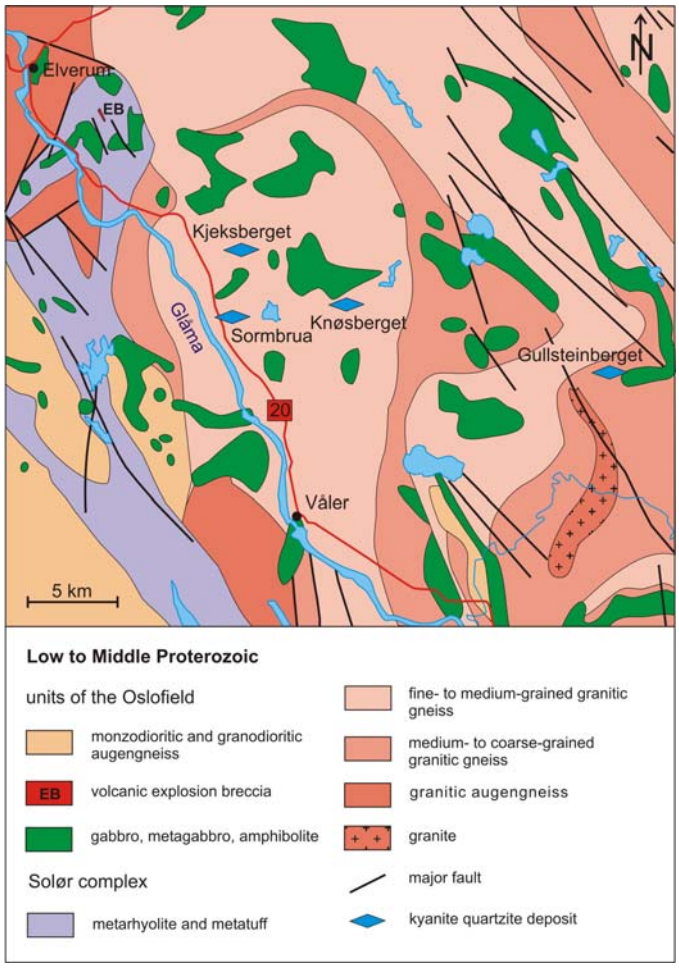

Figure 6. *Simplified geological map of Solør after Nordgulen (1999) and Gvein et al. (1974) with locations of the kyanite quartzite deposits.*

The *Gullsteinberget* deposit is situated 35 km SW of Elverum and about 6 km north of the state road 206 between Flisa and the border to Sweden. The deposit was identified and mapped by Jakobsen and Nielsen (1977). It is the largest known kyanite quartzite deposit in this area with a length of 1.8 km and a width of up to 300 m (Fig. 7). The lens-shape body strikes NE-SW and form the mountain ridge of the Gullsteinberget (516 m a.s.l.; Fig 8). The lens dips 50 to 60° to NW. Kyanite-rich layers alternate in m-scale with pyrophyllite-quartzite and minor biotite gneiss intercalations.

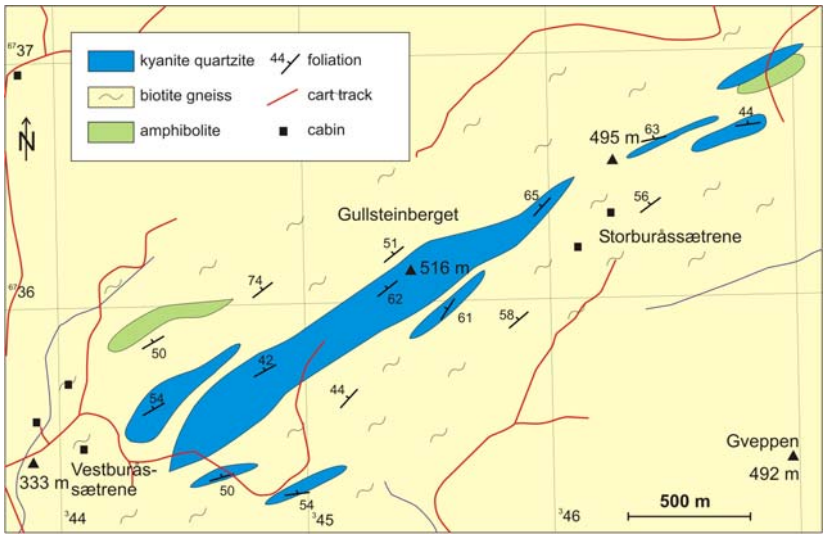

Figure 7. *Geological sketch map of the Gullsteinberget kyanite quartzite deposit according to Jakobsen and Nielsen (1977).*

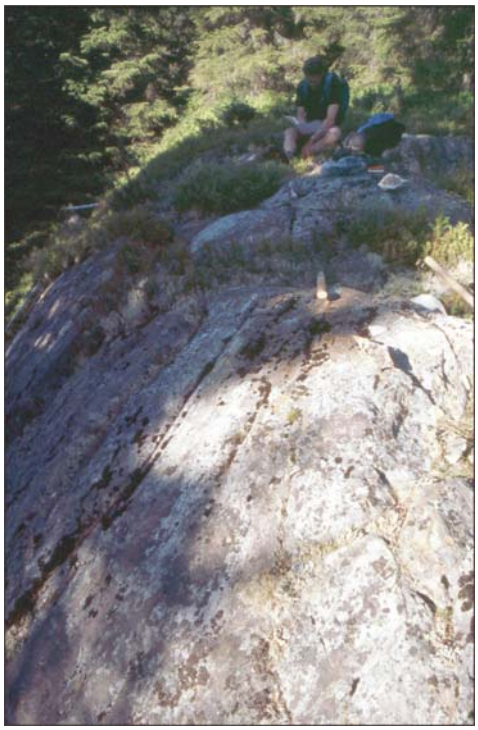

Figure 8. *Outcrop of massive kyanite quartzite near the top of the Gullsteinberget.*

The *Knøsberget* deposit forms a kinked lens with a total length of 2.2 km at the NW end of the Knøsberget plateau (355 m a.s.l.). The deposit is situated about 7 km by road from Braskereidfoss which lies at the state road 20. The western WSW-ENE striking part of the lens is 1.2 km long and consists predominantly of pyrophyllite quartzite (Fig. 5). The NE-SW striking and 1 km long eastern part comprises alternating layers of kyanite quartzite and pyrophyllite quartzite with minor intercalations of mafic gneiss. Here the lens is up to 200 m wide and dips 70-80° northwestward.

The *Kjeksberget* deposit is situated 2.5 km east by cart track from the state road 20, 5 km SE of Jømna. The lens-shaped, ENE-WSW striking body is about 2.5 km long, 200 m wide and dips presumably 50° SSE (Fig. 9). The deposit was mapped out by blocks of kyanite quartzite and no outcrops were found (Jakobsen and Nielsen 1977).

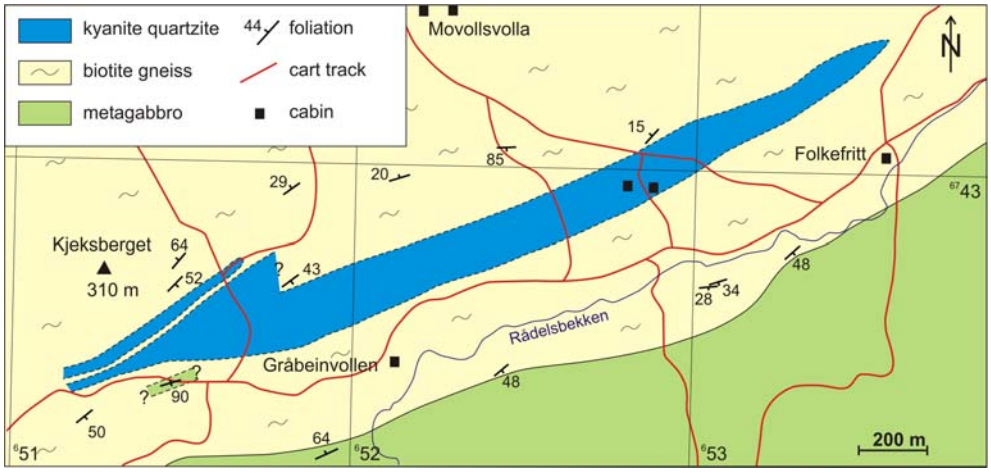

Figure 9. *Geological sketch map of the Kjeksberget kyanite quartzite deposit according to Jakobsen and Nielsen (1977).*

Fine-grained kyanite quartzite with blue nests of kyanite and lazulite is exposed below the old bridge *Sormbrua* of the old state road, 18 km SE of Elverum. The outcrop occurs at the SW edge of the S-shaped 3 km long kyanite quartzite body of Sormbrua. The outcrop was first described by Nystuen (1969a) who found kyanite crystals of up to 3 cm length at the outcrop. In other parts the kyanite quartzite is not exposed and was mapped using the distribution of kyanite quartzite blocks (Jakobsen and Nielsen 1977).

The Swedish kyanite quartzite *Hålsjöberg* in Värmland were sampled because it is probably genetically related to the Solør kyanite quartzite (Nystuen 1969a) and it was mined for alumina for refractories and for dimension stone. The Hålsjöberg deposit is situated 20 km NE of Torsby and about 100 km SE from Elverum. The deposit is together with other kyanite occurrences aligned to the Protogine Zone which separates granitic gneisses in the west (Solør Complex) and the Transscandinavian Granite-Porphyry Belt in the east (Lindh 1987). The supracrustals of the Protogine Zone consist of mica-schist and feldspar porphyry of dacitic composition which is overlain by the kyanite quartzite (Ek and Nysten 1990). The kyanite quartzite strikes N-S, dipping at various degrees eastward. Three separate bodies can be distinguished at Hålsjöberg covering an area of 1 km^2. In close contact with the kyanite quartzite a hyperite diabas occurs. Peak metamorphic conditions at Hålsjöberg were >2 kbar and between 520 and 575°C (Ek and Nysten 1990).

3.2. Tverrådalen, Surnadal

The kyanite quartzite of *Tverrådalen* is situated about 8 km beeline and 12 km by road SE of the community centre Skei at the innermost part of Øvstebødalen (Fig. 10). The valley is here called Tverrådalen. The kyanite quartzite occurs at the southern steep slope at the altitude 300 m a.s.l. and 100 m above the river Tverråa. The outcrop extends 10 x 5 m (Fig.11). The deposit was studied in detail by Wanvik (1998). Two core drill holes, 9 and 5 m in depth, were performed. The thickness of the kyanite quartzite lens dipping 85° southward is 5.5 m (Wanvik 1998; Fig. 12).

The deposit is situated in the border area between the basal, autochthonous Proterozoic gneiss units and the allochthon Caledonian nappe rocks that extends from the Trondheim region along Surnadal and further westwards to the Molde area. Detailed mapping of the area was carried out by Tørudbakken (1982). The kyanite quartzite lens is associated with small amphibolite lenses with a thickness of 5 to 50 m. Both units are hosted in granitic gneiss of Middle Proterozoic age (0.9-1.6 billion years) (Fig. 13). The thrust zone of the Caledonian nappes is about 1 km north of the deposit. A steep-dipping, E-W striking metaarkose-quartzite band (50-100 m in thickness) of Upper Proterozoic age (0.6-0.9 billion years) extends 100 to 200 m north of the kyanite quartzite. In contrast to the kyanite quartzite the metaarkose unit contains 10-30 vol.% feldspar and it is free of kyanite. However, kyanite-bearing metaarkose were found at the Gråsjøen dam in the valley Folldalen, 14 km east from the kyanite quartzite of Tverrådalen.

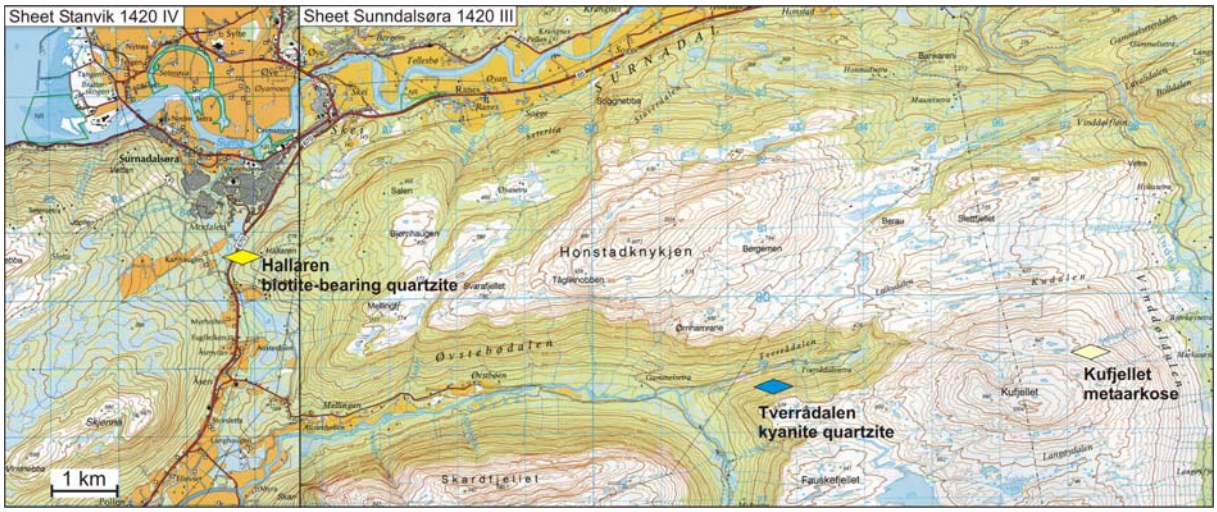

Figure 10. *Location of the kyanite quartzite deposit from Surnadal on the topographic 1 : 50.000 map sheet Snota 1420 I.*

Figure 11. *Outcrop of the small kyanite quartzite body in the Surnadal area. The fine-grained white rock has greenish and pinkish shades caused by variations of the kyanite and rutile concentration.*

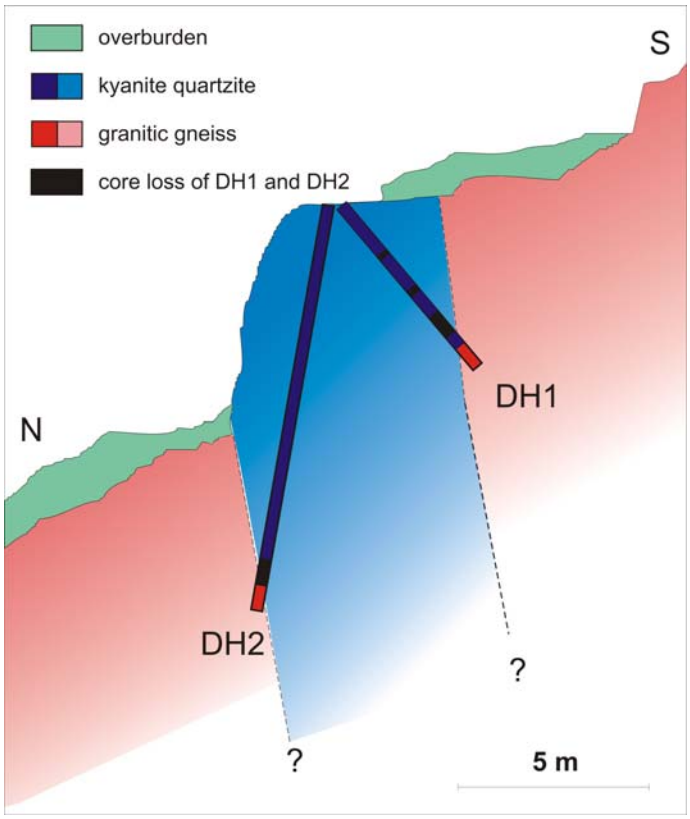

Figure 12. *Vertical N-S section of the kyanite quartzite deposit (Wanvik 1998) near Surnadal with the location of the two drill cores performed in 1998 by NGU.*

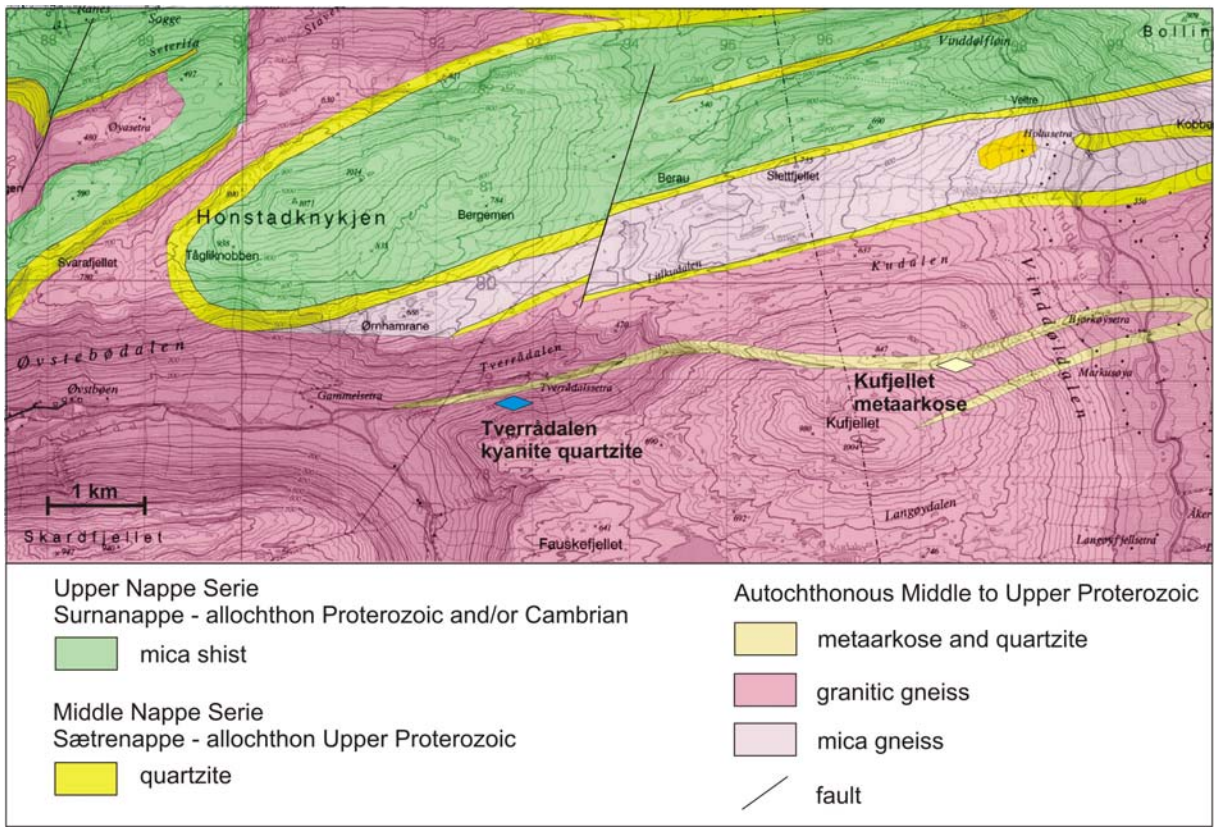

Figure 13. *Geological map of the upper Øvstebødalen in the Surnadal area. Modified after Tveden and Lutro (1998).*

3.3 Juovvačorrú, Skjomen

The quartz kyanite bodies of the Skjomen area are located 20 km SSE of the village Skjomen in northern Norway, 10 km S of the southern end of the Skjomendalen (Fig. 14). The rocks are exposed at a high plateau called Juovvačorrú ca. 1000 m a.s.l..

The quartz kyanite bodies of Juovvačorrú belong to Sørdalen Supracrustal Belt, which is part of the Lower Proterozoic Rombak Basement Window. The window is surrounded by allochthonous Caledonian nappe complexes. The sequence of the Sørdalen Supracrustal Belt is mainly composed of porphyritic, mafic, intermediate and felsic volcanites (Korneliussen and Sawyer 1989, Fig. 15). Debris flows and pyroclastic rocks are interbedded with the volcanites. Lenses of metasediments and kyanite quartzites are tectonically intercalated within the volcanic rocks. The rocks are assumed to have ages between 1.91 and 1.88 Ga (Korneliussen and Sawyer 1989). The age assumption bases on lithological relationships to similar rocks in northern Sweden which were dated by Frietsch and Perdahl (1987) and Widenfalk et al. (1987). The Sørdalen Supracrustal Belt is embedded in granites which are dated at 1.78 and 1.69 Ga by Gunner (1981) and Heier and Compston (1969), respectively. The rocks of the Sørdalen Supracrustal Belt were metamorphosed under amphibolite facies conditions at 6 kbar and ca. 575°C (Sawyer 1986). The age of the prograde metamorphism is unknown. Occasionally, the rocks were effected by greenschist-facies metamorphism related to the Caledonian deformation.

The kyanite quartzite occurrences are limited to a 3.5 km long, steep dipping, lens-shape body of volcanites at the southeastern edge of the Sørdalen Supracrustal Belt (Fig. 15). The kyanite quartzite lenses are 10 to 100 m long and 5 to 40 m wide and form aligned boudins (Figs. 16 and 17). Ca. 60 kyanite quartzite bodies were identified by Korneliussen (2005, person. comm.).

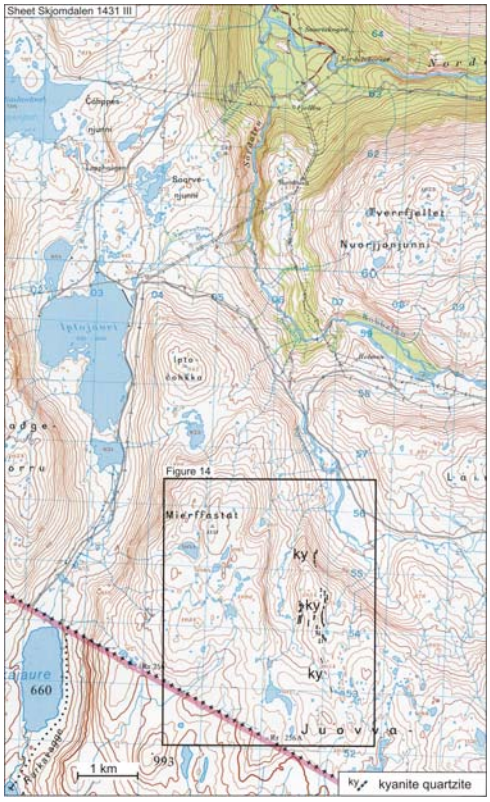

Figure 14. *Location of the kyanite quartzite occurrences in the Skjomen area.*

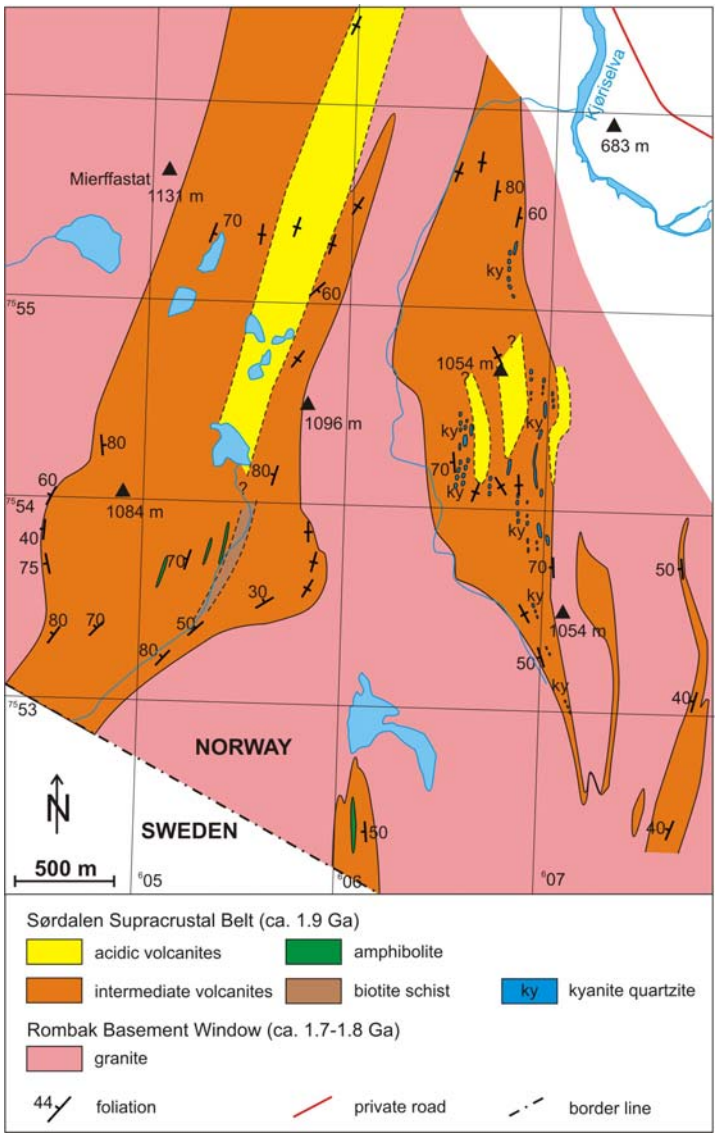

Figure 15. *Geological map of the southern part of the Sørdalen Supracrustal Belt (Korneliussen 2005, unpubl.) forming part of the Rombak Basement Window in northern Norway.*

Figure 16. *Ca. 30 m wide kyanite quartzite boudin in the centre of the photograph at Juovvačorrú wheathered out of volcanic rocks. (with permission of Are Korneliussen)*

Figure 17. *Fine-grained kyanite quartzite at Juovvačorrú with turquoise shades. The lower edge of the photograph is ca. 15 cm. (with permission of Are Korneliussen)*

3.4 Nasafjell, Mo i Rana

The kyanite quartzites form three WNW-ESE elongated lenses at the SW slope of the Nasafjell (1210 m a.s.l.) which is situated in the Saltfjell region, Nordland (Fig. 18). The three deposits are about 2, 4 and 7 km ESE of the Bolna railway station and the state road R6 along Lønsdalen. The kyanite quartzites are aligned along the SW margin of a basement dome consisting of granite. The granite dome forms a small basement window (~30 km^2) breaking through the Caledonian Gargatis nappe (Fig. 19), which consists of Svecokarelian deformed (1.6 to 1.9 Ga) granitic gneisses (Gjelle 1988). The basement granite (1.7 to 1.8 a) itself is considered as autochthonous. It is enclosed and bordered by onion-like shells of granitic gneiss, metagabbro, muscovite-quartzite schists, large lenses of hydrothermal quartz and kyanite quartzite (Gjelle 1988, Wanvik 2004). Both the kyanite quartzites and the hydrothermal quartz at Nasafjell were studied in detail by Wanvik (2003, 2004). The three kyanite quartzite deposits are 150, 400 and 600 m long and up to 30 m wide. They are embedded in muscovite schist.

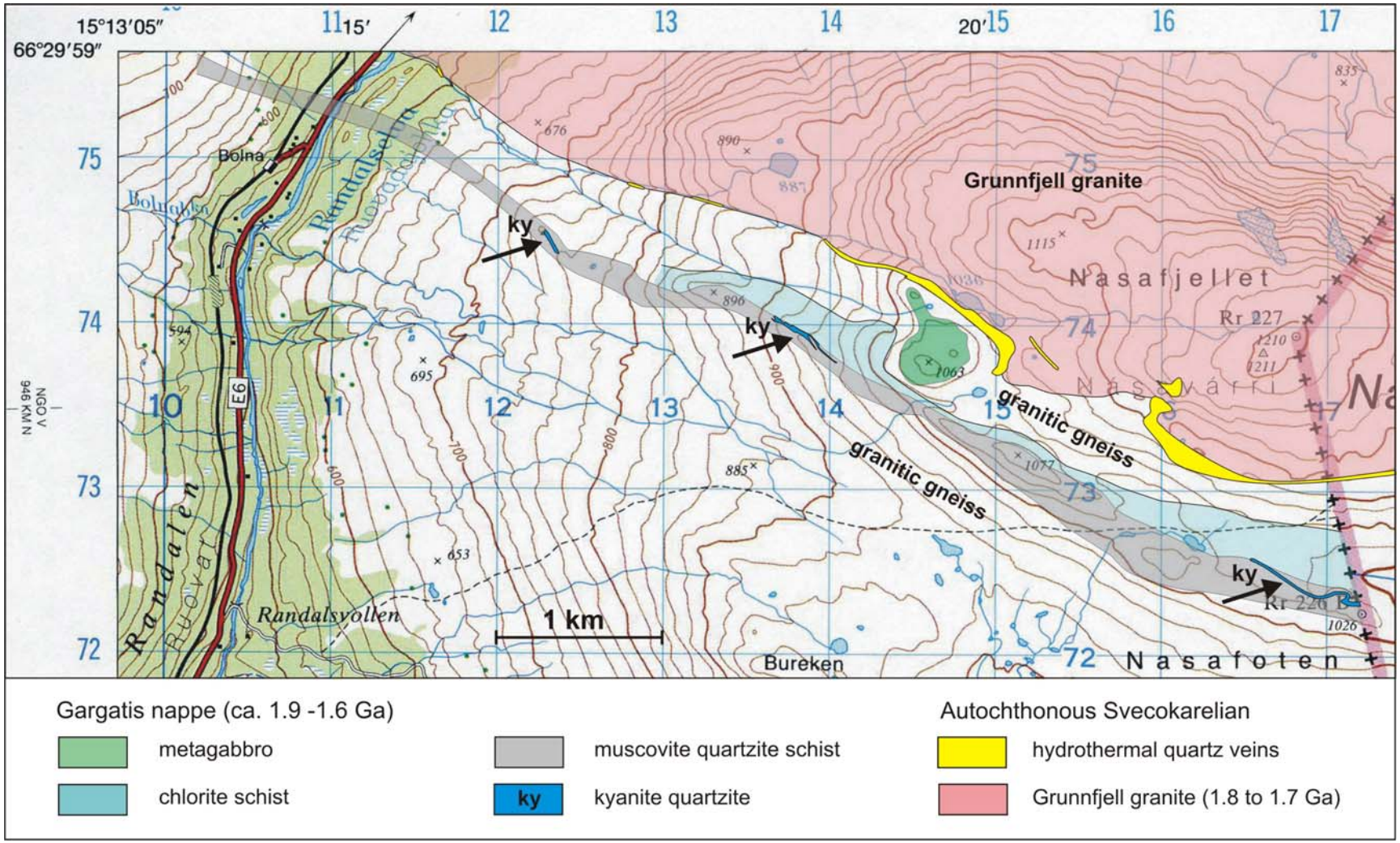

Figure 18. *Location of the kyanite quartzite occurrences at Nasafjell.*
Detail of the 1:50 000 topographic map Virvatnet with geological units mapped by Andersen (in: Dahl 1980) and Wanvik (2004).

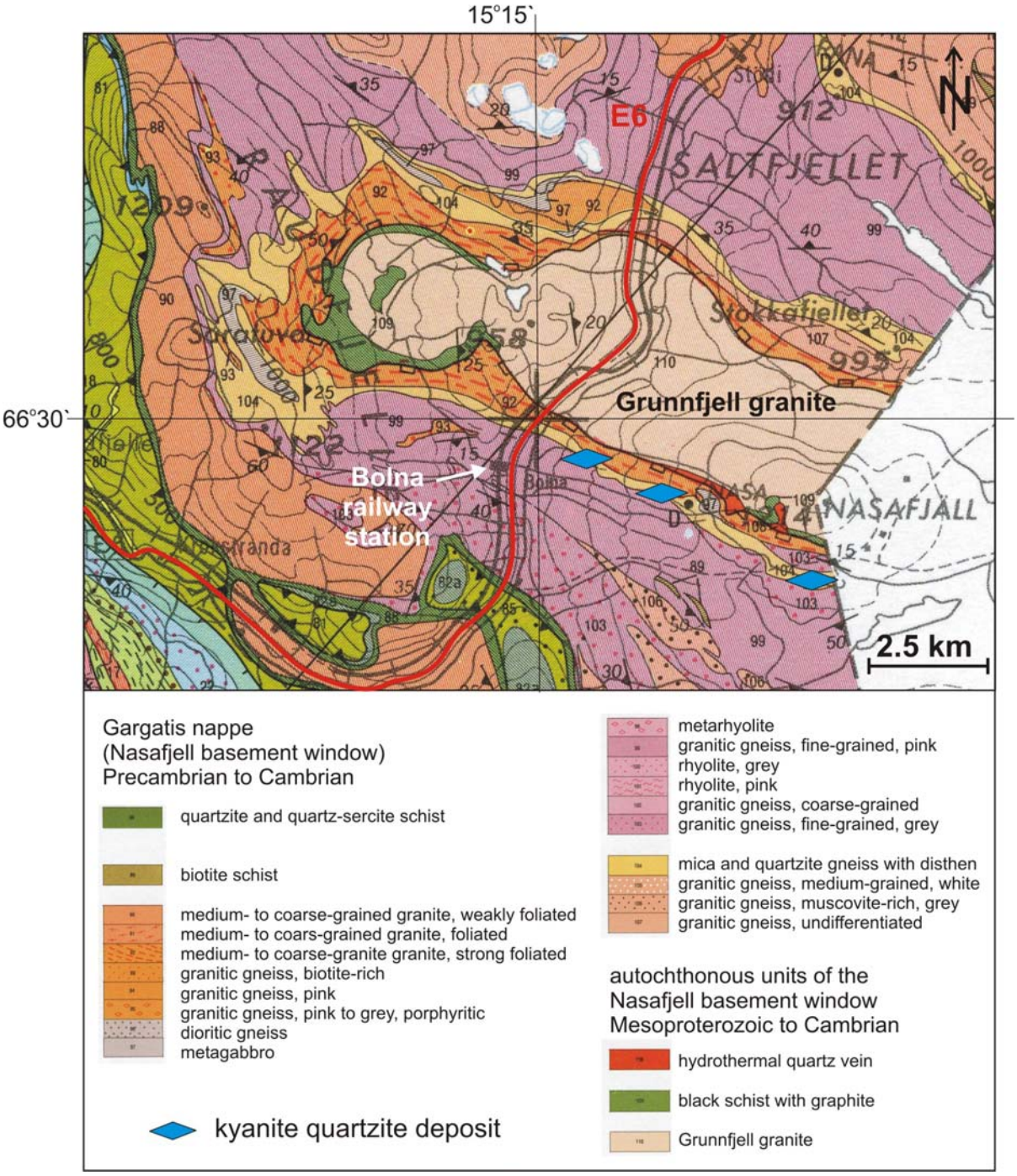

Figure 19. *Detail of the geological map of Saltdal M 1 : 250 000 (Gjelle 1988) showing the granite dome (Grunnfjell granite) and the kyanite quartzite deposits at its SW edge.*

4. Whole rock chemistry and petrography of kyanite quartzites

Kyanite quartzites are fine-grained and laminated rocks where quartz-rich layers alternate with kyanite-rich layers. The thickness of the layers varies between several centimeters up to several meters. Quartz-rich layers contain up to 80 wt.% quartz and kyanite-rich layers up to 45 wt.% kyanite. Occasionally, kyanite-rich layers are altered to muscovite- and/or pyrophyllite -rich layers due to retrograde processes. The muscovite and pyrophyllite content in these layers is up to 8 wt.%. Common accessory minerals are rutile (TiO_2), pyrite (FeS_2) and other Ti-Fe-bearing oxides and sulfides. Kyanite quartzite does not contain feldspar and biotite, which are common minor minerals in quartzites of sedimentary origin.

Whole rock analyses (XRF) of major and trace elements of quartz-rich and kyanite-rich layers of kyanite quartzites from Norway are listed in Table 5 and 6. In addition a quartzite (sample Hallaren) and metaarkoses (samples Kufjellet and Folldalen) which are regional related to the Tverrådalen kyanite quartzite, have been analysed to demonstrate the chemical contrast between kyanite quartzites and “ordinary” quartzites. Latter are of sedimentary origin whereas the origin of kyanite quartzites is still a matter of discussion (see chapters below). Kyanite quartzites contain between 10 and 32 wt.% Al_2O_3 whereas sedimentary quartzites and metaarkoses have Al_2O_3 concentrations below 9 wt.% (Fig. 20a). Kyanite quartzites contain almost no CaO, Na_2O and K_2O. Concentrations for the trace elements Ga, Cu, Ni, Co, Nd, Pr, Mo, Y, Pb, As, Hf, Sb, Sn, U, Cs, Ta, Yb, Sc, F and Cl are commonly below the detection limit. Kyanite quartzites have elevated concentrations of Ba, W, Zr, Sr, Cr and V. Zr seems to be a tracer of kyanite quartzite origin, because the kyanite quartzites from different areas vary in their Zr content (Fig. 20b). Au and Ag concentration were determined in pyrite-bearing samples from Gullsteinberget (2907410) and Sormbrua (2807401) (Table 6).

Table 5. *Whole rock analyses of major elements of kyanite quartzites (kyqtz) and associated quartzites (qtz) and metaarkoses (mar). Kyanite-poor (ky-poor) kyanite quartzites are considered here to have <25 wt.% kyanite which corresponds approximately <17.5 wt.% Al_2O_3 in the rock.*

locality	sample#	rock type	SiO_2	Al_2O_3	Fe_2O_3	TiO_2	MgO	CaO	Na_2O	K_2O	MnO	P_2O_5	LOI	total
Gullsteinberget	2907410	ky-poor kyqtz	76.09	17.70	1.42	0.32	0.07	0.01	<0.1	0.63	<0.01	0.02	2.32	98.58
Knøsberget	2907408	ky-rich kyqtz	75.89	19.39	0.71	0.23	0.05	<0.01	<0.1	0.05	<0.01	0.04	1.74	98.11
Kjeksberget	2907403	ky-rich kyqtz	66.96	30.19	0.64	0.31	0.08	0.02	<0.1	0.09	<0.01	0.08	0.9	99.33
	2907404	ky-poor kyqtz	82.54	12.76	1.67	0.48	<0.01	<0.01	<0.1	<0.01	<0.01	0.05	1.17	98.63
Sormbrua	2807401	ky-poor kyqtz	77.37	13.78	1.41	0.32	0.07	0.02	0.20	3.64	<0.01	0.04	2.38	99.24
	2907407	ky-poor kyqtz	78.90	17.72	0.19	0.36	0.01	0.01	<0.1	0.01	0.01	0.04	0.84	98.11
	2907406	ky-poor kyqtz	80.61	13.67	0.08	0.42	0.03	0.24	<0.1	0.05	<0.01	2.41	1.37	98.91
Halsjöberg	3107402	ky-rich kyqtz	67.35	31.55	0.46	0.09	0.12	0.01	0.12	0.09	<0.01	0.1	0.28	100.2
	3107401	ky-poor kyqtz	86.83	11.01	0.35	0.11	0.01	0.05	<0.1	0.14	<0.01	0.11	0.43	98.99
Tverrådalen	1907401	ky-poor kyqtz	82.67	14.28	0.13	0.44	0.06	0.01	<0.1	0.15	<0.01	0.03	0.62	98.33
	5*	ky-rich kyqtz	80.23	17.90	0.22	0.44	0.14	0.03	<0.1	0.38	<0.01	0.03	0.97	100.4
	6*	ky-rich kyqtz	67.62	30.75	0.26	0.35	0.14	0.04	<0.1	0.23	<0.01	0.05	0.75	100.2
	7*	ky-poor kyqtz	83.09	13.19	0.23	0.50	0.11	0.16	0.18	0.47	<0.01	0.12	0.84	98.89
	8*	ky-rich kyqtz	70.19	26.50	0.22	0.45	0.13	0.03	<0.1	0.18	<0.01	0.05	0.81	98.59
	9*	ky-poor kyqtz	81.76	15.10	0.15	0.51	0.09	<0.01	<0.1	0.20	<0.01	0.01	0.61	98.48
	DH1 0-3.5m*	ky-poor kyqtz	78.64	16.96	0.31	0.45	0.11	0.05	0.32	0.71	<0.01	0.05	1.89	99.48
	DH1 3.5-4.8m*	ky-rich kyqtz	75.49	21.81	0.10	0.47	0.11	0.02	<0.1	0.20	<0.01	0.03	1.14	99.38
	DH2 0-1.1m*	ky-rich kyqtz	80.26	18.15	0.19	0.35	0.09	0.02	<0.1	0.22	<0.01	0.02	0.93	100.3
	DH2 1.1-3.5m*	ky-rich kyqtz	69.38	27.88	0.27	0.46	0.11	0.07	<0.1	0.18	<0.01	0.07	1.02	99.47
	DH2 3.5-5.5m*	ky-rich kyqtz	78.35	18.82	0.24	0.38	0.10	0.05	<0.1	0.19	<0.01	0.04	0.70	98.88
	DH2 5.5-9.1m*	ky-rich kyqtz	75.83	20.62	0.20	0.39	0.11	0.04	0.16	0.28	<0.01	0.04	1.21	98.99
Kufjellet	2007405	mar	90.58	5.04	0.50	0.14	0.19	0.01	0.23	2.68	0.01	<0.01	0.47	99.86
Folldalen	2007410	mar	80.88	8.84	2.41	0.44	0.80	0.22	0.49	3.71	0.063	0.08	1.31	99.24
Hallaren	1907405	qtz	88.18	5.47	1.30	0.39	0.36	0.34	0.43	1.85	0.017	0.063	0.76	99.15
Jouvvačorrú	R1021a	ky-rich kyqtz	77.68	20.8	0.09	0.18	0.03	<0.01	<0.1	0.05	<0.01	0.02	0.21	99.05
	R1021b	quartzite	98.56	0.19	0.09	0.84	<0.01	<0.01	<0.1	0.03	<0.01	<0.01	0.15	99.89
Nasafjell	JW0315c		76.27	20.84	0.54	0.18	0.05	0.01	<0.1	0.32	<0.01	0.07	0.56	98.78

* data from Wanvik (1998)

Table 6. *Whole rock analyses of trace elements of kyanite quartzites and associated quartzites and metaarkoses. Concentrations for Sb, Sn, U, Cs, Ta and Sc are below the detection limit of 10 ppm, for Yb below 15 ppm and for F and Cl below 0.1 ppm. Trace element concentrations marked with yellow might be indicative for the origin of the rocks.*

locality	sample#	Ba	Ga	Zn	Cu	Ni	Co	Ce	La	Nd	W	Pr	Mo	Nb	Zr	Y	Sr	Rb	Th	Pb	Cr	V	As	Hf	S	Au*	Ag*
Gullsteinberget	2907410	422	11	17	<10	<5	5	<10	<10	<10	47	<10	<5	21	213	<5	26	22	<5	<10	68	<10	8	<10	0.32	2.2	32
Knøsberget	2907408	74	<10	8	<10	<5	8	<10	<10	<10	24	<10	<5	15	119	<5	47	<5	7	<10	17	19	<5	<10	0.32	n.d.	n.d.
Kjeksberget	2907403	2430	19	26	11	<5	<5	39	47	13	44	<10	8	13	231	6	120	<5	8	<10	50	32	<5	<10	0.13	n.d.	n.d.
	2907404	1722	<10	10	10	<5	<5	<10	11	<10	57	<10	<5	16	251	<5	92	<5	<5	<10	27	29	5	<10	0.36	n.d.	n.d.
Sormbrua	2807401	646	<10	13	<10	5	<5	104	63	50	35	14	7	13	227	7	73	78	12	21	65	23	<5	<10	0.32	0.9	5
	2907407	1274	<10	12	13	<5	<5	35	30	12	43	<10	<5	14	280	<5	55	<5	7	<10	40	19	<5	<10	<0.1	n.d.	n.d.
	2907406	136	10	10	<10	<5	<5	<10	<10	<10	39	<10	<5	15	312	<5	1206	<5	<5	<10	24	42	<5	20	<0.1	n.d.	n.d.
Halsjöberg	3107402	44	18	12	<10	<5	<5	<10	<10	<10	44	<10	<5	<5	36	<5	72	<5	5	<10	98	22	5	<10	<0.1	n.d.	n.d.
	3107401	121	<10	12	<10	<5	<5	<10	<10	<10	43	<10	<5	<5	30	<5	147	<5	<5	<10	42	<10	<5	<10	<0.1	n.d.	n.d.
Tverrådalen	1907401	399	<10	7	<10	<5	8	10	13	<10	31	<10	<5	16	310	<5	26	5	8	<10	<10	25	<5	14	<0.1	n.d.	n.d.
Kufjell	2007405	724	<10	13	<10	<5	<5	<10	<10	<10	38	<10	<5	5	127	12	39	88	6	<10	27	<10	<5	<10	<0.1	n.d.	n.d.
Folldalen	2007410	782	<10	32	<10	9	8	30	19	12	39	<10	<5	12	182	18	41	123	9	<10	30	33	<5	<10	<0.1	n.d.	n.d.
Hallaren	1907405	325	<10	15	10	<5	<5	29	16	<10	37	<10	<5	8	311	21	23	58	10	<10	22	14	<5	<10	<0.1	n.d.	n.d.
Jouvvačorrú	R1021a	<10	31	15	<10	<5	<5	<10	<10	<10	48	<10	<5	33	73	<5	5	<5	<5	<10	42	21	5	<10	<0.1	n.d.	n.d.
	R1021b	10	<10	10	<10	<5	<5	<10	<10	<10	51	<10	<5	16	155	<5	<5	<5	5	<10	13	<10	<5	<10	<0.1	n.d.	n.d.
Nasafjell	JW0315c	285	11	7	<10	<5	6	84	65	30	27	11	5	22	221	8	69	10	24	10	19	27	17	<10	<0.1	n.d.	n.d.

* Au and Ag were analysed by ICP-AES at ACME Analytical Laboratories LTD., Vancouver BC V6A 1R6, 852 E. Hastings St., Canada. Values are given in ppb.
n.d. – not determined

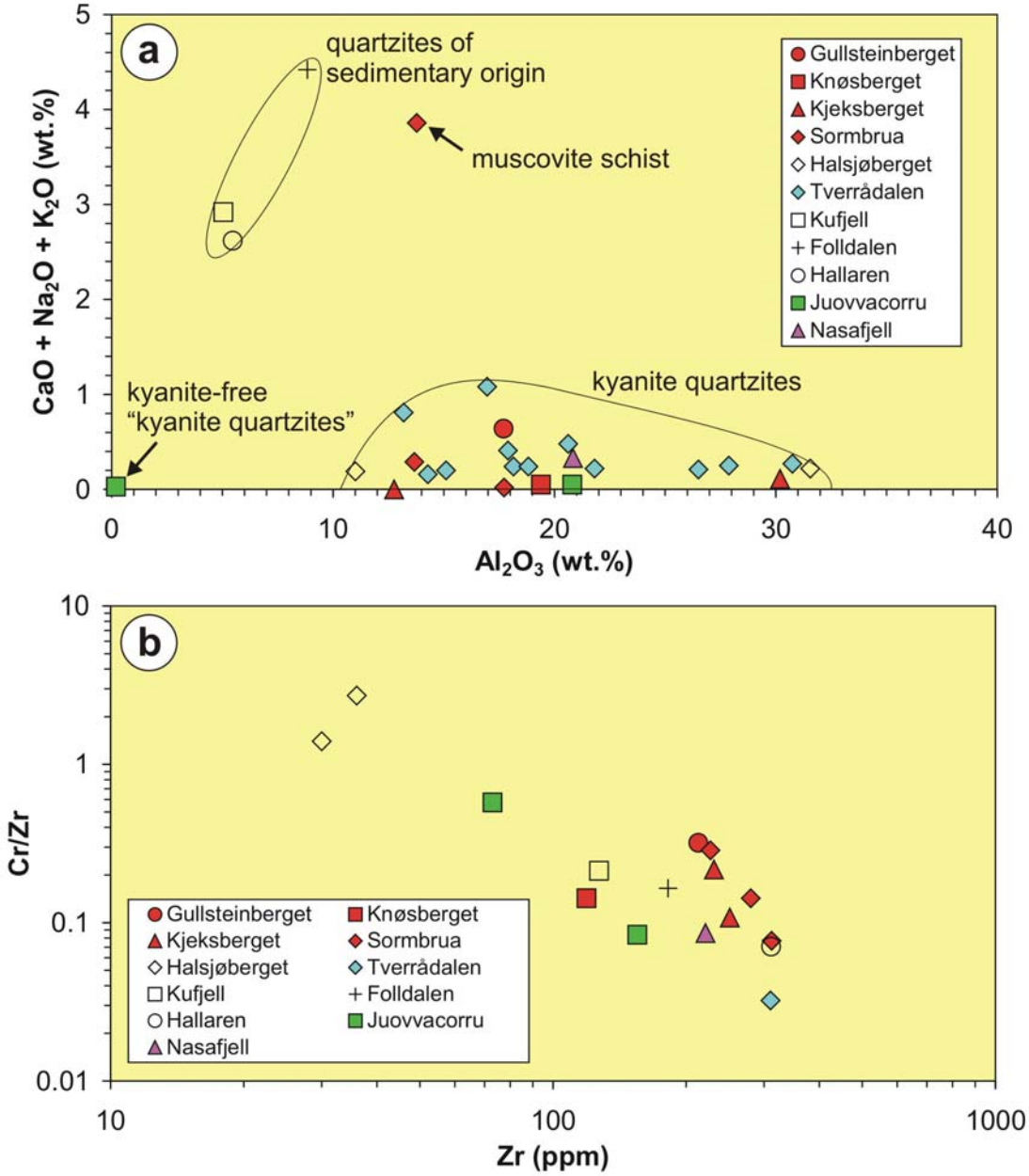

Figure 20. *a – Major element plot of kyanite quartzites and regional related quartzite (Hallaren) and metaarkoses (Kufjellet and Folldalen). b – Zr versus Cr/Zr plot of kyanite quartzites and regional related quartzite (Hallaren) and metaarkoses (Kufjellet and Folldalen).*

4.1. Solør

The concentration of SiO_2 of a representative sample from the *Gullsteinberget* deposit is 76.1 wt.% and of Al_2O_3 17.7 wt.% determined by XRF (Table 5). According to Jakobsen and Nielsen (1977) the average content (37 samples) of quartz from the Gullsteinberget is about 75 wt.%, of kyanite 22.9 wt.% and of rutile 0.18 wt.%. The rock has relative high Zr (213 ppm, Table 6) which is typically for all Solør kyanite quartzites. The quartz crystals have an average crystal size of 0.496 mm (200 measurements), which is relative high compared to the bulk of the Norwegian kyanite quartzites. 42.5 % of the quartz crystals are ≥0.5 mm. The maximum of crystal size distribution lies at ca. 0.15 mm (Fig. 21). The thin section scan in Fig. 22 shows the distribution of quartz (white) and kyanite (dark grey) in a kyanite-rich layer of the quartzite. Kyanite crystals are commonly embedded in pyrophyllite and muscovite (bright grey). Barite is a common accessory mineral. The rock contains slightly elongated quartz crystals (Figs. 23a, b). Some of the large crystals have undulatory extinction whereby the subgrains form a stripe-like pattern (Fig. 23c). Quartz shows straight grain boundaries and 120° triple-junctions between grains, indicating stable arrangement of the crystal framework due to grain boundary area reduction (Fig. 23d). Kyanite plates are about 480 µm in length and they are commonly altered to muscovite (Fig. 23e) and to sericite along grain boundaries and trans-granular cracks (Fig. 23f).

In scanning electron microscopy cathodoluminescence (SEM-CL) imaging quartz of the Gullsteinberget deposit has a more or less homogeneous and weak cathodoluminescence (CL) signal (Figs. 24a, c). The homogeneous and weak CL indicates relative low concentrations of lattice defects and luminescence active trace elements (CL activators) in the quartz lattice. Fe^{3+} is a CL activator in quartz and Al and Ti create presumably blue luminescence centres (e.g., Götze et al. 2001, Müller et al. 2002). Backscattered electron (BSE) imaging reveals that sericite films occur along some grain boundaries (Figs. 24b, d).

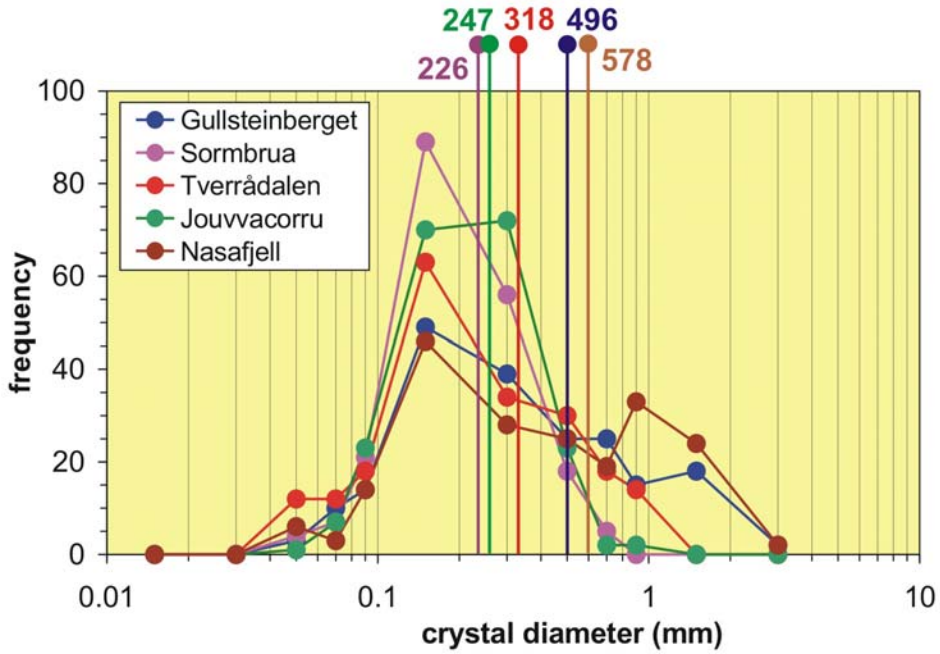

Figure 21. *Crystal size distribution of quartz in kyanite quartzites.*
200 crystals were measured for each sample. The vertical lines and numbers (in µm) indicate the average crystal size. The flat and wide pattern of Gullsteinberget and Nasafjell corresponds to a wide range of crystal sizes.

Figure 22. *Thin section scan of a kyanite-rich layer in the Gullsteinberget kyanite quartzite. Dark grey – kyanite, bright grey – pyrophyllite/muscovite, white – quartz.*

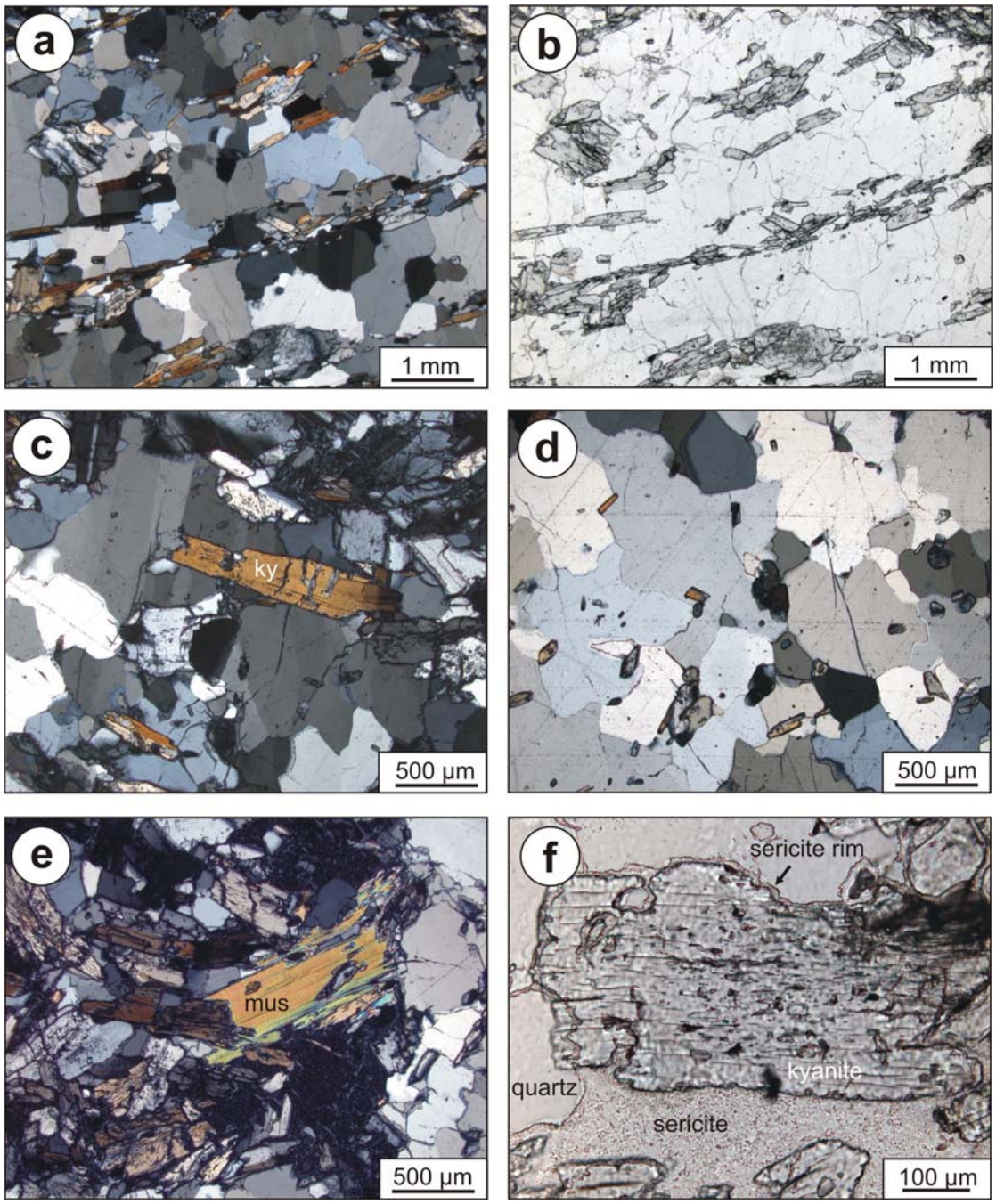

Figure 23. *Optical microscopy images of kyanite quartzites from the Gullsteinberget deposit. a – Laminated kyanite quartzite where quartz layers alternate with thin kyanite layers (dull brownish). Crossed nicols. b – Same section as (a). The dark grey crystals are kyanite. Plane light. c – Quartz crystal with stripe-like undulatory extinction enclosing a kinked kyanite (ky) crystal. Crossed nicols. d – Detail of quartz texture showing the straight grain boundaries. 120° triple-junctions between grains are common. Crossed nicols. e – Retrograde muscovite (mus) overgrowth on kyanite. Crossed nicols. f – Retrograde formed sericite along grain boundaries and trans-granular cracks of kyanite. Plane light.*

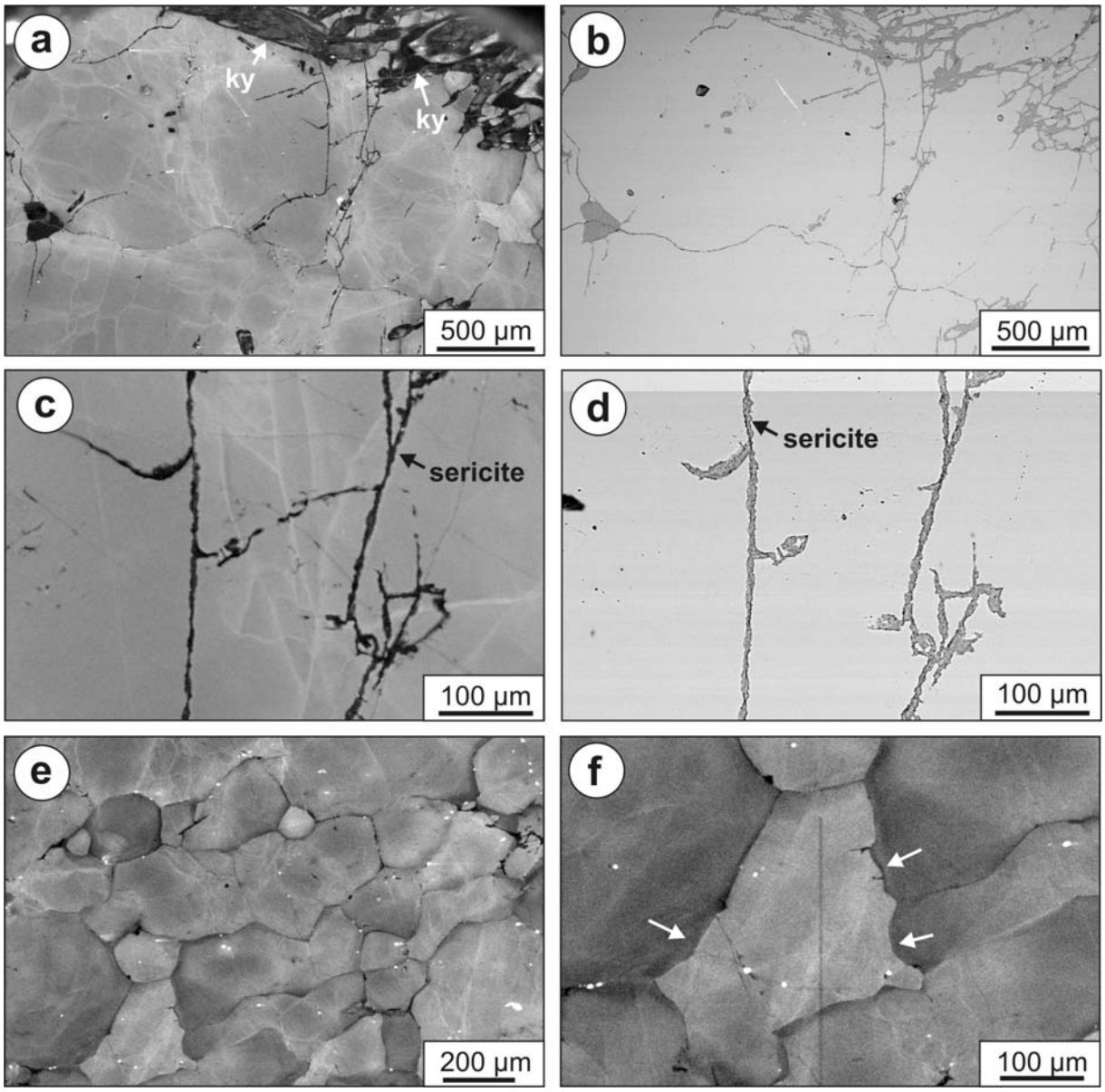

Figure 24. *Scanning electron microscopy cathodoluminescence (SEM-CL) and backscattered electron (BSE) images of kyanite quartzites from the Gullsteinberget and Kjeksberget deposits. a – SEM-CL image of quartz of the Gullsteinberget kyanite quartzite. CL is almost homogeneous. Vein-like shadows with slightly lighter CL cross-cut the grains. Kyanite (ky) appears dark grey with internal zoning. b – BSE image of the same section as (a). The darker structures are formed by sericite. c – Detail of (a). d – Detail of (b). e – SEM-CL image of quartz from the Kjeksberget deposit. Quartz grains show different grey shades of CL. f – Detail of (e). Dull luminescent defect-poor quartz replaces quartz with brighter CL by grain boundary migration (arrows).*

The average content (18 samples) of quartz, kyanite and rutile amounts 74, 23.1 and 0.59 wt.%, respectively, in the kyanite quartzite from *Knøsberget* (Jakobsen and Nielsen 1977). The Knøsberget sample has the lowest Ba content of 74 ppm detected in the kyanite quartzites from Solør. SiO_2 content in kyanite quartzites from the *Kjeksberget* deposit varies between 67 and 83 wt.%. Jakobsen and Nielsen (1977) analysed one sample from the Kjeksberget deposit with 21.5 wt.% kyanite and 1.14 wt.% rutile. The rocks of Kjeksberget have high Ba between

1722 and 2430 ppm (Table 6). Quartz grains of the Kjeksberget deposit show different grey shades in SEM-CL (Figs. 24e, f) which are caused by minor variations of the defect and CL activator concentration. Bright grains are richer in defects and/or trace elements than darker grains. Dull luminescent defect-poor quartz grains replace quartz grains with brighter CL and higher defect concentration by grain boundary migration (e.g., Van den Kerkhof et al. 2004; Fig. 24f). Therefore, the widespread grain boundary migration result in the purification of quartz whereby impurities were expelled to the grain boundaries.

The Al_2O_3 content of the *Sormbrua* deposit varies between 13 and 18 wt.%, which is relative low compared to the other deposits of Solør. Accordingly the SiO_2 content is higher with 77 to 81 wt.%. Nystuen (1969a) stated kyanite concentrations of 10 to 15 vol.% with kyanite crystals up to 3 cm in length from Sormbrua. Sample 2807401 has high K_2O of 3.64 wt.% due to muscovite which probably replaced kyanite completely during retrograde metamorphism. K_2O was probably introduced by metamorphic (metasomatic) processes. The sample represents an intercalation of muscovite schist in kyanite quartzites. The average crystal size of the slightly elongated quartz crystals is 0.226 mm (200 measurements). The maximum of crystal size distribution is at ca. 0.15 mm (Figs. 21). 11.5 % of the quartz crystals are ≥0.5 mm. The thin section scan in Fig. 25 shows the distribution of quartz (white), kyanite (dark grey), wavellite and topaz (grey batches) in a kyanite-rich layer of the Sormbrua deposit. The quartz fabric is almost equi-granular and crystals are slightly elongated (Fig. 26a). Crystals >500 µm show undulatory extinction (Fig. 26b). Quartz of the Sormbrua deposit has a dull CL indicating a low abundance of lattice defects and trace elements. Shadows of brighter CL reflect presumably old grain boundaries (Figs. 27a, b).

The blue batches observed in the hand specimen (Fig. 1) consist of kyanite needles, wavellite ($Al_3[(OH,F)_3/(PO_4)_2] \cdot 5H_2O$) and tiny lazulite crystals ($(Mg,Fe)Al_2(PO_4)_2(OH)_2$; Figs. 26c-f). Wavellite forms aggregates of up to 5 mm large crystals enclosing kyanite needles. Poikiolitic topaz ($Al_2SiO_4(F,OH)_3$)with drop-like quartz inclusions is common. The crystals are up to 2 mm in size. Other accessory minerals are rutile, zircon, barite, apatite and aluminium-strontium-phosphates. The kyanite needles are about 1.3 mm in length and rimmed by sericite (Fig. 28a). The quartz texture of the sample from the same kyanite quartzite body but about 2 km NE from the Sormbrua bridge shows granoblastic-polygonal crystal texture with planar high-angle boundaries („foam texture“) and 120° triple-junctions between grains due to lattice recovery (Figs. 28b-d). The sample contains about 1 vol.% pyrite (Fig. 28c) and does not contain kyanite but muscovite layers.

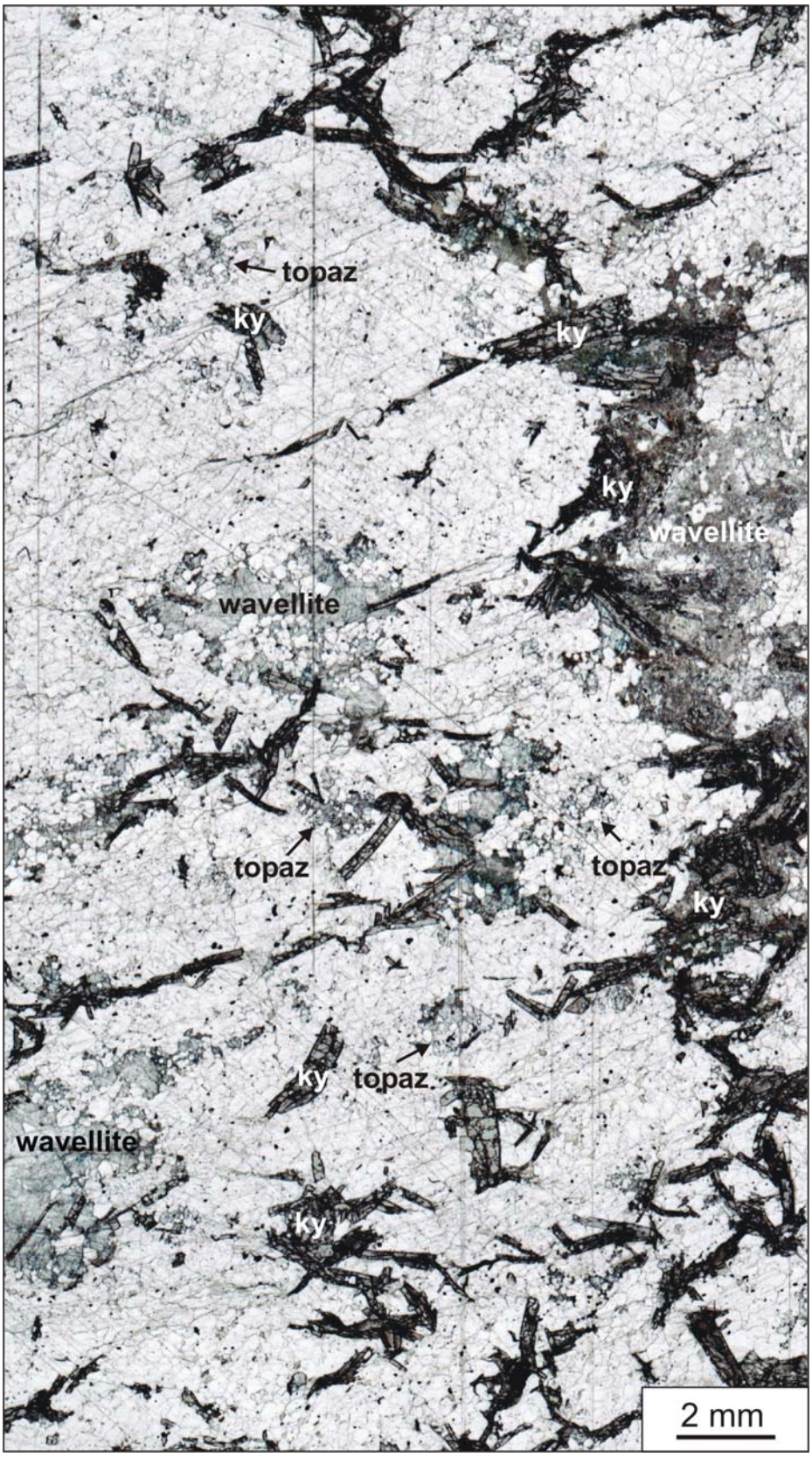

Figure 25. *Thin section scan of a kyanite-rich layer in the Sormbrua kyanite quartzite. Dark grey – kyanite (ky), grey batches – wavellite or topaz, white - quartz*

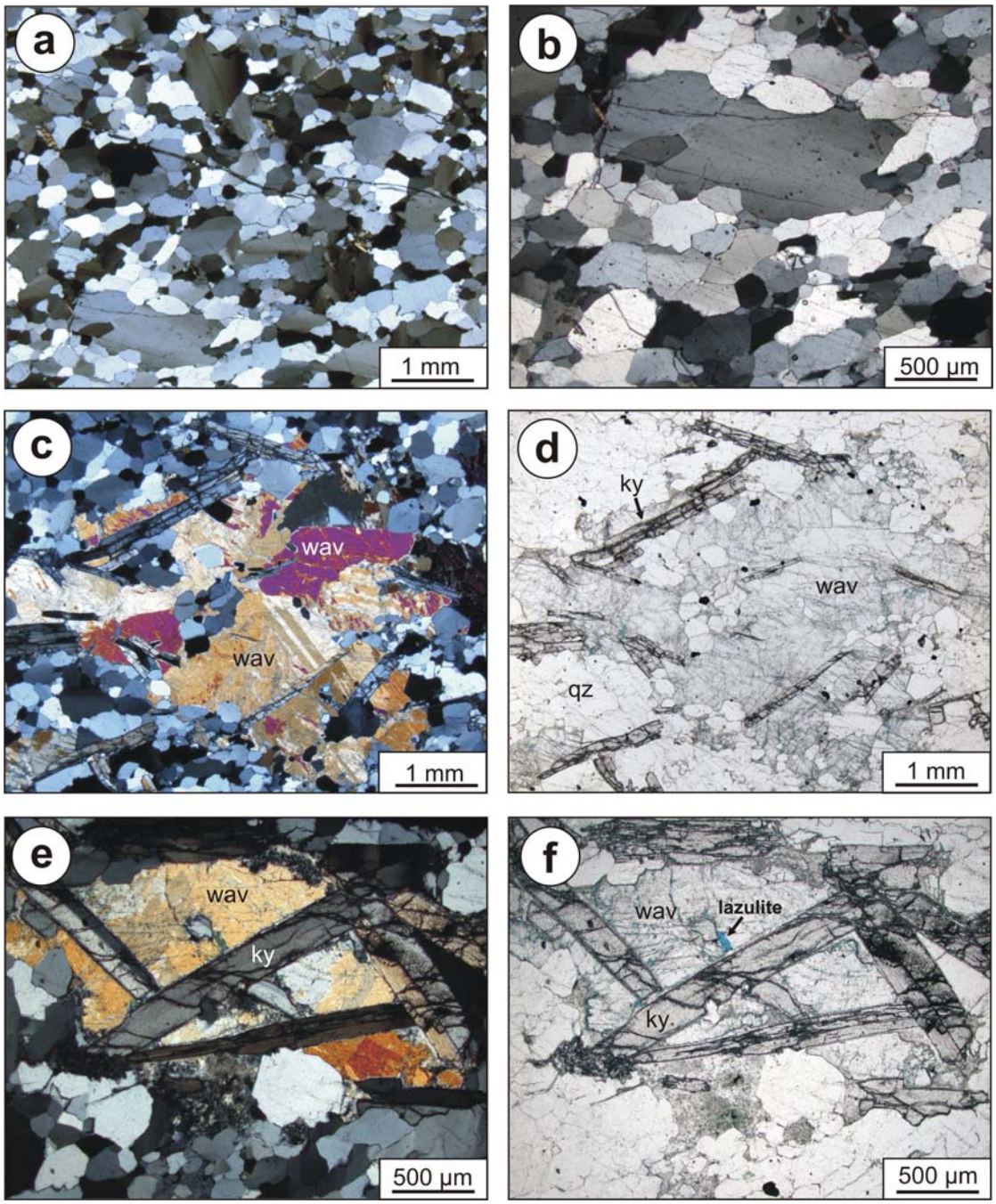

Figure 26. *Optical microscopy images of kyanite quartzites from the Sormbrua deposit. a – Overview of the quartz texture of the sample from the outcrop at the bridge Sormbrua. Crossed nicols. b - Large quartz crystal with undulatory extinction surrounded by small elongated crystals. Crossed nicols. c – Aggregate of wavellite (wav) enclosing kyanite needles (ky). Crossed nicols. d - Same section as (c). ky – kyanite, qz – quartz, wav - wavellite. Plane light. e - Nest of kyanite needles (ky) embedded in wavellite (wav). f - Same section as (e). Tiny blue lazulite crystals are at the grain boundaries of wavellite and kyanite. These wavellite-kyanite aggregates are the blue batches observed in the hand specimen (Fig. 1b).*

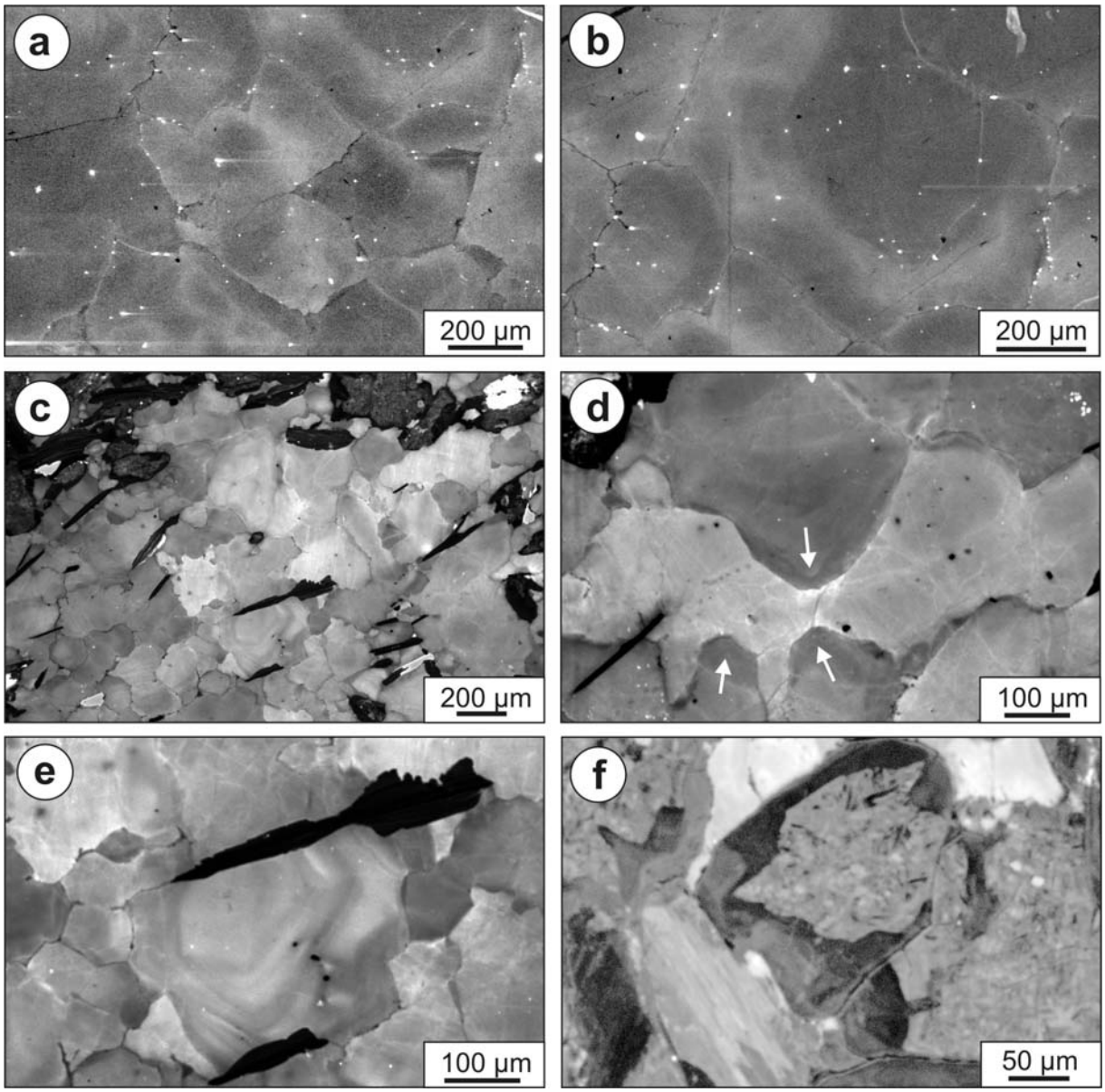

Figure 27. *Scanning electron microscopy cathodoluminescence (SEM-CL) images of kyanite quartzites from the Sormbrua and Tverrådalen deposits. a - Quartz of the Sormbrua deposit with dull CL. Shadows of brighter CL reflect presumably old grain boundaries. The bright spots are caused by mineral inclusions which are probably apatite. b – Large quartz grain with a concentric shadow of brighter CL which probably marks an old grain boundary. c – Overview SEM-CL image of quartz of the Tverrådalen deposit. Quartz grains show different grey shades of CL. d – Dull luminescent defect-poor quartz replaces quartz with brighter CL by grain boundary migration (arrows). Tverrådalen deposit. e – Detail of (c). Quartz with blurred euhedral zoning. The zoning resembles the zoning pattern of quartz phenocrysts of volcanic rocks (e.g. Müller et al. 2005). f - Kyanite with a grey irregular core surrounded by dull luminescent kyanite. Tverrådalen deposit.*

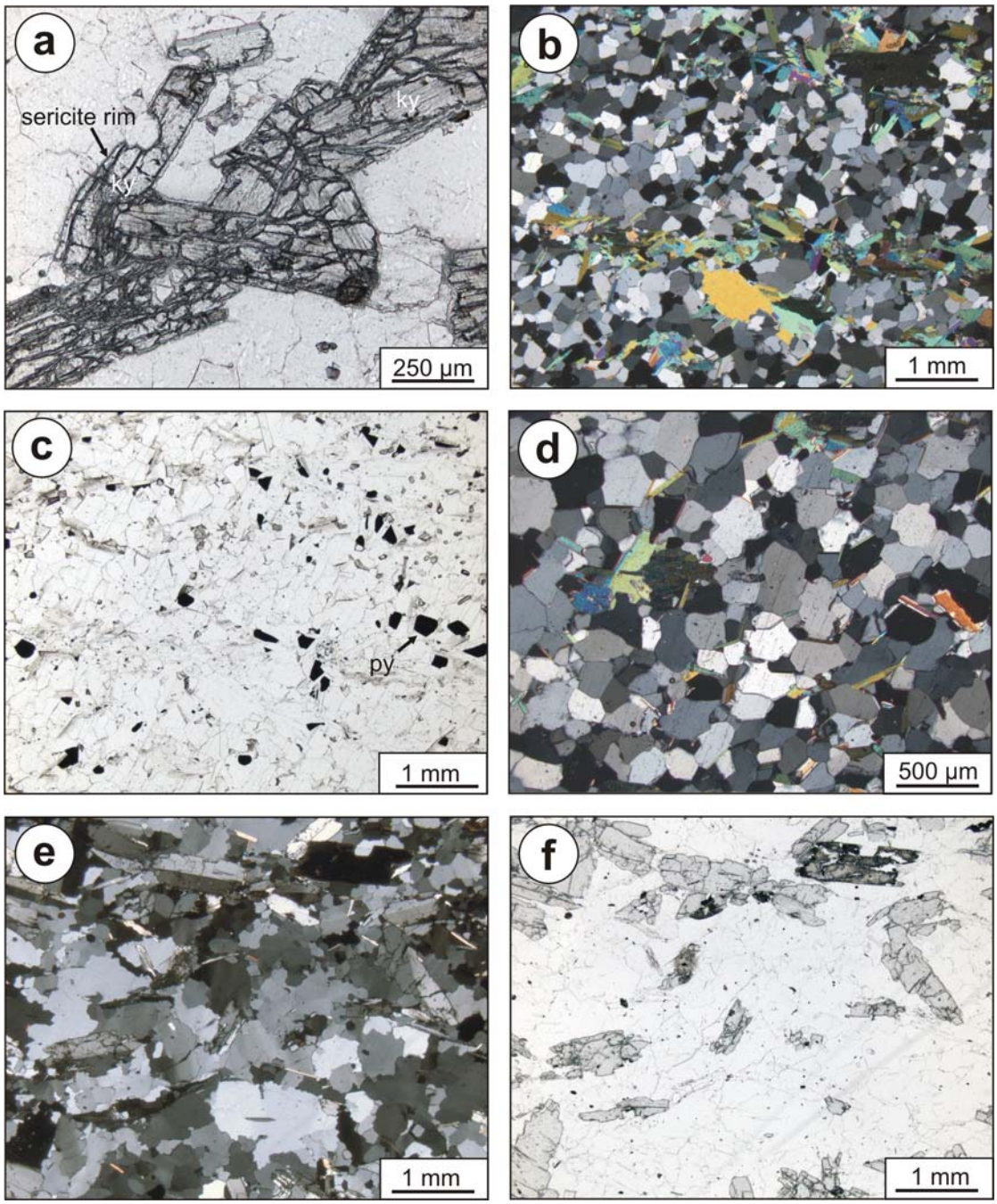

Figure 28. *Optical microscopy images of kyanite quartzites from the Sormbrua and Tverrådalen deposits. a – Kyanite in the sample from bridge Sormbrua rimmed by sericite. Plane light. b - Granoblastic-polygonal texture of quartz intercalated by muscovite-rich layers. Sormbrua deposit. Crossed nicols. c – Same section as (b). Pyrite (py) is common accessory. Plane light. d - Granoblastic-polygonal crystal texture with planar high-angle boundaries („foam texture“) and 120° triple-junctions between grains. Crossed nicols. e – Quartz texture of the kyanite quartzite from Tverrådalen, Surnadal. Quartz crystals have a wide range of size and exhibits sutured and irregular grain boundaries. Crossed nicols. f – Same section as (e). Kyanite crystals are dark grey. Plane light.*

4.2. Tverrådalen, Surnadal

The average composition of 11 samples from the kyanite quartzite of Tverrådalen is 65 wt.% quartz, 31 wt.% kyanite, 3-5 wt.% muscovite and 0.5 wt.% rutile wherby the quartz content varies between 75 and 55 wt.% and the kyanite content between 20 and 44 wt% (Wanvik 1998). Muscovite is poor in Fe. Zircon is a common accessory mineral which is reflected in the relative high Zr concentration of 310 ppm (Table 6). SiO_2 varies between 68 and 83 wt.% and Al_2O_3 between 13 and 31 wt.% (Table 5).

The average crystal size of quartz is 0.318 mm (n=200). The maximum of the crystal size distribution is at ca. 0.15 mm (Fig. 21). 31 % of the quartz crystals are ≥0.5 mm. The thin section scan in Fig. 29 shows the distribution of quartz (white) and kyanite (dark grey) in a kyanite-rich layer of the Tverrådalen sample. Quartz has strongly sutured and irregular grain boundaries (Fig. 28e, f, 30a-d). Some large quartz grains show stripe-like undulatory extinction due to subgrain formation (Fig. 30c). The irregular boundaries are non-equilibrium "frozen" mobile boundaries formed by late stage deformation, probably of Caledonian age. The texture is attributed to strain-induced grain boundary migration. Deformation of a previously deformed quartzite with straight grain boundaries produces strain which is evenly distributed within grains but is heterogeneously distributed along boundaries. Incipient recrystallisation results in slight boundary movements from less-strained into more-strained regions so as to reduce the total amount of strained crystal. The "teeth" on the boundary represent greater grain boundary movement into small regions of higher strain. The grain boundary migration causes the release and replacement of impurities (trace elements) from the newly formed quartz. The impurities are enriched at the crystal growth front (grain boundary; Fig. 30d). Quartz from Tverrådalen has generally low CL intensity which indicates a low abundance of lattice defects and trace elements. The different grey shades of quartz in the overview image (Fig. 28c) are caused by minor variations of the defect and activator element concentration. Bright grains are richer in defects and/or trace elements than darker grains (e.g., Van den Kerkhof et al. 2004). Fig. 28d illustrates how defect-poor quartz (dark grey) grows (arrows) at the cost of the defect-rich crystal (bright grey). The widespread grain boundary migration result in the formation of defect- and trace-element-poor quartz. Fig. 28e shows a quartz grain with blurred euhedral zoning. It is the only zoned crystal which has been found. The zoning resembles the zoning observed in quartz phenocrysts of volcanic rocks (e.g., Müller et al. 2005).

Kyanite plates are about 800 µm in length and contain common inclusion of quartz (Fig. 30e). In SEM-CL kyanite shows internal zoning where irregular cores with common inclusions of quartz are overgrown by dull luminescent kyanite (Fig. 28f). Occasionally, kyanite is overgrown by retrograde muscovite along micro-shear zones (Fig. 30f). About 10% of the kyanite crystals are completely sericitised (Figs. 29, 31a).

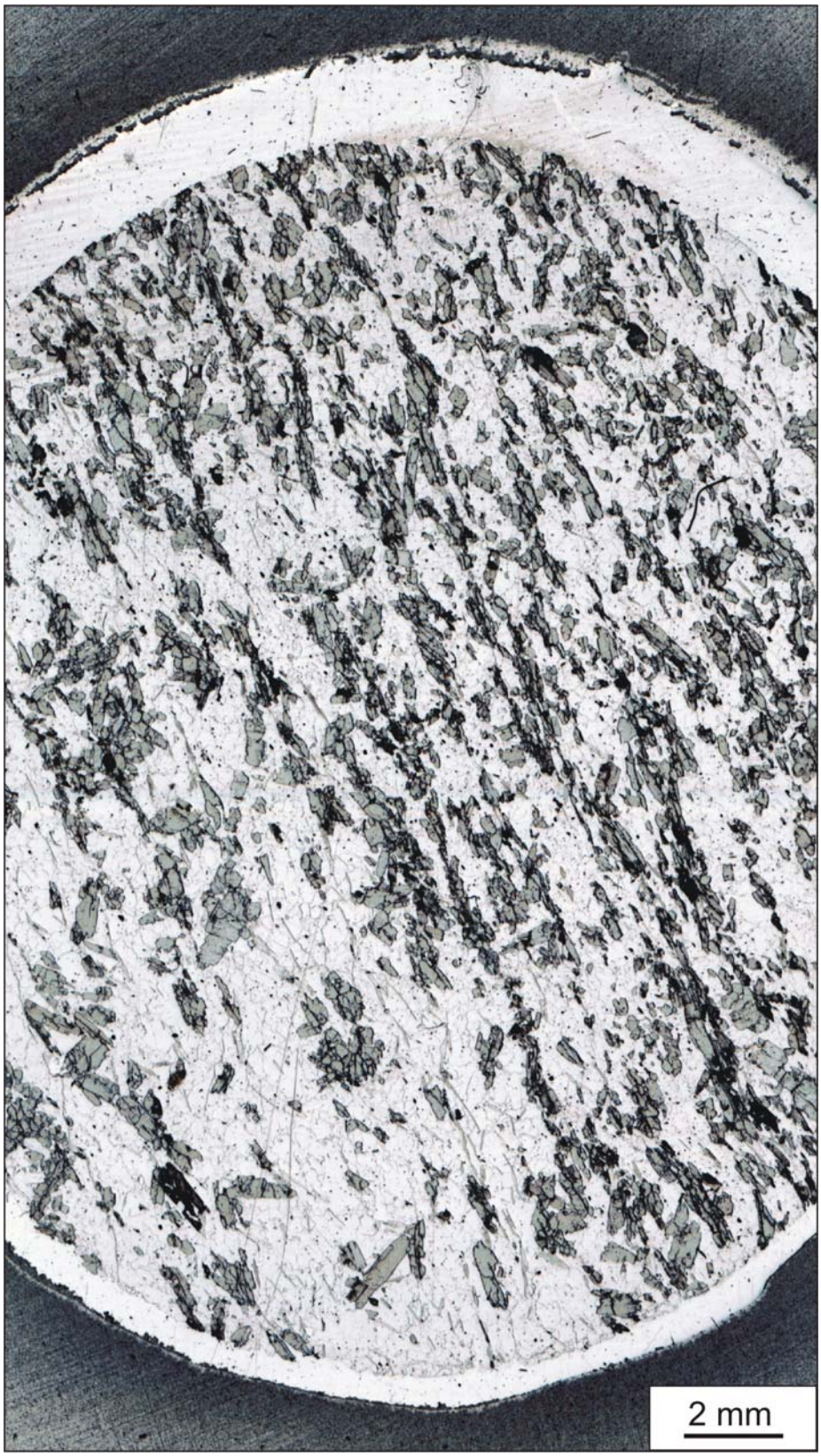

Figure 29. *Thin section scan of a kyanite-rich layer in the Tverrådalen kyanite quartzite (drill core). Dark grey – kyanite, black – sercitised kyanite, white – quartz.*

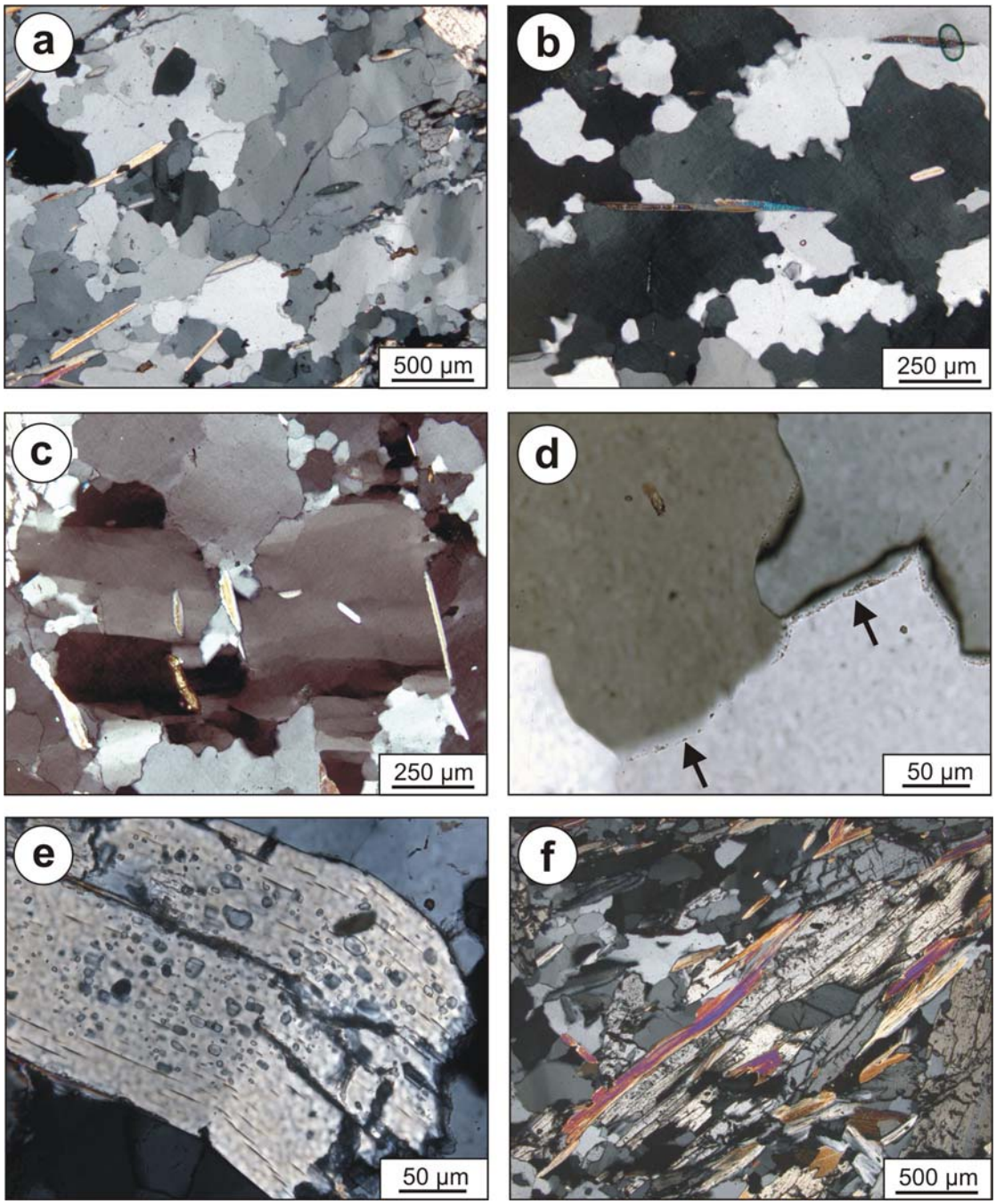

Figure 30. *Optical microscopy images of kyanite quartzites from the Tverrådalen deposit. a- Quartz texture showing the wide range of crystal sizes. Crossed nicols. b – Detail of quartz texture with strongly sutured grain boundaries. Crossed nicols. c - Large quartz crystal with stripe-like undulatory extinction due to subgrain formation. Crossed nicols. d - Enrichment of impurities at the growth front (grain boundary) due to grain boundary migration. Crossed nicols. e – Quartz inclusions in kinked kyanite. Crossed nicols. f – Sheared kyanite crystals partly overgrown by retrograde muscovite. Crossed nicols.*

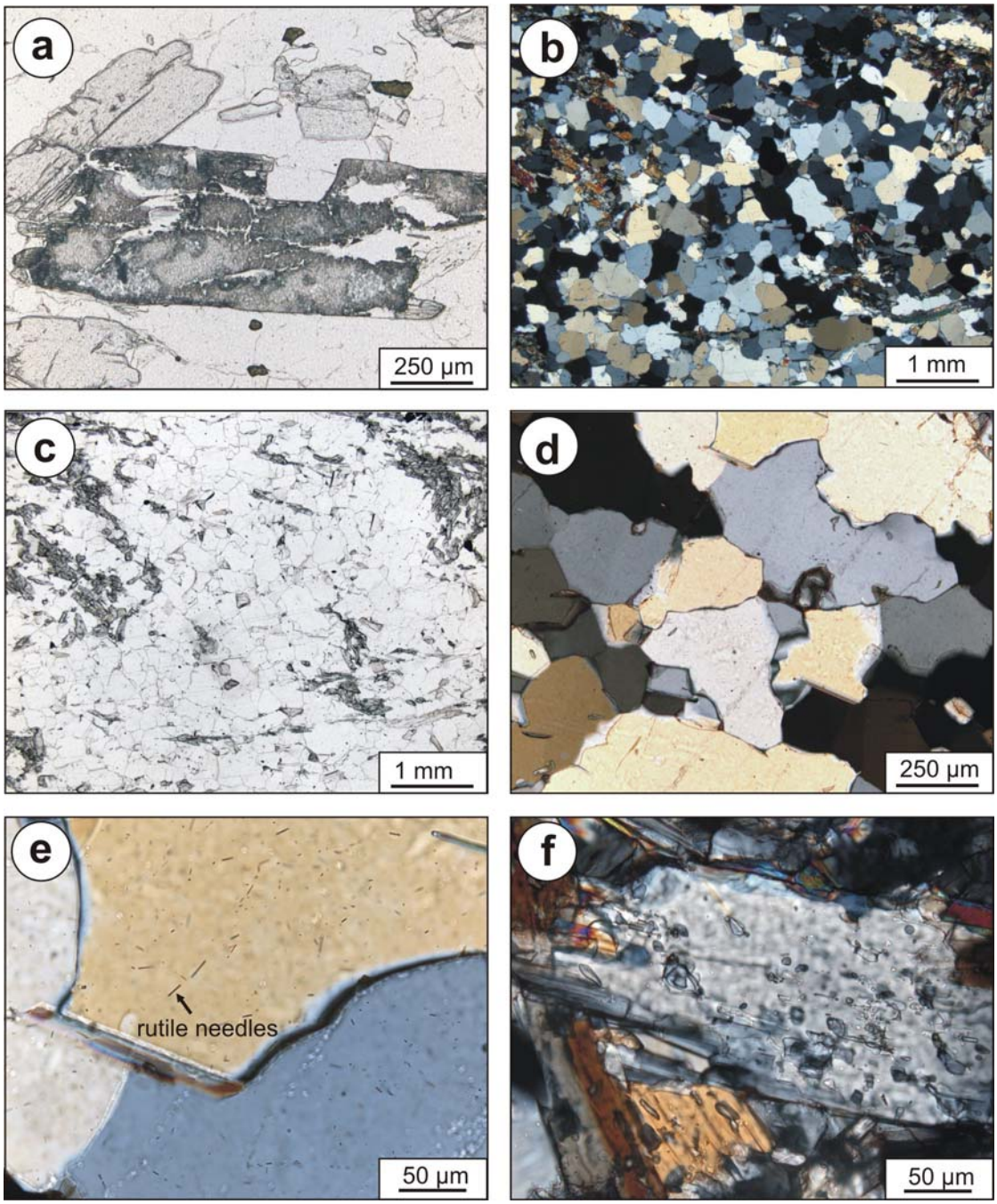

Figure 31. *Optical microscopy images of the kyanite quartzites from the Tverrådalen and Juovvačorrú deposits. a – Completely sercitised kyanite in a sample from the Tverrådalen deposit. Plane light. b – Overview of quartz texture of the kyanite quartzite from Juovvačorrú, Skjomen. Crossed nicols. c – Same section as (b). Plane light. d – Detail of quartz texture from the Juovvačorrú deposit. Quartz has planar grain boundaries and occasionally 120° triple-junctions between grains. Crossed nicols. e – Rutile needles in quartz of the Juovvačorrú deposit. Crossed nicols. f – Quartz inclusions in kyanite of the Juovvačorrú deposit. Crossed nicols.*

4.3 Juovvačorrú, Skjomen

The kyanite content of the Juovvačorrú deposit is below 25 wt.% and the quartz content varies from 75 to 98 wt.%. Latter are almost pure quartzites with 98.6 wt.% SiO_2 (Table 5). The Juovvačorrú kyanite quartzite is depleted in Ba, Zr and Sr compared to the other Norwegian kyanite quartzites (Table 6). Accessory minerals are rutile and zircon. The average crystal size of quartz is 0.247 mm (200 measurements). The maximum of the crystal size distribution is at ca. 0.2 mm (Fig. 21). 13.5 % of the quartz crystals are ≥0.5 mm. Quartz has planar grain boundaries and occasionally 120° triple-junctions between grains (Figs. 31b-e). It contains commonly tiny rutile needles (Fig. 31e). Kyanite plates are about 160 µm in length. They are the smallest kyanite crystals observed in the Norwegian kyanite quartzite deposits. The crystals contain common quartz inclusions (Fig. 31f).

4.4 Nasafjell, Mo i Rana

The Nasafjell kyanite quartzite contains about 30 wt.% kyanite, 60 wt.% quartz and up to 10 wt.% muscovite (Dahl 1980). The kyanite-rich spot check sample JW0135c contains 76.3 wt.% SiO_2 and 20.8 wt.% Al_2O_3. Concentrations of Ba are 285 ppm, of Zr 221 ppm and Sr 69 ppm (Table 6). Accessory minerals are pyrite, barite, rutile, zircon, REE-rich (Ce) aluminium-phosphates (no monazite) and strontium-bearing minerals. The average crystal size of quartz is 0.578 mm (200 measurements). This is the largest average crystal size determined in the investigated kyanite quartzites. The quartz shows two maxima in the crystal size distribution plot; at 0.15 mm and 0.9 mm (Fig. 21). 51.5 % of the quartz crystals are ≥0.5 mm. In quartz-rich layers quartz forms clear crystals with sutured grain boundaries (Figs. 33a, b). In kyanite-rich layers quartz is more fine-grained (Figs. 33c, d). Impurities and accessory minerals are preferentially enriched along intragranular microcracks and grain boundaries (Fig. 33e). The kyanite forms euhdral clear crystals which contain commonly rutile inclusions (Fig. 33f). In the CL image quartz crystals of the Nasafjell deposit shows a rather homogenous CL (Fig. 34a). Tongues along the margin of large crystals have lower CL intensity due to quartz recrystallisation by grain boundary migration (Fig. 34b). The recrystallised quartz domains of kyanite-rich layers contain common zircon inclusions causing CL-active radiation halos in the host quartz (Fig. 34b). Kyanite forms clear crystals with an average length of 800 µm and width of 160 µm (Fig. 34d). Pyrite crystals up to 1 cm in size are common. Occasionally they contain zircons (Figs. 34e, f).

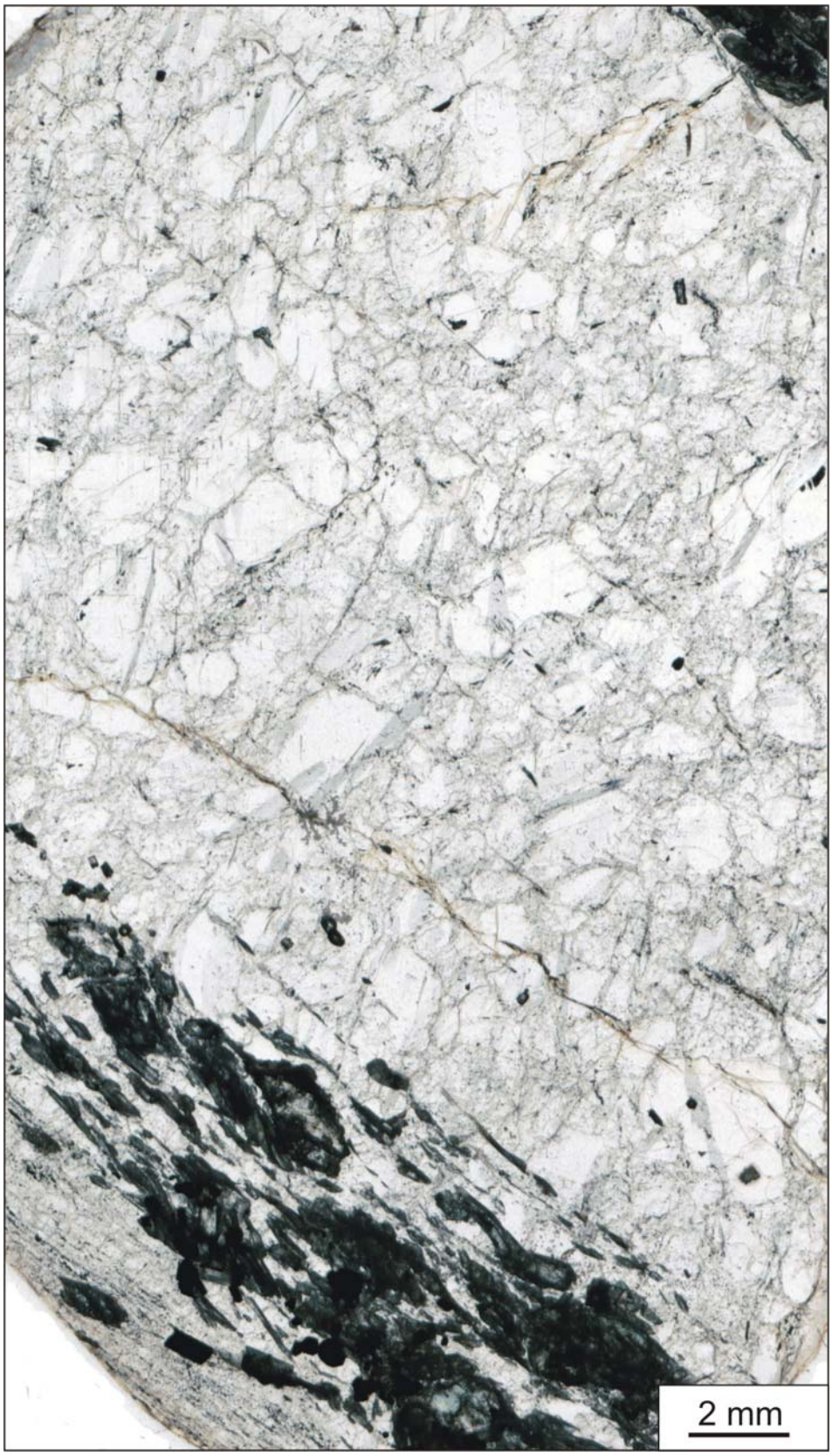

Figure 32. *500 µm-thin section scan of a quartz layer in the Nasafjell kyanite quartzite. Black – kyanite, white – quartz.*

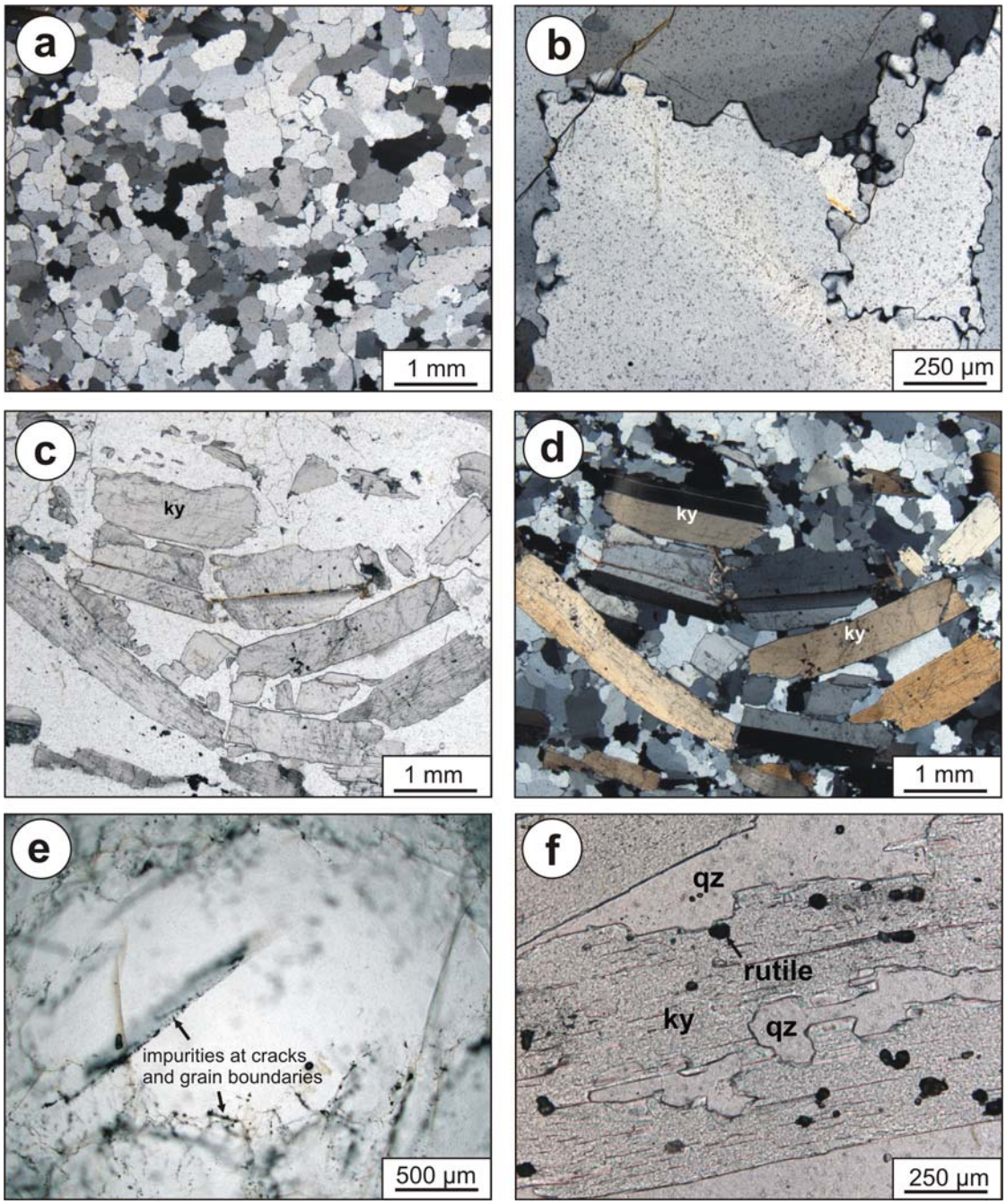

Figure 33. *Optical microscopy images of kyanite quartzites from the Nasafjell deposits. a – Quartz fabric consisting of isometric quartz grains with sutured grain bounadries. Crossed nicols. b – Sutured grain boundaries of quartz. Plane light. c - Large euhdral kyanite crystals (brownish grey) in a kyanite-rich layer. Plane light. d – Same section as (c). Crossed nicols. e – Large, clear and elongated quartz crystals in a quartz-rich layer. Crossed nicols. e – Enrichment of impurities and accessory minerals along intragranular cracks and grain bounadries. Plane light. f – Clear kyanite crystal with rutile inclusions. ky – kyanite, qz – quartz. Plane light.*

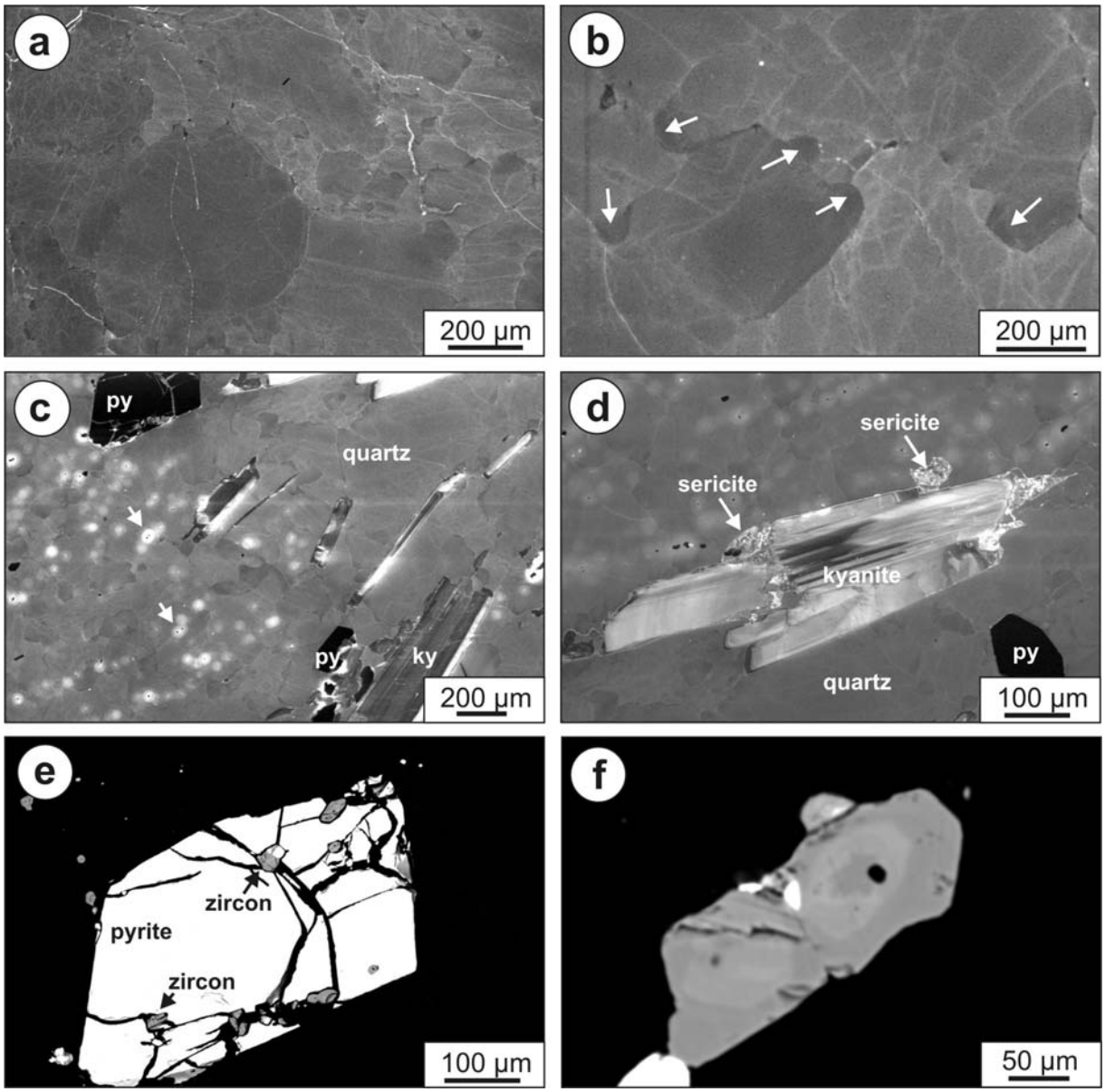

Figure 34. *Scanning electron microscopy cathodoluminescence (SEM-CL) and backscattered electron (BSE) images of kyanite quartzites from the Nasafjell deposits. a – SEM-CL image of quartz with dull and homogenous CL. b – SEM-CL image of quartz. Tongues along the margin of large crystals (arrows) have lower CL intensity due to quartz recrystallisation by grain boundary migration. c –SEM-CL image of quartz within a kyanite-rich layer. Quartz shows CL-active radiation halos around small zircon inclusions. ky – kyanite, py – pyrite. d – SEM-CL image of a zoned kyanite. py - pyrite. e – BSE image of a pyrite crystal (white) embedded in quartz (black). The pyrite contains a number of zircon inclusions. f – BSE image of zircon in quartz.*

5. Trace elements in quartz of Norwegian kyanite quartzites

Trace element concentrations of quartz from kyanite quartzites and regional related quartzite (Folldalen) determined by LA-ICP-MS are listed in Table 7. Concentrations marked in yellow are considered as "high purity quartz" with Al <25 ppm and Ti <10 ppm. Al and Ti are commonly the most frequent trace elements in quartz and they reflect the general trace element abundance of quartz. Li^+, Na^+, K^+ and H^+ are interstitial charge compensators of substitutional incorporated Al^{3+}. P^{5+} entered the quartz lattice according to the berlinite substitution $P^{5+} + Al^{3+} = Si^{4+} + Si^{4+}$ (Maschmeyer and Lehmann 1983). Therefore, low concentrations of Al cause low concentrations of Li, Na, K, H and P in the quartz lattice. Fig. 35 shows element plots of quartz from kyanite quartzites and of quartz products of Norwegian and foreign companies.

The distinction of "high purity quartz" from quartz with lower purity bases on concentrations of trace elements in "high purity quartz products" which are sold worldwide (Table 8). Norwegian Crystallites AS mines high quality pegmatite quartz at Drag in the Tysfjord, northern Norway. The reference sample "Drag" where analysed at NGU by LA-ICP-MS and concentrations of the quartz products "Drag NC1 100-300 µm" and "Drag NCA 100-300 µm" are given by Norwegian Crystallites AS (Norwegian Crystallites AS 2005). Iota STD and Iota 8 are a refined quartz products of the company IOTA® which is one of the world-leading producers of high purity quartz (IOTA® 2005). For comparison analysis, done by LA-ICP-MS at NGU, of the quartz product of North Cape Minerals AS from Glamsland pegmatite deposits in southern Norway is given. The Glamsland quartz product is not considered as "high purity quartz".

The relative large ablation volume of the LA-ICP-MS (180 x 250 x 40 µm) during sampling involves the risk that fluid and mineral inclusions in quartz "contaminate" the concentrations of trace elements which are incorporated in the quartz lattice. The quartz of kyanite quartzites is almost free of fluid inclusions but contains common micro inclusions of minerals, such as rutile, pyrite and apatite.

5.1. Solør

Most of the concentrations of trace elements in quartz from the Solør kyanite quartzites lie in the "high purity quartz" field. Al varies from 10.9 to 32.8 ppm (average 19.8 ppm) and Ti from <0.09 to 31.3 ppm (average 5.2 ppm). Quartz from the Knøsberget and Sormbrua deposits has remarkably low Ti concentrations. Li, Be, B, Mn, Ge, K, Ca and Fe are generally below the limit of detection. Outstanding concentrations of Ti, Al and Fe of analyses 2907406-A and 2907404-A, respectively, are probably caused by mineral micro inclusion in quartz.

The quartz of the Swedish Halsjöberget kyanite quartzites has much higher Al and Ti. Quartz of the Halsjöberget sample has a smoky colour which indicates a relative high Al content because the smoky colour of quartz is caused by Al-defects which were exposed to natural radioactive radiation. The K concentration is also relative high. The relative closely situated kyanite quartzite deposits of Solør and Halsjöberget show large variations of trace element concentrations in quartz. Therefore, the low concentrations of quartz observed in the Solør kyanite quartzites is not a universal feature of kyanite quartzites.

Table 7. *Laser ablation ICP-MS analyses of trace elements in quartz from kyanite quartzites and associated quartzites and metaarkoses. Concentrations are in ppm. Concentrations marked in yellow are considered as high purity quartz (Al <25 ppm and Ti <10 ppm).*

locality	sample#	Li	Be	B	Mn	Ge	Na	Al	P	K	Ca	Ti	Fe
Gullsteinberget	2907411-A	<1	<2	3.0	<0.3	<0.5	<100	21.5	<5	<3	<60	7.4	<2
	2907411-B	<1	<2	<3	<0.3	<0.5	<100	31.1	<5	<3	<60	16.0	<2
	2907411-C	<1	<2	<3	<0.3	<0.5	<100	22.7	<5	<3	<60	5.2	<2
Knøsberget	2907408-A	<1	<2	<3	<0.3	<0.5	<100	20.4	<5	<3	<60	0.3	<2
	2907408-B	<1	<2	3.6	0.4	<0.5	<100	15.9	<5	<3	<60	0.2	<2
	2907408-C	<1	<2	<3	<0.3	<0.5	<100	20.9	<5	<3	72	3.8	<2
Kjeksberget	2907404-A	<1	<2	<3	<0.3	<0.5	<100	28.5	<5	<3	<60	6.0	18.8
	2907404-B	<1	<2	<3	<0.3	<0.5	<100	16.6	<5	<3	<60	2.5	<2
	2907404-C	<1	<2	<3	<0.3	<0.5	<100	18.1	<5	<3	<60	0.2	<2
Sormbrua	2907406-A	<1	<2	<3	<0.3	<0.5	<100	32.8	<5	11.7	<60	31.3	<2
	2907406-B	<1	<2	<3	0.36	<0.5	<100	12.6	<5	<3	<60	0.1	<2
	2907406-C	<1	<2	<3	<0.3	<0.5	<100	16.2	<5	<3	<60	4.0	4.8
	2907407-A	<1	<2	<3	<0.3	<0.5	<100	10.9	<5	<3	<60	<0.09	<2
	2907407-B	<1	<2	<3	<0.3	<0.5	<100	11.6	<5	<3	<60	<0.09	<2
	2907407-C	1.0	<2	<3	0.3	<0.5	<100	16.8	<5	<3	<60	<0.09	<2
Halsjöberget	3107401-A	<1	<2	<3	<0.3	<0.5	<100	97.7	<5	30.5	<60	7.5	8.8
	3107401-B	<1	<2	<3	<0.3	0.6	<100	968.0	<5	282.5	<60	19.2	87.8
	3107401-C	<1	<2	<3	<0.3	<0.5	<100	48.2	<5	12.6	<60	107.0	5.3
Tverrådalen	1907401-A	<1	<0.4	<1	<0.1	0.4	<20	14.0	<5	<0.2	<15	8.0	<0.4
	1907401-B	<1	<0.4	<1	<0.1	0.5	<20	18.5	<5	<0.2	<15	10.3	0.4
	1907401-C	<1	<0.4	<1	<0.1	0.4	<20	13.9	<5	0.49	<15	13.6	<0.4
Folldalen	2007410-A	2.4	<0.4	<1	<0.1	0.7	<20	13.5	<5	<0.2	<15	4.3	<0.4
	2007410-B	1.9	<0.4	<1	<0.1	0.8	<20	15.0	<5	<0.2	<15	4.9	<0.4
	2007410-C	<1	<0.4	<1	<0.1	0.6	<20	13.1	<5	0.57	<15	4.8	<0.4
Juovvačorrú	R1021B-A	<2	1.1	<6	2.4	0.8	<400	5.3	<13	<10	<70	6.1	<1
	R1021B-B	<2	<0.1	<6	<0.8	<0.7	<400	6.2	<13	<10	<70	2.9	<1
	R1021B-C	<2	0.1	<6	1.0	<0.7	<400	12.0	<13	<10	<70	0.2	<1
	R1021B-D	2.4	0.1	<6	<0.8	0.8	<400	12.8	<13	<10	<70	5.8	<1
	R1021B-E	<2	<0.1	<6	<0.8	0.8	<400	12.0	<13	<10	<70	0.2	<1
	R1021B-F	<2	0.1	<6	<0.8	1.0	<400	14.6	<13	<10	<70	2.4	<1
Nasafjell	JW02-61*	0.5	n.d.	<1.0	n.d.	n.d.	<1.0	9.2	n.d.	<1.0	n.d.	2.1	<0.5
	JW03-15A-1*	<0.5	n.d.	0.6	n.d.	n.d.	<1.0	16.8	n.d.	0.6	11.6	2.5	<0.5
	JW03-15B-1*	<0.5	n.d.	0.2	n.d.	n.d.	<1.0	<5.0	n.d.	0.2	<5.0	2.3	<0.5
	JW03-15C-1*	<0.5	n.d.	0.6	n.d.	n.d.	6.1	17.7	n.d.	0.6	<5.0	3.0	<0.5
	JW03-15A-2**	<0.5	n.d.	0.4	n.d.	n.d.	6.4	20.4	n.d.	0.4	<5.0	3.2	1.0
	JW03-15B-2**	<0.5	n.d.	0.5	n.d.	n.d.	5.6	14.8	n.d.	0.5	<5.0	3.7	5.2
	JW03-15C-2**	<0.5	n.d.	0.5	n.d.	n.d.	<1.0	14.5	n.d.	0.5	22	2.2	6.6
Rio Levele	MOZAM1-A	<1	<2	<3	<0.3	<0.5	<100	34.9	<5	<3	<60	6.8	<2
	MOZAM1-B	<1	<2	<3	<0.3	0.6	<100	52.7	<5	<3	<60	9.6	<2
	MOZAM1-C	<1	<2	<3	<0.3	<0.5	<100	37.3	<5	<3	<60	6.8	<2

* data from Wanvik (2004). Quartz without inclusions.
** data from Wanvik (2004). Quartz with inclusions.
n.d. – not determined.

Table 8. *Concentrations of trace elements in quartz products of Norwegian and foreign companies. Products "Drag" and "Glamsland" were analysed by LA-ICP-MS at NGU. Concentration for P in the Glamsland sample is set in brackets due to the poor accuracy (see method chapter 2.4).*

	Li	Al	Ti	Fe	Na	K	P	B	Ca
Drag	6.0	24.3	5.1	<0.5	1.3	<0.8		0.8	3.5
Drag NC1*	4.0	26.0	4.0	0.5	2.7	0.7		<0.4	0.6
Drag NCA*	0.7	7.0	4.0	0.1	0.7	0.3			0.1
Iota STD**	0.9	16	1.3	0.2	0.9	0.6	0.1	0.08	0.5
Iota 8**	<0.02	7.0	1.2	<0.03	0.03		0.05	<0.04	
Glamsland	8.3	44.1	6.0	<2.6	<50.0		(14.1)	<2.0	

* Norwegian Crystallites AS (2005)
** IOTA® (2005)

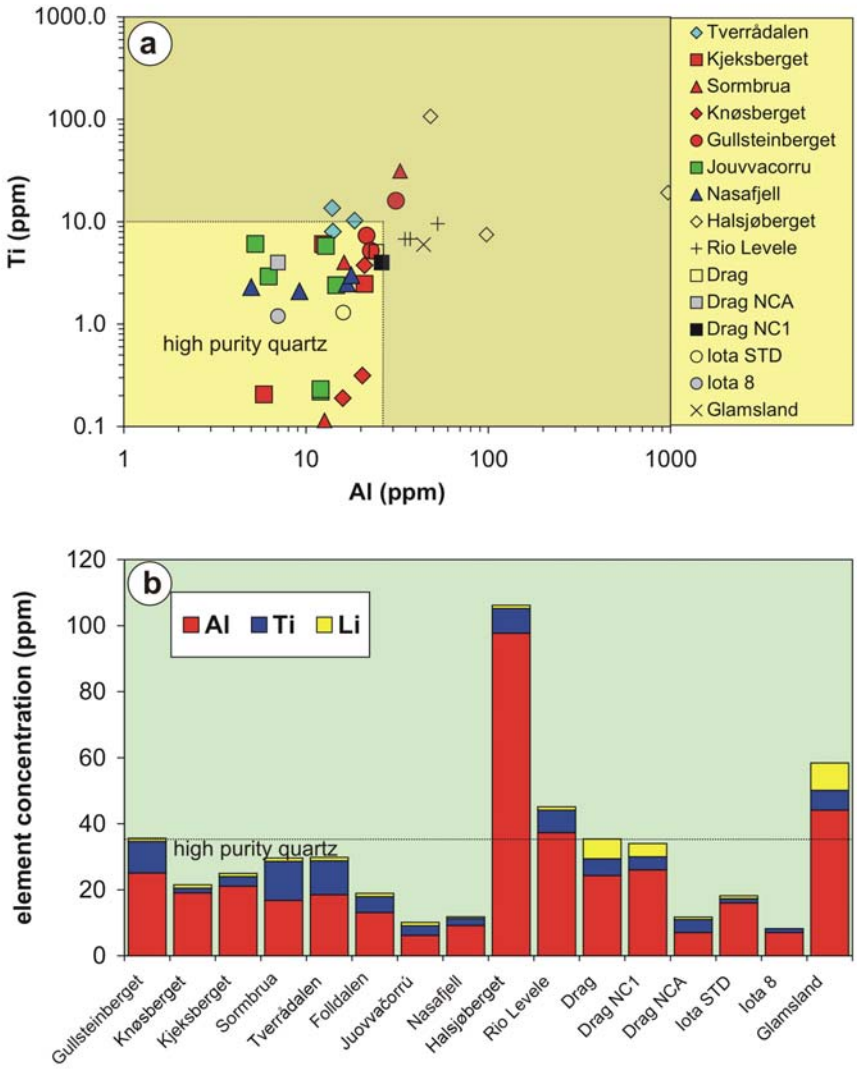

Figure 35. *a – Al versus Ti plot of quartz in kyanite quartzites from Norway (coloured symbols), Sweden (Halsjöberget) and Mozambique (Rio Levele) and of high purity quartz products (Drag, Drag NCA, Drag NC1, Iota STD, Iota 8). "Glamsland" is the quartz product of North Cape Minerals AS. Quartz with Al <25 ppm and Ti <10 ppm is considered as "high purity quartz". b – Stacked column diagram of Al, Ti and Li in quartz of kyanite quartzites and quartz products. "Folldalen" is kyanite-bearing metaarkose near to the Tverrådalen kyanite quartzite. For further explanation of sample names see (a).*

5.2. Tverrådalen, Surnadal

Quartz of the Tverrådalen deposit has higher average Ti of 10.6 ppm compared to quartz of the other Norwegian kyanite quartzites and, therefore lies at the boundary of the "high purity quartz" field (Fig. 35a). Al varies between 14.0 and 18.5 ppm. Li, Be, B, Mn, K, Ca and Fe are generally below the limit of detection. The average Ge concentration is 0.43 ppm.

The quartz of regional related kyanite-bearing metaarkose of Folldalen has also remarkable low trace element concentrations. The average of Al amounts 13.9 ppm and of Ti 4.7 ppm.

5.3. Juovvačorrú, Skjomen

Quartz from the Juovvačorrú deposit exhibits the lowest average concentration of Al with 10.5 ppm and of Ti with 2.9 ppm. Concentrations of Ge and Be are about 0.8 and 0.1 ppm, repectively. Li, B, Mn, K, Ca and Fe are generally below the limit of detection. The quartz of the Juovvačorrú kyanite quartzite is the purest among the Norwegian kyanite quartzite deposits.

5.4. Nasafjell, Mo I Rana

Quartz from the Nasafjell deposits is one the purest Norwegian kyanite quartzites which gave originally the reason for this study. Average concentrations for Al and Ti are 12.2 and 2.5 ppm, respectively, for inclusion free quartz (Wanvik 2004). Li and Fe are below 0.5 ppm and B below 1 ppm. Wanvik (2004) could achieve much lower detection limits for N, K and Ca (1, 1 and 5 ppm) with the LA-ICP-MS. Ranges of concentrations are for Na <1.0 to 6.1 ppm, K <1.0 to 1.8 ppm and Ca <5.0 to 11.6 ppm (inclusion-free quartz). Wanvik (2004) analysed also quartz containing micro inclusions of minerals and fluids. The average concentrations 16.6 ppm Al and 3.0 ppm Ti are only somewhat higher than of clear quartz.

5.5. Rio Levele, Mozambique

The average concentration of Al and Ti in quartz of the kyanite quartzite from Rio Levele amounts 41.6 and 7.7 ppm, respectively. Due to the relative high Al concentration it cannot be considered as a "high purity quartz". Li, Be, B, Mn, Ge, K, Ca and Fe are below the limit of detection. The example shows again, that low trace element concentrations are not a universal feature of quartz in kyanite quartzites.

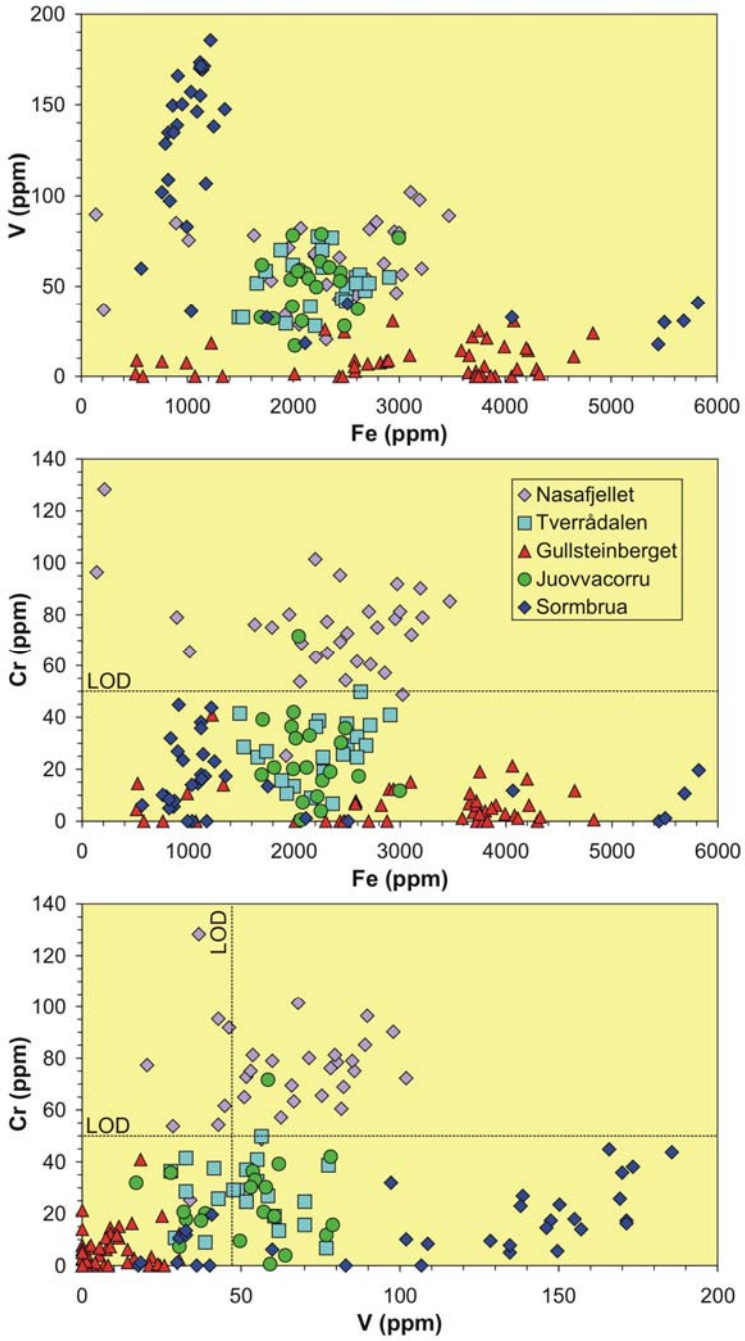

Figure 36. *Fe, V and Cr concentrations in kyanite from Norwegian kyanite quartzite deposits.*

6. Chemistry of kyanite

Major and trace elements of kyanite from Gullsteinberget, Sormbrua, Tverrådalen, Juovvačorrú and Nasafjell were analysed by electron micro probe at the Geowissenschaftliches Zentrum Göttingen, Germany. Concentrations are listed in Appendix B. Concentrations of Fe, V and Cr are generally above the limit of detection.These three trace elements may be indicative for the kyanite quartzite origin. Element plots in Fig. 36 reveal a great variation of Fe, V and Cr concentration. The Nasafjell and Juovvačorrú kyanite have a similar trace element signature. Fe varies between 1487 and 2997 ppm, V between 17 and 79

ppm and Cr between 0 and 72 ppm. Kyanite from Nasafjellet is enriched in Cr. The average Cr content is 75 ppm which is three times higher than for the other kyanites. The kyanites from Solør, Gullsteinberget and Sormbrua, have high Fe in the crystal cores up to 5820 ppm and low Fe in the crystal margin (511 to 1354 ppm; Fig. 37). The Fe-poor margin of the Sormbrua kyanite shows high average V (139 ppm) whereas the core is depleted in V (31 ppm). In the cathodoluminescence image the kyanites from Sormbrua are zoned (Fig. 37).

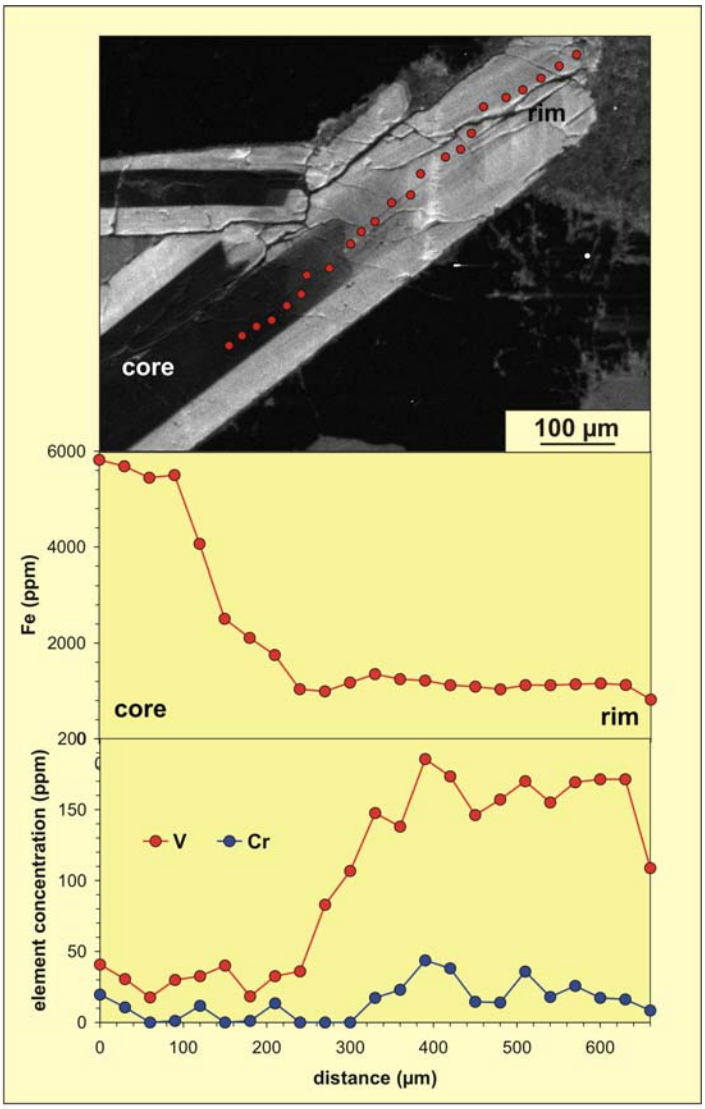

Figure 37. *Concentration profile of Fe, V and Cr across a kyanite crystal from Sormbrua measured by electron micro probe. The euhdral crystal zoning in the SEM-CL image is probably caused by variations of the Cr content, because Cr^{3+} is luminescence activator.*

7. Origin of kyanite quartzites

Knowledge about the origin and the evolution of kyanite quartzites is essential to understand the processes generating low concentrations of trace elements in quartz of Norwegian kyanite quartzites. Kyanite quartzites exhibit a number of features which distinguish them from “ordinary” quartzites originating from sandstone and arkose:

1) Kyanite quartzites form rare lens-shaped bodies from meter-scale up to a length of several kilometers and a thickness of several hundred meters
2) Kyanite quartzites are hosted in supracrustal units of greenschist facies.
3) Kyanite quartzites are commonly associated with metamorphosed acidic and intermediate volcanic and subvolcanic rocks or with mafic volcanites and intrusives of island arc setting (e.g. McCauley 1961, Nystuen 1968b, Spence et al. 1980, Bibikova et al. 2001).
4) Kyanite quartzite does not contain feldspar.
5) Common accessories in kyanite quartzites are rutile, zircon, pyrite and other Fe-Ti-bearing oxides and sulfides. Sporadic accessories are topaz, fluorite, titanite, lazulite, apatite, Cr-mica and gold (e.g., Spence et al. 1980).

A number of models regarding the formation of kyanite quartzites, have been presented over the last 60-70 years to explain the often stratabound, but also discordant, nature of the kyanite quartzite units, occurring commonly within meta-volcanic sequences and immediately overlying meta-sedimentary rocks. The rare mineral assemblages, e.g. Al-phosphate minerals and Cr-mica, and very low contents of prograde metamorphic potassium silicates are additional characteristic features of the kyanite quartzites. Ek and Nysten (1990) and Ihlen (2000) gave reviews of discussions and distinguished three general models for the development of kyanite quartzites as illustrated in Figure 38:

(1) Pre-metamorphic advanced argillic alteration zones in felsic and intermediate volcanites and subvolcanic intrusions of island arc settings. A number of authors have concluded that the kyanite quartzites developed from pre-metamorphic hydrothermal alteration of volcanic rocks in conjunction with hot-spring activity (e.g., Espenshade and Potter 1960, Schreyer 1987, Hora 1998, Owens and Dickerson 2001, Pasek and Owens 2002). This activity is caused by fluid convection above hot granitic magma bodies giving off acid volatiles during degassing and resurgent boiling. They have generally an island arc setting, some situated below sea-floor exhalation centres (1a in Fig. 38; Valliant et al. 1983, Willner et al. 1990, Bibikova et al. 2001, Greiner 2003), others below sub-aerial hot-springs within geothermal systems (1b in Fig. 38; Spence 1975, Spence et al. 1980, Schmidt 1985, Ek and Nysten 1990, Larsson 2001) or above porphyry-style intrusions (1c in Fig. 38). These authors agree that the alteration occurred in response to strong acid leaching of volcanic and sub-volcanic rocks, leading to the development of zones with advanced argillic alteration composed dominantly of quartz, Al-silicates (clays) and subordinate Al-hydroxides (gibbsite). The advanced argillic alteration grades upwards into pervasively silicified rocks, frequently with an overlying silica-capping at surface/seafloor and downwards into more potassium-rich argillic alteration with quartz, sericite, kaolinite and/or adularia (Spence 1975). During metamorphism clay minerals like halloysite, dickite and kaolinite break down to quartz and kyanite, andalusite or sillimanite, dependent on prevailing metamorphic grade (Fig. 39).

(2) Metamorphism of high-alumina sediments. Willner et al. (1990) and Schreyer (1987) suggests that kyanite quartzites originate from metamorphosed aluminous clays and quartz sand which are weathering products of altered subvolcanic and volcanic rocks (1c and 2 in Fig. 38). The Al-rich siliceous sediments were redistributed and deposited in basins were further Al-enrichment occurred due to hydrothermal activity of adjacent volcanic centres. A number of the fine-grained kyanite quartzite deposits in the Applachian belt (Horton 1981, 1989), including the largest and most productive kyanite deposits in the world,

appear to be of this type. They form persistent stratigraphical units locally with relicts of sedimentary structures like quartz conglomerates cemented by kyanite quartzites which are in strong support of a sedimentary origin. However, these water-lain sediments represent most probably short-range transport into adjacent basins, since no separation of clay minerals and silica appears to have occurred. Some authors advocate modification of aluminous sediments by emanating hydrothermal fluids in areas of igneous activity (Geijer 1963, Wise 1977) or by metasomatic fluids during regional metamorphism (Corey 1960, Schreyer and Chinner 1966, Gresens 1972, Flicoteaux and Lucas 1984, Liu and Hu 1999)

(3) *Structurally controlled syn-metamorphic metasomatism.* The close proximity of some kyanite quartzites to faults and shears in metamorphic terrains have lead to models advocating shear-induced syn-metamorphic metasomatism of quartzofeltspatic rocks (3 in Fig. 38; Banerji 1981, Andréasson and Dallmeyer 1995, Ihlen and Marker 1998). Andréasson and Dallmeyer (1995) made a well-founded model for the kyanite-rich metasomatic rocks along the Protogine Zone in southern Sweden, which they concluded were formed by shear-induced fluid migration and acid leaching of Palaeoproterozoic supracrustal sequences and granites. Such a model is supported by the invariable presence of syn-metamorphic, hydrothermal veins and segregations of kyanite and sillimanite in the deposits (Espenshade and Potter 1960, de Jager and von Backström 1961, Schreyer 1987, Lundegårdh 1995, Ihlen et al. 1993, Ihlen and Marker 1998).

The three models of kyanite quartzite formation explain in different ways the strong enrichment of alumina and silica in the protoliths and the depletion of alkalis which makes the source rocks and their metamorphic products unique in a chemical sense. However, the distinction between the three models based on field evidence is difficult, because both pre-metamorphic syn-volcanic and syn-metamorphic shear-induced metasomatism occur along fault zones, potentially giving rise to the assumption that are bedding parallel sedimentary bodies.

Most of the Norwegian kyanite quartzites are associated with volcanites. The Juovvačorrú deposits are hosted in the volcanic suite of the Sørdalen Supracrustal Belt (Korneliussen and Sawyer 1989) and the Solør kyanite quartzites occur about 12 km south of Proterozoic ash-flow tuffs and associated volcanic rocks (Nystuen 1969b). However, amphibolites and metagabbros (hyperites) are also commonly associated with the Norwegian kyanite quartzites. Some of the Norwegian kyanite quartzites are associated with major shear zones, e.g. the Nasafjell kyanite quartzites. Therefore, the models 1 and 3 are most likely processes of the formation of Norwegian kyanite quartzites. This implies that the quartz in the protolith was hydrothermal in origin. This is important to note, because hydrothermal quartz has low Ti concentration (<20 ppm; e.g. Schrön et al. 1982, Müller et al. 2003) but it can contain up to several thousands ppm of Al (Mullis and Ramseyer 1999, Müller 2000). However, Al and its interstitial charge compensators Li^+, K^+, Na^+ and H^+ can be removed from the quartz lattice during metamorphism >350ºC and >1.5 kbar whereas structural Ti in quartz is mostly kept in the lattice (Müller et al. 2002). The *P-T* conditions affecting the kyanite quartzite during metamorphism are not sufficient enough to sweep out structural bound Ti from the quartz lattice. Therefore, the low Ti in the protolith is an important prerequisite for the general low trace element concentration in quartz of kyanite quartzites. The contrasting trace element signatures of kyanite suggest that the Nasafjell deposit were derived from a hydrothermal altered mafic protolith, whereas the protoliths of the Solør, Tverrådalen and Juovvačorrú deposits were more evolved.

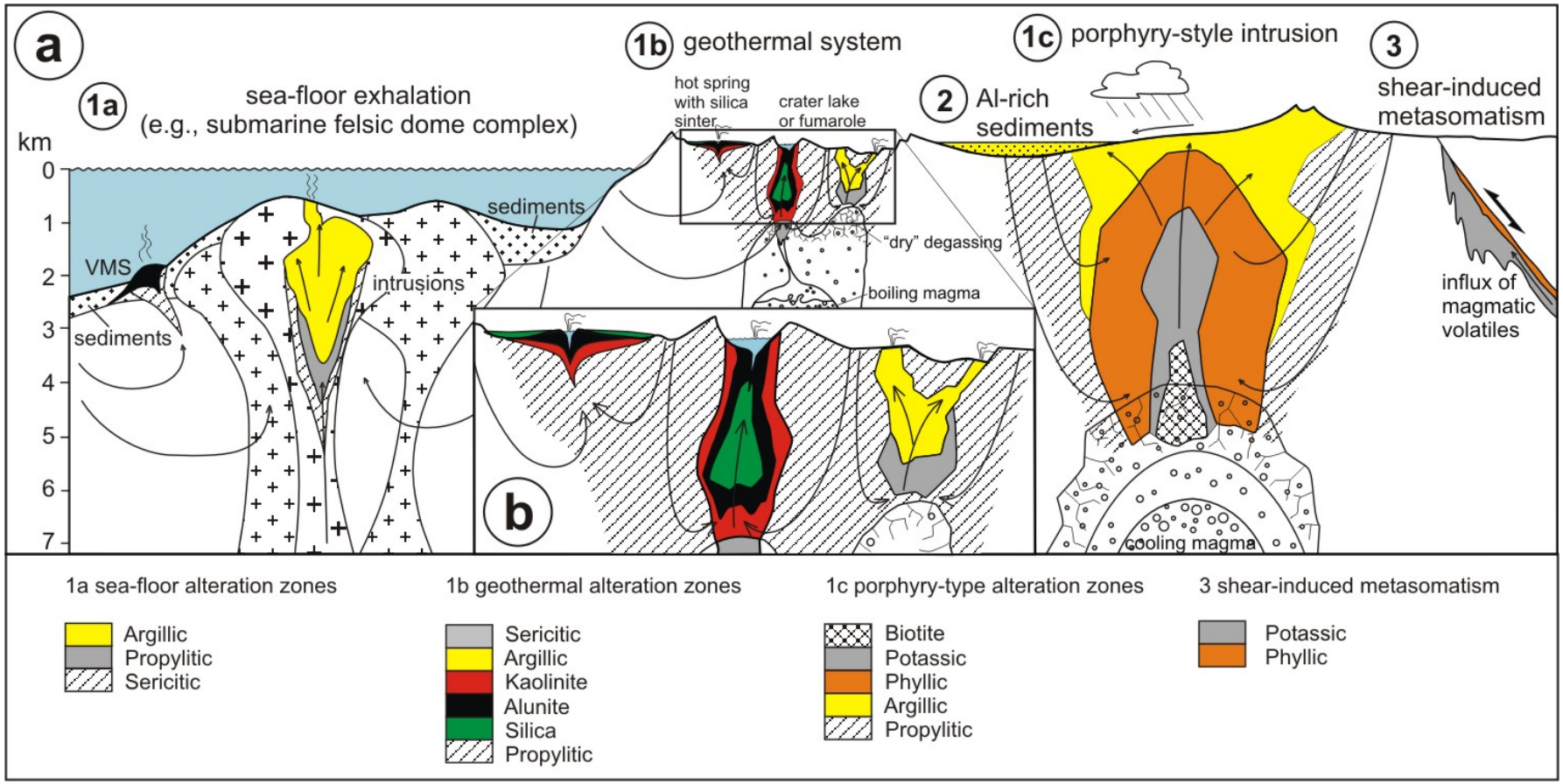

Figure 38. *a - Possible scenarios of the origin of high-Al silica rocks which result in kyanite quartzites after regional metamorphism: 1a –sea-floor Kuroko-type smoker system, 1b - hot spring geothermal system, 1c – porphyry-style alterations and 2 – Al- and silica-rich sediments which are the weathering product of acid-leaching alteration zones, 3 – shear-induced metasomatism of aluminous rock whereby acid magmatic or metamorphic fluids migrate along major shear zones. The Jiaojia-type Au-deposits in Jiaodong, China (Qiu et al. 2002), are an examples of the magmatic style. The argillic, kaoliniti, phyllic and silicic altered rocks and their weathering products (Al- and silica-rich sediments) are considered as protoliths of kyanite quartzites. Modified and compiled after Giggenbach (1992) and Sillitoe et al. (1996). b – Inset showing the enlargement of the caldera-related geothermal system (2b) with different styles of alteration zones modified after Giggenbach (1992).*

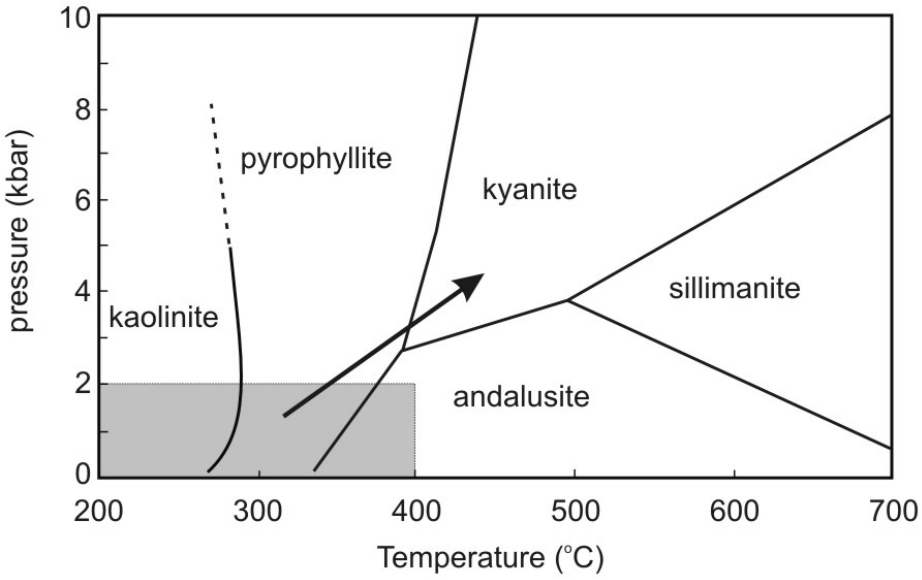

Figure 39. *Stability field of aluminosilicates expected to occur in acid-leached rocks, their sedimentary products and their metamorphic equivalents. Shaded area represents the approximate P-T interval in which argillic alteration take place. The arrow indicates the general P-T path of kyanite quartzites.*

8. Summary and Outlook

The study of trace element concentrations in quartz of the kyanite quartzite from Gullsteinberget, Knøsberget, Kjeksberget, Sormbrua, Tverrådalen, Juovvačorrú and Nasafjell deposits in Norway reveals that the trace element concentrations in quartz are low. Quartz, which forms 70 – 85 vol.% of these rocks, contains 5 – 30 ppm Al, 0.2 – 16 ppm Ti, <1 ppm Li, <1 ppm B and <2 ppm Fe. Concentrations were determined by LA-ICP-MS. Due to the low trace element concentrations, the quartz in the investigated kyanite quartzites can be considered as "high purity quartz" (Al <25 ppm and Ti <10 ppm). The concentrations are in the same range of concentrations of high purity quartz products, which are mined and produced in Norway (e.g., products "Drag NC1" and "Drag NCA" of Norwegian Crystallites AS) and elsewhere.

Taking the three models of kyanite quartzite formation in account four individual and fundamental processes are involved in the formation of high purity quartz and their host rocks, the kyanite quartzites:

Process 1: Fluid-induced recrystallisation of magmatic quartz during hydrothermal alteration of quartzofeldspatic protoliths.

Process 2: Precipitaton of hydrothermal quartz during the alteration of the protoliths (argillisation, silicification, fine-grained silica sinters with chalcedon, etc.).

Process 3: Precipitation of diagenetic quartz during lithification of alumina-rich siliceous sediments.

Process 4: Recrystallisation and redistribution of quartz during prograde regional metamorphism (rotation recrystallisation, grain boundary migration, mobilisation into fractures, etc.) at: (a) anhydrous, dry conditions or (b) hydrous conditions at sites affected by structurally bound migration of metamorphic fluids.

The relative importance of the individual processes listed above in the formation of high purity quartz is at present only vaguely known.

Advantages of Norwegian kyanite quartzite deposits from the economic perspective are:

1) Low concentrations of trace elements in quartz
2) Quartz is almost free of fluid inclusions
3) Straight and planar grain boundaries of quartz in the Skjomen, Solør and Nasafjell deposits reducing the energy consumption during rock crushing and lessens the intergrowth problem in grain liberation
4) Size and exposure of kyanite quartzite bodies allows open pit mining in the Skjomen, Solør and Nasafjell area. The largest deposit is the Gullsteinberget kyanite quartzite in Solør where more than 30 mill. ton of kyanite quartzite are available assuming a open pit depth of 40 m.
5) Quartz and kyanite can be separated after rock crushing by flotation because of their density contrast. Quartz has a density of 2.62 $g \cdot cm^{-1}$ and kyanite of 3.61 $g \cdot cm^{-1}$. Kyanite separates can be used for alumina production
6) Kyanite quartzites with high kyanite content (Gullsteinberget) and with lazulite (Sormbrua) are possibly attractive dimension stones. The Halsjöberg kyanite quartzite in Värmland, Sweden, was temporarily used as dimension stone, known as "Caribbean Blue" (trade name), due to its bluish, greenish and turquoise colouration.

Disadvantages from the economic perspective are:

1) Intergrowths of quartz with kyanite and mica.
2) The heterogeneous distribution of kyanite and mica in the rock (cm- to m-scale layering)
3) The small average crystal size of quartz (100 – 600 µm).
4) Former trace elements of the quartz lattice are enriched at the grain boundaries
5) Common mineral micro inclusions in quartz of rutile, apatite, zircon, titanite, pyrite, and other Fe-Ti oxides and sulfides.
6) The cleavage of the rock makes it difficult to produce large blocks for dimension stone

Taken all advantages and disadvantages of the investigated Norwegian kyanite quartzites in account, these kyanite quartzites can be considered as potential resources of high purity quartz. The quartz is suitable for high purity silica glass and silicon production for the high tech industry. The most attractive deposits from the economic view is the Gullsteinberget deposit in Solør. However, this pilot study provides only a few preliminary results of spot checks. For resource evaluation a much more extensive study of the Norwegian kyanite quartzites has to be carried out.

References

Andréasson, P.G. and Dallmeyer, R.D. 1995. Tectonothermal evolution of high-alumina rocks within the Protogin Zone, southern Sweden. Journal of Metamorphic Geology 13: 461-474.

Banerji, A.K. 1981. On the genesis of Lapsa Buru kyanite, Singhbhum District, Bihar. Journal Geological Society of India 22: 496-501.

Bibikova, E.V., Ihlen, P.M., Marker, M. 2001. Age of the hydrothermal alteration leading to garnetite and kyanite pseudo-quartzite formation in the Khizovaara segment of the late Archean Keret Greenstone Belt, Russian Karelia. EUG XI Strassbourg, 8.-12.4.2001, Journal of Conference Abstracts 6: p. 277.

Corey, A.F. 1960. Kyanite occurrences in the Petaca district, Rio Arriba County, New Mexico. New Mexico Institute of Mining and Technology, State Bureau of Mines and Mineral Ressources Bulletin 47.

Dahl, Ø. 1980. Nasa og Stødi kyanitfelter – resultater fra diamantboring og geologiske undersøkelser sommeren 1980. Aspro rapport 1115. Bergvesenrapport BV 3506.

de Jager, D.H., von Backström, J.W. 1961. The sillimanite deposits in Namaqualand near Pofadder. Geological Survey of South Africa Bulletin 33: 49 pp.

Ek, R., Nysten, P. 1990. Phosphate mineralogy of the Hålsjöberg and Hökensås kyanite deposits. Geologiska Föreningens i Stockholm GFF 112: 9-18.

Espenshade, G.H., Potter, D.B. 1960. Kyanite, sillimanite, and andalusite deposits of the Southeastern States. United States Geological Survey Professional Paper 336: 1-121.

Flem, B., Larsen, R.B., Grimstvedt, A., Mansfeld, J. 2002. In situ analysis of trace elements in quartz by using laser ablation inductively coupled plasma mass spectrometry. Chemical Geology 182: 237-247.

Flicoteaux, R. and Lucas, J. 1984. Weathering of phosphate minerals. In: Nriagu, J.O. and Moore, P.B. (eds.). Phosphate minerals. p. 292-317.

Frietsch, R., Perdahl, J.-A. 1987. On the nature of lower Proterozoic volcanic rocks in southern Norrbotten, northern Sweden. Proterozoic Geochemistry (Symp.), IGCP 217, Lund, (Abstr.), p. 35.

Geijer, P. 1963. Genetic relationships of the paragnesis Al_2O_3-SiO_2-lazulite-rutile. Arkiv för Mineralogi och Geologi 3: 423-464.

Giggenbach, W. F. 1992. SEG distinguished lecture: Magma degassing and mineral deposition in hydrothermal systems along convergent plate boundaries. Economic Geology 97: 1927-1944.

Gjelle, S. 1988. Geologisk kart over Norge, berggrunnskart Saltdal, M 1 : 250 000. Norges Geologiske Undersøkelse.

Götze, J., Plötze, M., Habermann, D. 2001. Origin, spectral characteristics and practical applications of the cathodoluminescence (CL) of quartz – a review. Mineralogy and Petrology 71: 225-250.

Greiner, E.M. 2003. A metallogenetic study of gold-bearing pyritic quartz-pebble conglomerates, Woodburn Lake Group, western Churchill province, Nunavut. Master's, University of Western Ontario, Canada.

Gresens, R.L. 1972. Staurolite-quartzite bands in kyanite quartzite at Big Rock, Rio Arriba County, New Mexico – a discussion. Contributions to Mineralogy and Petrology 35: 193-199.

Gunner, J.D. 1981. A reconnaissance Rb-Sr study of Precambrian rocks from the Sjangeli-Rombak Window and the pattern of initial 87Sr/86Sr ratios from northern Scandinavia. Norges Geologiske Tidskrift 61: 281-290.

Gvein, Ø., Skålvoll, H., Sverdrup, T. 1974. Geologisk kart over Norge, Berggrunnskart Torsby, M 1 : 250.000. Norges Geologiske Undersøkelse.

Heier, K., Compston, W. 1969. Interpretation of Rb-Sr age pattern in high-grade metamorphic rocks, North Norway. Norges Geologiske Tidskrift 49: 257-283.

Hora, Z.D. 1998. Industrial minerals in island arcs. In: Metallogeny of volcanic arcs. B.C. Geological Survey, Short Course Notes, Open File 1998-8, Section L. Accessed 20th May 2005. <http://www.em.gov.bc.ca/Mining/Geolsurv/MetallicMinerals/metallogeny/L98_Abstract_Hora.HTM>

Horton, Jr.W. 1981. Geological map of the Kings Mountain belt between Gaffney, South Carolina, and Lincolnton, North Carolina. In: Horton, J.W. et al. (eds.) Geological investigations of the Kings Mountain belt and adjacent areas in the Carolinas. Carolina Geological Society field trip guidebook, Columbia, S.C., South Carolina Geological Survey, p. 6-18.

Horton, Jr.W. 1989: Kyanite and sillimanite in high-alumina quartzite of the Battleground Formation, Kings Mountain belt. In: Gair, J.E. (ed.), Mineral resources of the Charlotte 1°x2° Quadrangle, North Carolina and South Carolina. United States Geological Survey Professional Paper 1462, 107-110.

Ihlen, P.M. 2000. Utilisation of sillimanite minerals, their geology, and potential occurrences in Norway – an overview. Norges Geologiske Undersøkelse Bull. 436: 113-128.

Ihlen, P.M. and Marker, M. 1998. Kyanite-rich metasomatic rocks along crustal-scale shear zones in the Baltic Shield: Evidence of shear induced fluid migration during tectonic dissection of Palaeoproterozoic supracrustal sequences? In: Phillippov, N. (ed) Abstract volume for Svekalapko Europrobe project Workshop 1998, Repino, Russia. The Ministry of Natural Resources of Russian Federation/State Company 'Mineral', 25-26.

Ihlen, P.M., Often, M., Marker, M. 1993. The geology of the Late Archean sequence at Khisovaara, Russian Karelia, and associated metasomatites: Implications for the interpretation of the Raitevarri Cu-Au deposit in the Karasjok Greenstone Belt, North Norway. In: Abstract volume for the Norwegian-Russian Collaboration Programme in the "North Area", 1st International Barents Symposium, 1993, Kirkenes, Norway. Norges geologiske undersøkelse.

IOTA® 2005. IOTA® high purity quartz. Accessed 20th May 2005. <http://www.iotaquartz.com/welcome.html>

Jakobsen, B.M., Nielsen, E. 1977. Kyanite kvartsit projektet 1976-1977. Laboratorienrapport. Endogen Laboratorium. Geol Institut Århus Universitet. p.19.

Korneliussen, A., Sawyer, E.W. 1989. The geochemistry of Lower Proterozoic mafic to felsic igneous rocks, Rombak Window, North Norway. Norges Geologiske Undersøkelse Bull. 415: 7-21.

Kyanite Mining Cooperation 2005. Kyanite Mining Cooperation – our facilities. Accessed 10th May 2005. <http://www.kyanite.com/willmountain.html>

Larsson, D. 2001. Transition of granite to quartz-kyanite rock at Hålsjöberg, southern Sweden: Consequence of acid leaching and later metamorphism. GFF 123: 237-246.

Lindh, A. 1987. Westward growth of the Baltic Shield. Precambrian Research 35: 53-70.

Liu, Y. and Hu, K.1999. Ultrahigh-pressure metamorphic aluminium-rich rocks in central China. Yanshi Xuebao (Acta Petrologica Sinica) 15/4: 548-556.

Lundegårdh, P.H. 1995. Beskrivning till berggrundskartan över Värmlands län. Östra och mellersta Värmlands berggrund. Fyndigheter av nyttosten och malm i Värmlands län. Sveriges geologiska undersøkning Ba 45: 1-167.

Maschmeyer, D. and Lehmann, G. 1983. A trapped-hole center causing rose colouration in natural quartz. Zeitschrift für Kristallographie 163: 181–196.

McCauley, J.F. 1961. Carolina Geological Society Guidebook. Division of Geology, State Development Board, Columbia, S.C., Geological Notes 5/5. p. 13.
Müller, A. 2000. Cathodoluminescence and characterisation of defect structures in quartz with applications to the study of granitic rocks. Ph.D. Thesis, University Göttingen, Germany.
Müller, A., Lennox, P., Trzebski, R. 2002. Cathodoluminescence and micro-structural evidence for crystallisation and deformation processes of granites in the Eastern Lachlan Fold Belt (SE Australia). Contributions to Minerlogy and Petrology 143: 510-524.
Müller, A., Wiedenbeck, M., Van den Kerkhof, A.M., Kronz, A. & Simon, K. 2003. Trace elements in quartz – a combined electron microprobe, secondary ion mass spectrometry, laser-ablation ICP-MS, and cathodoluminescence study. European Journal of Mineralogy 15: 747-763.
Müller, A., Breiter, K., Seltmann, R., Pécskay, Z. 2005. Quartz and feldspar zoning in the Eastern Erzgebirge pluton (Germany, Czech Republic): evidence of multiple magma mixing. Lithos 80: 201-227.
Mullis, J. & Ramseyer, K. 1999. Growth related Al-uptake in fissure quartz, Central Alps, Switzerland. Terra Nostra 99/6: p. 209.
Nordgulen, Ø. 1999. Geologisk kart over Norge, Berggrunnskart Hamar, M 1 : 250.000. Norges geologiske undersøkelse.
Norwegian Crystallites AS 2005. Norwegian Crystallites AS – Products – Crystal quartz analyses. Accessed 20th May 2005. <http://www.norcryst.no>
Nystuen, J.P. 1969a. Kyanitt-førende kvartsitt i Elverum-Våler, en mulig ekvivalent til Hårrsböbergets kvartsitt? Norges Geologiske Undersøkelse Bull. 258: 237-240.
Nystuen, J.P. 1969b. Precambrian ash-flow tuff and associated volcanic rocks at Elverum, southern Norway. Norges Geologiske Undersøkelse Bull. 258: 241-240.
Owens, B.E., Dickerson, S.E., 2001. Kyanite color as a clue to contrasting protolith compositions for kyanite quartzites in the Piedmont Province of Virginia. Southeastern Geology 40/4: 285-298.
Pasek, M.A., Owens, B.E. 2002. Regional geochemical constraints on the petrogenesis of kyanite quartzites in the Piedmont province of Virginia and an evaluation of anomalous Ga/Al values. GSA Joint Annual Meeting 3.-5. April 2002, Lexington Kentucky, abstracts with programs, Geological Society of America 34/2: p- 4.
Qiu, Y., Grives, D.I., McNaughton, N.J., Wang, L., Zhou, T. 2002. Nature, age and tectonic setting of the granitoid-hosted, orogenic gold deposits of the Jiaodong Peninsula, eastern North China craton, China. Mineralium Deposita 37: 283-305.
Sawyer, E. 1986. Metamorphic assemblages and conditions in the Rombak basement window. Norges Geologiske Undersøkelse, unpubl. Report 88.116. 11p.
Schmidt, R.G. 1985. High-alumina hydrothermal systems in volcanic rocks and their significance to mineral prospecting in the Carolina Slate Belt. United States Geological Survey Bulletin 1562, 1-59.
Schreyer, W. 1987. Pre- or synmetamorphic metasomatism in peraluminous metamorphic rocks. In: Helgeson H.C. (ed) Chemical transport in metasomatic processes. Reidel Berlin, 265-296.
Schreyer, W., Chinner, G.A. 1966. Staurolite-quartz bands in kyanite quartzite at Big Rock, Rio Arriba County, New Mexico. Contributions to Mineralogy and Petrology 12: 223-244.
Schrön, W., Baumann, L., Rank, K. 1982. Zur Charakterisierung von Quarzgenerationen in den postmagmatogenen Erzformationen des Erzgebirges. Zeitschrift für geologische Wissenschaften 10: 1499-1521.
Sillitoe, R.H., Hannington, M.D., Thompson, F.H. 1996. High sulfidation deposits in the volcanogenic massive sulfide environment. Economic Geology 91: 204-212.

Spence, W.H. 1975. A model for the origin of the pyrophyllite deposits in the Caroline Slate Belt. Geological Society of America Abstracts with Programs 7/4: p. 536.
Spence, W.H., Worthington, J.P., Jones, E.M., Kiff, I.T. 1980. Origin of the gold mineralization at the Haile Mine, Lancaster County, South Carolina. Mining Engineering 32: 70-73.
Tveden, E., Lutro, O. 1998. Berggrunnskart Ålesund 1 : 250.000, foreløpig. Norges geologiske undersøkelse.
Tørudbackken, B.O. 1982. En geologisk undersøkelse av nordre Trollheimen ved Surnadal, med hovedvekt på sammenhengen mellom strukturer, metamorphose og aldersforhold. Hovedoppgave i geologi – Universitet i Oslo.
Valliant, R.I., Barnett, R.L., Hodder, R.W. 1983. Aluminium silicate-bearing rock and its relation to gold mineralization; Bousquet Mine, Bousquet Township, Quebec. Canadian Institute of Mining, Metallurgy and Petroleum Bulletin 76: 81-90.
Van den Kerkhof, A.M., Kronz, A., Simon, K., Scherer, T. 2004. Fluid-controlled quartz recovery in granulite as revealed by cathodoluminescence and trace element analysis; Bamble sector, Norway. Contributions to Mineralogy and Petrology 146: 637-652.
Wanvik, J.E. 1998. Kyanite investigations in Tverrådalen, Surnadal. Norwegian Geological Survey, Report 1998.080.
Wanvik, J.E. 2003. Nasafjell kvartsforekomst. Norwegian Geological Survey, Report 2003.047.
Wanvik, J.E. 2004. Supplerende kvartsundersøkelser på Saltfjellet. Norwegian Geological Survey, Report 2003.106.
Widenfalk, L., Claesson, L.-Å., Skiöld 1987. Rocks associated with uplift of a Proterozoic continental margin, N. Sweden. Proterozoic Geochemistry (Symp.), IGCP 217, Lund, (Abstr.), p. 92.
Willner, A., Schreyer, W., Moore, J.M. 1990. Peraluminous metamorphic rocks from the Namaqualand Metamorphic Complex (South Africa): Geochemical evidence of an exhalation-related, sedimentary origin on a Mid-Proterozoic rift system. Chemical Geology 81: 221-240.
Wise, W.S. 1977. Mineralogy of the Champion Mine, White Mountains, California. Mineralogical Record 7: 478-486.

Appendix A. *Sample locations and descriptions.*

locality	zone	E	N	1:50000 sheet	sample#	locality description	rock description
Tverrådalen	32 V	492 817	6978679	Snota	1907401	Tverrådalen, 500 m SW Tverrådalsetra	fine-grained kyanite quartzite, kyanite-rich
Tverrådalen	32 V	492 817	6978679	Snota	5*	Tverrådalen, 500 m SW Tverrådalsetra	fine-grained kyanite quartzite, kyanite-rich
Tverrådalen	32 V	492 817	6978679	Snota	6*	Tverrådalen, 500 m SW Tverrådalsetra	fine-grained kyanite quartzite, kyanite-rich
Tverrådalen	32 V	492 817	6978679	Snota	7*	Tverrådalen, 500 m SW Tverrådalsetra	fine-grained kyanite quartzite, kyanite-poor
Tverrådalen	32 V	492 817	6978679	Snota	8*	Tverrådalen, 500 m SW Tverrådalsetra	fine-grained kyanite quartzite, kyanite-rich
Tverrådalen	32 V	492 817	6978679	Snota	9*	Tverrådalen, 500 m SW Tverrådalsetra	fine-grained kyanite quartzite, kyanite-poor
Tverrådalen	32 V	492 817	6978679	Snota	DH1 0-3.5m*	Tverrådalen, 500 m SW Tverrådalsetra	fine-grained kyanite quartzite, kyanite-poor
Tverrådalen	32 V	492 817	6978679	Snota	DH1 3.5-4.8m*	Tverrådalen, 500 m SW Tverrådalsetra	fine-grained kyanite quartzite, kyanite-rich
Tverrådalen	32 V	492 817	6978679	Snota	DH2 0-1.1m*	Tverrådalen, 500 m SW Tverrådalsetra	fine-grained kyanite quartzite, kyanite-rich
Tverrådalen	32 V	492 817	6978679	Snota	DH2 1.1-3.5m*	Tverrådalen, 500 m SW Tverrådalsetra	fine-grained kyanite quartzite, kyanite-rich
Tverrådalen	32 V	492 817	6978679	Snota	DH2 3.5-5.5m*	Tverrådalen, 500 m SW Tverrådalsetra	fine-grained kyanite quartzite, kyanite-rich
Tverrådalen	32 V	492 817	6978679	Snota	DH2 5.5-9.1m*	Tverrådalen, 500 m SW Tverrådalsetra	fine-grained kyanite quartzite, kyanite-rich
Hallaren	32 V	484 799	6980738	Stangvik	1907405	20 m E of Street 670 S of Surnadalsøra, next to Hallaren	5 cm thick fine-grained quartzite layer containing muscovite and biotite
Kufjellet	32 V	497375	6979120	Snota	2007405	Vinddøldalen, 1.5 km NE of Kufjellet	Fine-grained metaarkosewith muscovite
Folldalen	32 V	506 374	6978266	Snota	2007410	Folldalen, 700 m NNE Gråhaugen, N at the foot of the dam	muscovite-rich, medium-grained metaarkose with kyanite
Sormbrua	32 V	650 855	6738948	Elverum	2807401	500 m NNE from Sormbrua bridge, 5 km SE Jømna	Greenish white, fine-grained muscovite/pyrophyllite-rich kyanite quartzite with pyrite
Kjeksberget	32 V	651 144	6742248	Elverum	2907403	Kjeksberget kyanite quartzite, 300 m W Jensbekkoia, 3 km SE Jømna	Boulder of fine-grained greenish and pinkish kyanite quartzite with pyrite
Kjeksberget	32 V	651 144	6742248	Elverum	2907404	Kjeksberget kyanite quartzite, 300 m W Jensbekkoia, 3 km SE Jømna	Boulder of fine-grained white kyanite-poor quartzite with minor muscovite/pyrophyllite and pyrite
Sormbrua	32 V	650 517	6738723	Elverum	2907406	Sormbrua bridge, 5 km SE Jømna	Fine-grained kyanite quartzite with turquoise nests (2 to 5 mm) of kyanite and lazulite
Sormbrua	32 V	650 517	6738723	Elverum	2907407	Sormbrua bridge, 5 km SE Jømna	Laminated, fine-grained kyanite quartzite with pinkish (rutile) and bluish colour

Appendix A. *Sample locations and descriptions. Continued.*

locality	zone	E	N	1:50000 sheet	sample#	locality description	rock description
Knøsberget	32 V	657 454	6739983	Kynna	2907408	1 km NE Knøsen, 500 m ESE Åroskoia	Fine-grained kyanite-poor kyanite quartzite with long (up to 1 cm) pyrophyllite
Gullsteinberget	V 33	345 345	6736074	Flisa	2907410	50 m NW summit of Gullsteinberget, 10 km NE Sønsterud	Greenish white fine-grained, muscovite/pyrophyllite-rich kyanite quartzite
Gullsteinberget	V 33	345 371	6736097	Flisa	2907411	summit of Gullsteinberget, 10 km NE Sønsterud	Greenish white fine-grained kyanite quartzite
Hålsjøberget	V 33	402 319	6683610		3107401	Hålsjøberget, 20 km NE of Torsby, Vaermland, Sweden	quartz-rich layer (smoky quartz) within laminated kyanite quartzite
Hålsjøberget	V 33	402 319	6683610		3107402	Hålsjøberget, 20 km NE of Torsby, Vaermland, Sweden	kyanite-rich layer within laminated kyanite quartzite
Juovvačorrú	V 33	606 904	7553985	Skjomen	R1021a	high plane Juovvačorrú 20 km SSE of Skjomen, 10 km S of the southern end of the Skjomendalen, .	Fine-grained turquoise kyanite quartzite with minor pyrophyllite
Juovvačorrú	V 33	606 904	7553985	Skjomen	R1021b	high plane Juovvačorrú 20 km SSE of Skjomen, 10 km S of the southern end of the Skjomendalen, .	Kyanite-poor, fine-grained quartzite with rusty batches, traces of mica, rutile
Nasafjell	V 33	513840	7373910	Virvatnet	JW0315C	3 km W of top of Nasafjellet (1210 m), 4 km ESE of the Bolna railway station	Kyanite-rich, fine- to medium grained quartzite

Appendix B. *Kyanite chemistry determined by electron probe micro analysis.*

locality	Nasafjell	Nasafjell	Nasafjell	Nasafjell	Nasafjell	Nasafjell	Nasafjell	Nasafjell	Nasafjell	Nasafjell	Nasafjell	Nasafjell	Nasafjell	Nasafjell	Nasafjell	Nasafjell	Nasafjell
sample nr.	JW03-15C	JW03-15C	JW03-15C	JW03-15C	JW03-15C	JW03-15C	JW03-15C	JW03-15C	JW03-15C	JW03-15C	JW03-15C	JW03-15C	JW03-15C	JW03-15C	JW03-15C	JW03-15C	JW03-15C
	profile 1	profile 1	profile 1	profile 1	profile 1	profile 1	profile 1	profile 1	profile 1	profile 1	profile 1	profile 1	profile 1	profile 1	single pt	single pt	single pt
distance (µm)	0	18	36	54	90	108	126	144	162	180	198	216	234	252			
Major and trace elements (wt%)																	
Al_2O_3	62.53	63.35	62.98	62.52	63.46	62.64	63.03	62.65	62.57	63.08	63.08	62.58	62.60	63.20	63.22	63.00	62.07
SiO_2	35.60	34.96	35.08	35.24	35.53	35.22	35.20	35.05	34.99	34.94	35.01	35.36	35.24	35.28	35.74	35.10	35.12
TiO_2	0	0.004	0.001	0	0	0.001	0.001	0	0.002	0.005	0.007	0.002	0.007	0.002	0	0	0.004
FeO	0.389	0.284	0.313	0.283	0.252	0.411	0.413	0.334	0.358	0.380	0.400	0.446	0.350	0.298	0.115	0.386	0.368
MnO	0.001	0	0	0	0.001	0.001	0.003	0.002	0	0.001	0	0	0.001	0.001	0	0.006	0
MgO	0	0.017	0	0.003	0.004	0.005	0.008	0.004	0.004	0.004	0.002	0.006	0.003	0.001	0	0.004	0.003
V_2O_3	0.008	0.010	0.006	0.01	0.011	0.014	0.009	0.007	0.013	0.012	0.015	0.013	0.012	0.008	0.012	0.012	0.009
Cr_2O_3	0.009	0.011	0.017	0.018	0.014	0.016	0.014	0.011	0.013	0.014	0.013	0.015	0.011	0.012	0.014	0.014	0.010
CaO	0.008	0.001	0.001	0.008	0.005	0.005	0.004	0.004	0.002	0.005	0.006	0.006	0.003	0.003	0.002	0	0.004
Na_2O	0	0	0.002	0.007	0	0	0	0.002	0	0	0	0	0.001	0	0	0	0.001
K_2O	0.003	0.004	0	0.003	0.003	0.002	0.002	0.003	0	0.002	0.004	0	0	0.002	0.001	0.002	0
total	98.55	98.65	98.40	98.08	99.28	98.32	98.69	98.07	97.95	98.45	98.54	98.43	98.23	98.81	99.10	98.52	97.59
Trace elements (ppm)																	
Ti	<51	<51	<51	<51	<51	<51	<51	<51	<51	<51	<51	<51	<51	<51	<51	<51	<51
Fe	3025	2205	2433	2200	1955	3192	3212	2595	2785	2955	3108	3470	2721	2314	892	3000	2856
Mn	<69	<69	<69	<69	<69	<69	<69	<69	<69	<69	<69	<69	<69	<69	<69	<69	<69
Mg	<54	103	<54	<54	<54	<54	<54	<54	<54	<54	<54	<54	<54	<54	<54	<54	<54
V	56	67	<48	68	71	98	60	<48	86	80	102	89	82	51	85	80	62
Cr	<51	63	95	101	80	90	79	62	75	78	72	85	60	65	79	81	57
Ca	54	<45	<45	61	<45	<45	<45	<45	<45	<45	45	<45	<45	<45	<45	<45	<45
Na	<132	<132	<132	<132	<132	<132	<132	<132	<132	<132	<132	<132	<132	<132	<132	<132	<132
K	<57	<57	<57	<57	<57	<57	<57	<57	<57	<57	<57	<57	<57	<57	<57	<57	<57

Appendix B. *Kyanite chemistry determined by electron probe micro analysis. Continued.*

locality	Nasafjell	Nasafjell	Nasafjell	Nasafjell	Nasafjell	Nasafjell	Nasafjell	Nasafjell	Nasafjell	Nasafjell	Nasafjell	Nasafjell	Nasafjell	Nasafjell	Tverrådalen	Tverrådalen
sample nr.	JW03-15C	JW03-15C	JW03-15C	JW03-15C	JW03-15C	JW03-15C	JW03-15C	JW03-15C	JW03-15C	JW03-15C	JW03-15C	JW03-15C	JW03-15C	JW03-15C	980051	980051
	profile 2	profile 2	profile 2	profile 2	profile 2	profile 2	profile 2	profile 2	profile 2	single pt	single pt	single pt	single pt	single pt	profile 1	profile 1
distance (µm)	0	20	40	60	80	100	120	140	160						0	29
major and trace elements (wt%)																
Al_2O_3	62.64	62.52	62.60	62.71	63.03	63.38	62.56	62.11	62.01	62.86	62.72	62.52	62.26	63.60	63.02	62.20
SiO_2	35.27	35.15	34.83	35.31	35.13	35.65	35.59	36.08	35.31	35.96	35.53	35.69	35.54	35.14	35.15	35.01
TiO_2	0.005	0.002	0.004	0.003	0.003	0.001	0	0.001	0	0.002	0.006	0.008	0.004	0.001	0	0.004
FeO	0.348	0.382	0.313	0.322	0.266	0.130	0.027	0.018	0.210	0.248	0.297	0.230	0.320	0.264	0.322	0.334
MnO	0.001	0	0	0.002	0	0	0.007	0	0.002	0.004	0.002	0	0	0.003	0.001	0
MgO	0.012	0.006	0.004	0.007	0.007	0	0.001	0	0.002	0.002	0.003	0.003	0.005	0.001	0	0
V_2O_3	0.008	0.007	0.010	0.008	0.012	0.011	0.005	0.013	0.012	0.005	0.003	0.008	0.006	0.004	0.007	0.008
Cr_2O_3	0.014	0.016	0.012	0.013	0.012	0.012	0.023	0.017	0.014	0.004	0.014	0.013	0.010	0.010	0.005	0.006
CaO	0.006	0.001	0.001	0.006	0.002	0.003	0.003	0.005	0.000	0.004	0	0.005	0	0.004	0.007	0.004
Na_2O	0	0.001	0	0	0.002	0	0	0	0.005	0.002	0	0	0	0.009	0.004	0.003
K_2O	0.003	0.004	0.006	0	0	0.001	0.002	0.002	0.004	0	0.001	0.004	0	0	0.001	0.004
total	98.31	98.09	97.78	98.38	98.47	99.19	98.22	98.25	97.58	99.09	98.57	98.48	98.14	99.04	98.52	97.58
trace elements (ppm)																
Ti	<51	<51	<51	<51	<51	<51	<51	<51	<51	<51	<51	<51	<51	<51	<51	<51
Fe	2706	2973	2436	2501	2071	1013	210	137	1628	1924	2310	1791	2486	2056	2502	2595
Mn	<69	<69	<69	<69	<69	<69	<69	<69	145	<69	<69	<69	<69	<69	<69	<69
Mg	69	<54	<54	<54	<54	<54	<54	<54	<54	<54	<54	<54	<54	<54	<54	<54
V	54	<48	66	52	82	75	<48	90	78	<48	<48	53	<48	<48	49	55
Cr	81	92	69	73	69	66	128	96	76	<51	77	75	54	54	<51	<51
Ca	<45	<45	<45	<45	<45	<45	<45	<45	<45	<45	<45	<45	<45	<45	51	<45
Na	<132	<132	<132	<132	<132	<132	<132	<132	<132	<132	<132	<132	<132	<132	<132	<132
K	<57	<57	<57	<57	<57	<57	<57	<57	<57	<57	<57	<57	<57	<57	<57	<57

Appendix B. *Kyanite chemistry determined by electron probe micro analysis. Continued.*

locality	Tverrådalen	Tverrådalen	Tverrådalen	Tverrådalen	Tverrådalen	Tverrådalen	Tverrådalen	Tverrådalen	Tverrådalen	Tverrådalen	Tverrådalen	Tverrådalen	Tverrådalen	Tverrådalen	Tverrådalen
sample nr.	980051	980051	980051	980051	980051	980051	980051	980051	980051	980051	980051	980051	980051	980051	980051
	profile 1	profile 1	profile 1	profile 1	profile 1	profile 1	profile 1	profile 1	profile 1	profile 1	profile 1	profile 1	profile 1	profile 1	profile 1
distance (µm)	58	87	116	145	174	203	232	261	290	319	348	377	406	435	464
major and trace elements (wt%)															
Al_2O_3	62.55	62.57	62.85	62.52	62.13	62.22	61.74	61.65	62.47	62.54	62.76	62.44	62.23	61.35	63.07
SiO_2	35.31	35.72	35.10	35.28	34.73	34.90	34.97	35.04	35.14	35.36	35.57	35.30	35.19	36.37	34.53
TiO_2	0	0.003	0.001	0	0	0.002	0.001	0.003	0.009	0.002	0	0	0.003	0.004	0.004
FeO	0.213	0.257	0.224	0.287	0.248	0.293	0.338	0.345	0.278	0.284	0.191	0.196	0.242	0.317	0.334
MnO	0.002	0.001	0.003	0	0.003	0.002	0.003	0.002	0.001	0.004	0	0	0	0	0.004
MgO	0	0	0	0	0.001	0.008	0.006	0.010	0.009	0	0	0	0	0	0
V_2O_3	0.008	0.009	0.009	0.011	0.004	0.009	0.008	0.007	0.006	0.004	0.005	0.005	0.010	0.006	0.0076
Cr_2O_3	0.004	0.002	0.005	0.007	0.002	0.003	0.009	0.005	0.002	0.006	0.007	0.005	0.002	0.005	0.0044
CaO	0.004	0.005	0.005	0.002	0.003	0.004	0.004	0.004	0.004	0.006	0.002	0.002	0.003	0.004	0.0033
Na_2O	0	0.005	0	0	0.004	0	0.009	0	0.002	0.004	0.003	0	0	0	0
K_2O	0.003	0	0.003	0.002	0.002	0	0.003	0	0	0.002	0.002	0	0	0.001	0.0005
total	98.10	98.58	98.20	98.11	97.13	97.44	97.09	97.07	97.93	98.21	98.55	97.95	97.67	98.06	97.96
trace elements (ppm)															
Ti	<51	<51	<51	<51	<51	<51	<51	<51	54	<51	<51	<51	<51	<51	<51
Fe	1657	1994	1739	2233	1931	2279	2628	2679	2161	2206	1487	1524	1882	2462	2595
Mn	<69	<69	<69	<69	<69	<69	<69	<69	<69	<69	<69	<69	<69	<69	<69
Mg	<54	<54	<54	<54	<54	<54	<54	60	<54	<54	<54	<54	<54	<54	<54
V	52	62	58	77	<48	60	56	48	<48	<48	<48	<48	70	<48	52
Cr	<51	<51	<51	<51	<51	194	<51	<51	<51	<51	<51	<51	<51	<51	<51
Ca	<45	<45	<45	<45	<45	<45	<45	<45	<45	<45	<45	<45	<45	<45	<45
Na	<132	<132	<132	<132	<132	<132	<132	<132	<132	<132	<132	<132	<132	<132	<132
K	<57	<57	<57	<57	<57	<57	<57	<57	<57	<57	<57	<57	<57	<57	<57

Appendix B. *Kyanite chemistry determined by electron probe micro analysis. Continued.*

Locality	Tverrådalen	Tverrådalen	Tverrådalen	Tverrådalen	Tverrådalen	Gullsteinberget	Gullsteinberget	Gullsteinberget	Gullsteinberget	Gullsteinberget	Gullsteinberget	Gullsteinberget	Gullsteinberget
sample nr.	980051	980051	980051	980051	980051	2907411	2907411	2907411	2907411	2907411	2907411	2907411	2907411
	profile 1	profile 1	profile 1	profile 1	profile 1	profile 1	profile 1	profile 1	profile 1	profile 1	profile 1	profile 1	profile 1
distance (µm)	493	522	551	580	609	0	15	30	45	60	75	90	105
major and trace elements (wt%)													
Al_2O_3	62.62	63.49	62.88	62.99	62.48	62.52	62.99	62.92	63.14	62.88	62.95	62.53	62.04
SiO_2	34.85	34.96	35.07	34.98	35.42	36.04	35.06	34.99	35.59	35.46	35.51	35.70	35.65
TiO_2	0.003	0.004	0.006	0.007	0.003	0.002	0.001	0	0	0	0.001	0	0.001
FeO	0.304	0.292	0.374	0.350	0.321	0.47	0.489	0.475	0.514	0.479	0.525	0.522	0.553
MnO	0.002	0	0	0.005	0	0	0.001	0.003	0.001	0	0	0	0.003
MgO	0.013	0.011	0.011	0.009	0	0.004	0.004	0.013	0.019	0.003	0.006	0	0.002
V_2O_3	0.011	0.010	0.008	0.008	0.006	0	0.001	0.003	0.002	0	0.004	0	0.001
Cr_2O_3	0.001	0.004	0.007	0.007	0.007	0.001	0.001	0.001	0	0.001	0	0.004	0
CaO	0.008	0.003	0.002	0.002	0.005	0.003	0.004	0.004	0.003	0.001	0.002	0.002	0.003
Na_2O	0.003	0	0.011	0.002	0.006	0	0.001	0	0.001	0.004	0	0	0.006
K_2O	0	0.005	0.002	0.001	0	0.004	0.002	0	0	0.001	0	0	0
total	97.82	98.78	98.36	98.36	98.25	99.05	98.56	98.40	99.26	98.84	99.00	98.76	98.26
trace elements (ppm)													
Ti	<51	<51	<51	<51	<51	<51	<51	<51	<51	<51	<51	<51	<51
Fe	2363	2273	2906	2717	2497	3653	3803	3691	3992	3722	4082	4061	4296
Mn	<69	<69	<69	<69	<69	<69	<69	<69	<69	<69	<69	<69	<69
Mg	76	68	66	<54	<54	<54	<54	76	116	<54	<54	<54	<54
V	77	70	55	52	<48	<48	<48	<48	<48	<48	<48	<48	<48
Cr	<51	<51	<51	<51	<51	<51	<51	<51	<51	<51	<51	<51	<51
Ca	55	<45	<45	<45	<45	<45	<45	<45	<45	<45	<45	<45	<45
Na	<132	<132	<132	<132	<132	<132	<132	<132	<132	<132	<132	<132	<132
K	<57	<57	<57	<57	<57	<57	<57	<57	<57	<57	<57	<57	<57

Appendix B. *Kyanite chemistry determined by electron probe micro analysis. Continued.*

Locality	Gullsteinberget	Gullsteinberget	Gullsteinberget	Gullsteinberget	Gullsteinberget	Gullsteinberget	Gullsteinberget	Gullsteinberget	Gullsteinberget	Gullsteinberget	Gullsteinberget	Gullsteinberget
sample nr.	2907411	2907411	2907411	2907411	2907411	2907411	2907411	2907411	2907411	2907411	2907411	2907411
	profile 1	profile 1	profile 1	profile 1	profile 1	profile 1	profile 1	profile 1	profile 1	profile 1	profile 1	profile 1
distance (µm)	120	135	150	165	180	195	210	225	240	255	270	285
major and trace elements (wt%)												
Al_2O_3	62.55	62.55	63.00	62.39	63.72	62.64	63.27	63.25	63.38	62.70	62.66	62.98
SiO_2	35.76	35.41	35.59	35.30	35.32	35.26	35.34	35.16	35.56	35.53	35.61	35.35
TiO_2	0	0.001	0	0	0.003	0	0.001	0	0.001	0.002	0	0.002
FeO	0.479	0.487	0.479	0.483	0.066	0.158	0.172	0.138	0.067	0.363	0.313	0.319
MnO	0.004	0.001	0	0	0	0	0	0	0.001	0.001	0.001	0
MgO	0.007	0.018	0.020	0	0	0.012	0.012	0	0	0.003	0.001	0
V_2O_3	0	0	0	0.004	0	0.003	0	0	0.001	0.001	0	0.004
Cr_2O_3	0	0	0.001	0.003	0.001	0.007	0.002	0	0.003	0.001	0	0
CaO	0.001	0.003	0	0.004	0.001	0	0.002	0.004	0.003	0	0.003	0
Na_2O	0.008	0	0.007	0.008	0	0.002	0	0.006	0	0.004	0.005	0.010
K_2O	0.001	0	0	0.005	0.001	0	0.004	0.003	0	0.002	0	0.002
total	98.82	98.47	99.10	98.20	99.11	98.08	98.80	98.57	99.02	98.61	98.59	98.67
trace elements (ppm)												
Ti	<51	<51	<51	<51	<51	<51	<51	<51	<51	<51	<51	<51
Fe	3724	3784	3720	3754	511	1226	1333	1073	523	2822	2433	2482
Mn	<69	<69	<69	<69	<69	<69	<69	<69	<69	<69	<69	<69
Mg	<54	112	118	<54	<54	70	74	<54	<54	<54	<54	<54
V	<48	<48	<48	<48	<48	<48	<48	<48	<48	<48	<48	<48
Cr	<51	<51	<51	<51	<51	<51	<51	<51	<51	<51	<51	<51
Ca	<45	<45	<45	<45	<45	<45	<45	<45	<45	<45	<45	<45
Na	<132	<132	<132	<132	<132	<132	<132	<132	<132	<132	<132	<132
K	<57	<57	<57	<57	<57	<57	<57	<57	<57	<57	<57	<57

Appendix B. *Kyanite chemistry determined by electron probe micro analysis. Continued.*

locality	Gullsteinberget	Gullsteinberget	Gullsteinberget	Gullsteinberget	Gullsteinberget	Gullsteinberget	Gullsteinberget	Gullsteinberget	Gullsteinberget	Gullsteinberget	Gullsteinberget	Gullsteinberget
sample nr.	2907411	2907411	2907411	2907411	2907411	2907411	2907411	2907411	2907411	2907411	2907411	2907411
	profile 1	profile 1	profile 1	profile 2	profile 2	profile 2	profile 2	profile 2	profile 2	profile 2	profile 2	profile 2
distance (µm)	300	315	330	0	15	30	45	60	75	90	105	120
major and trace elements (wt%)												
Al_2O_3	62.76	62.55	62.23	62.43	62.61	61.83	62.42	62.39	62.20	61.92	62.21	62.47
SiO_2	35.06	35.44	34.98	34.93	34.90	34.83	34.87	35.01	35.38	34.80	36.17	34.78
TiO_2	0	0.003	0.002	0.001	0	0.002	0	0.001	0	0	0	0
FeO	0.332	0.370	0.373	0.317	0.482	0.462	0.399	0.543	0.348	0.540	0.098	0.259
MnO	0	0.001	0.001	0.001	0.004	0.001	0	0	0	0	0.003	0.002
MgO	0	0	0	0	0	0.002	0.003	0.007	0.005	0.001	0	0
V_2O_3	0	0.001	0.001	0	0	0.002	0.002	0.002	0.001	0.002	0.001	0
Cr_2O_3	0.001	0	0.002	0	0	0.002	0.003	0.001	0	0.003	0	0
CaO	0.003	0.002	0	0.002	0.003	0.004	0.001	0.002	0.004	0.002	0.003	0
Na_2O	0	0	0	0.011	0	0.002	0.004	0.006	0.007	0.006	0	0.001
K_2O	0	0.001	0	0	0.001	0.001	0.001	0.001	0	0	0.001	0
total	98.16	98.37	97.59	97.69	98.00	97.14	97.70	97.96	97.95	97.28	98.48	97.51
trace elements (ppm)												
Ti	<51	<51	<51	<51	<51	<51	<51	<51	<51	<51	<51	<51
Fe	2583	2878	2898	2466	3750	3587	3099	4218	2703	4199	762	2012
Mn	<69	<69	<69	<69	<69	<69	<69	<69	<69	<69	<69	<69
Mg	<54	<54	<54	<54	<54	<54	<54	<54	<54	<54	<54	<54
V	<48	<48	<48	<48	<48	<48	<48	<48	<48	<48	<48	<48
Cr	<51	<51	<51	<51	<51	<51	<51	<51	<51	<51	<51	<51
Ca	<45	<45	<45	<45	<45	<45	<45	<45	<45	<45	<45	<45
Na	<132	<132	<132	<132	<132	<132	<132	<132	<132	<132	<132	<132
K	<57	<57	<57	<57	<57	<57	<57	<57	<57	<57	<57	<57

Appendix B. *Kyanite chemistry determined by electron probe micro analysis. Continued.*

Locality	Gullsteinberget	Gullsteinberget	Gullsteinberget	Gullsteinberget	Gullsteinberget	Gullsteinberget	Gullsteinberget	Gullsteinberget	Gullsteinberget	Gullsteinberget	Gullsteinberget	Gullsteinberget
sample nr.	2907411	2907411	2907411	2907411	2907411	2907411	2907411	2907411	2907411	2907411	2907411	2907411
	profile 2	profile 2	profile 2	profile 2	profile 2	profile 2	profile 2	profile 2	profile 2	profile 2	profile 2	profile 2
distance (µm)	135	150	165	180	195	210	225	240	255	270	285	300
major and trace elements (wt%)												
Al_2O_3	63.37	62.40	61.82	62.14	61.44	62.22	61.87	62.18	62.42	62.01	62.30	62.97
SiO_2	35.32	35.63	35.84	35.11	35.60	35.15	35.94	35.66	35.72	35.30	35.22	35.50
TiO_2	0	0.002	0.002	0.005	0.003	0	0.002	0	0.002	0.003	0	0
FeO	0.128	0.378	0.529	0.556	0.492	0.502	0.497	0.471	0.075	0.598	0.621	0.332
MnO	0	0	0	0.001	0	0.002	0	0	0	0.003	0	0.002
MgO	0.002	0.007	0.011	0.005	0.029	0.022	0	0.005	0	0.005	0.004	0.004
V_2O_3	0.001	0.004	0.001	0	0.003	0	0	0.002	0	0.002	0.004	0.001
Cr_2O_3	0.002	0.002	0	0	0	0.001	0.001	0.002	0	0.002	0	0.001
CaO	0.003	0.005	0.004	0.005	0.004	0.005	0.005	0	0	0.001	0.005	0.001
Na_2O	0	0	0	0	0	0.002	0.004	0	0.004	0	0.008	0
K_2O	0.002	0	0.001	0	0.003	0	0.002	0	0.001	0	0.001	0.001
total	98.82	98.43	98.21	97.82	97.57	97.91	98.32	98.32	98.22	97.92	98.15	98.81
trace elements (ppm)												
Ti	<51	<51	<51	<51	<51	<51	<51	<51	<51	<51	<51	<51
Fe	992	2938	4113	4323	3826	3905	3865	3661	580	4649	4829	2579
Mn	<69	<69	<69	<69	<69	<69	<69	<69	<69	<69	<69	<69
Mg	<54	<54	68	<54	177	132	<54	<54	<54	<54	<54	<54
V	<48	<48	<48	<48	<48	<48	<48	<48	<48	<48	<48	<48
Cr	<51	<51	<51	<51	<51	<51	<51	<51	<51	<51	<51	<51
Ca	<45	<45	<45	<45	<45	<45	<45	<45	<45	<45	334	<45
Na	<132	<132	<132	<132	<132	<132	<132	<132	<132	<132	<132	<132
K	<57	<57	<57	<57	<57	<57	<57	<57	<57	<57	<57	<57

Appendix B. *Kyanite chemistry determined by electron probe micro analysis. Continued.*

Locality	Gullsteinberget	Gullsteinberget	Jouvvacorru	Jouvvacorru	Jouvvacorru	Jouvvacorru	Jouvvacorru	Jouvvacorru	Jouvvacorru	Jouvvacorru	Jouvvacorru	Jouvvacorru	Jouvvacorru	Jouvvacorru
sample nr.	2907411	2907411	R1021A	R1021A	R1021A	R1021A	R1021A	R1021A	R1021A	R1021A	R1021A	R1021A	R1021A	R1021A
	profile 2	profile 2	profile 1	profile 1	profile 1	profile 1	profile 1	profile 1	profile 1	profile 1	profile 1	profile 1	profile 1	profile 1
distance (µm)	315	330	0	15	30	45	60	75	90	105	120	135	150	165
major and trace elements (wt%)														
Al_2O_3	62.42	62.62	62.02	62.98	62.05	62.07	60.14	61.87	61.85	62.20	62.60	62.01	62.05	62.31
SiO_2	35.63	35.78	35.14	35.52	35.12	35.30	37.45	35.52	35.28	35.05	35.65	35.45	35.75	35.64
TiO_2	0	0	0	0	0.001	0.002	0	0	0	0	0.005	0.002	0.004	0.002
FeO	0.332	0.296	0.254	0.256	0.336	0.268	0.266	0.272	0.276	0.315	0.285	0.290	0.314	0.263
MnO	0	0	0.002	0	0.001	0	0	0	0	0	0	0.003	0	0
MgO	0.004	0	0	0	0.001	0.008	0	0	0.003	0.008	0	0.001	0	0.001
V_2O_3	0.001	0.004	0.008	0.006	0.006	0.004	0.009	0.008	0.008	0.008	0.007	0.009	0.008	0.009
Cr_2O_3	0.001	0	0.006	0.004	0.003	0.001	0	0.004	0.006	0.005	0.002	0.001	0.005	0.013
CaO	0.002	0.003	0.004	0.003	0.005	0.001	0.006	0.004	0	0.002	0.002	0.007	0.004	0.001
Na_2O	0.006	0	0	0.001	0	0	0.005	0	0.004	0.003	0	0.005	0	0.004
K_2O	0	0	0	0.003	0	0	0.003	0.001	0	0	0	0.002	0	0.001
total	98.39	98.70	97.43	98.77	97.52	97.66	97.88	97.68	97.43	97.59	98.55	97.78	98.14	98.25
trace elements (ppm)														
Ti	<51	<51	<51	<51	<51	<51	<51	<51	<51	<51	<51	<51	<51	<51
Fe	2578	2298	1976	1991	2609	2081	2064	2118	2145	2446	2218	2253	2442	2043
Mn	<69	<69	<69	<69	<69	<69	<69	<69	<69	<69	<69	<69	<69	<69
Mg	<54	<54	<54	<54	<54	<54	<54	<54	<54	<54	<54	<54	<54	<54
V	<48	<48	54	<48	<48	<48	59	57	54	58	50	64	53	58
Cr	<51	<51	<51	<51	<51	<51	<51	<51	<51	<51	<51	<51	<51	72
Ca	<45	<45	<45	<45	<45	<45	<45	<45	<45	<45	<45	53	<45	<45
Na	<132	<132	<132	<132	<132	<132	<132	<132	<132	<132	<132	<132	<132	<132
K	<57	<57	<57	<57	<57	<57	<57	<57	<57	<57	<57	<57	<57	<57

Appendix B. *Kyanite chemistry determined by electron probe micro analysis. Continued.*

Locality	Jouvvacorru	Jouvvacorru	Jouvvacorru	Jouvvacorru	Jouvvacorru	Jouvvacorru	Jouvvacorru	Jouvvacorru	Jouvvacorru	Sormbrua	Sormbrua	Sormbrua	Sormbrua	Sormbrua	Sormbrua
sample nr.	R1021A	R1021A	R1021A	R1021A	R1021A	R1021A	R1021A	R1021A	R1021A	2907406	2907406	2907406	2907406	2907406	2907406
	profile 2	profile 2	profile 2	profile 2	profile 2	profile 2	profile 2	profile 2	profile 2	profile 1	profile 1	profile 1	profile 1	profile 1	profile 1
distance (µm)	0	15	30	45	60	75	90	105	120	0	21	42	63	84	105
major and trace elements (wt%)															
Al_2O_3	62.81	62.17	62.09	62.50	62.70	62.78	63.56	62.70	62.66	63.21	62.69	62.35	62.31	62.42	63.06
SiO_2	35.66	35.50	35.10	35.39	35.11	34.97	35.11	35.07	35.05	34.97	35.01	35.16	35.08	35.03	34.50
TiO_2	0.005	0	0.005	0	0.001	0.005	0	0	0	0.005	0.003	0.001	0.002	0.001	0
FeO	0.257	0.386	0.292	0.319	0.259	0.301	0.218	0.233	0.219	0.073	0.102	0.107	0.098	0.111	0.106
MnO	0.002	0.002	0	0	0.006	0.004	0.001	0	0	0	0	0	0.002	0.001	0
MgO	0	0	0.003	0.015	0.005	0.002	0.004	0.002	0	0	0	0	0.001	0	0
V_2O_3	0.012	0.011	0.012	0.004	0.002	0.009	0.005	0.005	0.009	0.009	0.019	0.014	0.015	0.022	0.020
Cr_2O_3	0.008	0.002	0.003	0.006	0.006	0.003	0.003	0.004	0.007	0.001	0.002	0.006	0.002	0.001	0.001
CaO	0.002	0.004	0.001	0.003	0.003	0	0.001	0.002	0.004	0.005	0.002	0	0	0.005	0.002
Na_2O	0.006	0	0.010	0	0	0.008	0.002	0	0	0	0	0	0	0	0.001
K_2O	0.002	0.003	0.004	0	0.005	0	0.001	0	0	0	0	0	0	0	0
total	98.77	98.08	97.51	98.24	98.10	98.08	98.90	98.02	97.95	98.27	97.83	97.64	97.51	97.58	97.69
trace elements (ppm)															
Ti	<51	<51	<51	<51	<51	<51	<51	<51	<51	<51	<51	<51	<51	<51	<51
Fe	1995	2997	2266	2483	2015	2341	1694	1812	1704	564	793	835	760	862	821
Mn	<69	<69	<69	<69	<69	<69	<69	<69	<69	<69	<69	<69	<69	<69	<69
Mg	<54	<54	<54	93	<54	<54	<54	<54	<54	<54	<54	<54	<54	<54	<54
V	78	77	79	<48	<48	60	<48	<48	62	60	128	97	102	150	135
Cr	<51	<51	<51	<51	<51	<51	<51	<51	<51	<51	<51	<51	<51	<51	<51
Ca	<45	<45	<45	<45	<45	<45	<45	<45	<45	<45	<45	<45	<45	<45	<45
Na	<132	<132	<132	<132	<132	<132	<132	<132	<132	<132	<132	<132	<132	<132	<132
K	<57	<57	<57	<57	<57	<57	<57	<57	<57	<57	<57	<57	<57	<57	<57

Appendix B. *Kyanite chemistry determined by electron probe micro analysis. Continued.*

Locality	Sormbrua	Sormbrua	Sormbrua	Sormbrua	Sormbrua	Sormbrua	Sormbrua	Sormbrua	Sormbrua	Sormbrua	Sormbrua	Sormbrua	Sormbrua	Sormbrua	Sormbrua	Sormbrua	Sormbrua	Sormbrua
sample nr.	2907406	2907406	2907406	2907406	2907406	2907406	2907406	2907406	2907406	2907406	2907406	2907406	2907406	2907406	2907406	2907406	2907406	2907406
	profile 1	profile 1	profile 1	profile 1	profile 2	profile 2	profile 2	profile 2	profile 2	profile 2	profile 2	profile 2	profile 2	profile 2	profile 2	profile 2	profile 2	profile 2
distance (µm)	126	147	168	189	0	30	60	90	120	150	180	210	240	270	300	330	360	390
major and trace elements (wt%)																		
Al_2O_3	63.13	62.76	62.79	62.42	62.11	63.02	62.28	62.30	62.06	62.45	63.18	62.33	63.53	63.55	62.72	62.76	62.80	62.33
SiO_2	35.10	35.04	35.16	35.72	34.95	34.85	34.38	34.41	34.67	34.75	34.68	34.92	34.63	34.64	35.06	34.30	34.58	34.74
TiO_2	0	0.002	0	0.001	0	0	0.002	0	0.001	0.004	0	0	0.003	0.002	0.001	0.003	0.001	0.001
FeO	0.116	0.117	0.122	0.112	0.749	0.732	0.701	0.708	0.523	0.323	0.272	0.225	0.133	0.128	0.151	0.174	0.161	0.157
MnO	0.004	0	0.001	0	0.004	0.003	0.002	0	0.001	0.002	0	0	0.002	0	0	0.004	0	0.001
MgO	0.003	0	0.001	0	0	0.001	0	0.002	0	0	0.001	0	0	0	0.002	0	0.005	0
V_2O_3	0.020	0.024	0.022	0.020	0.006	0.004	0.003	0.004	0.005	0.006	0.003	0.005	0.005	0.012	0.016	0.022	0.020	0.027
Cr_2O_3	0.005	0.008	0.004	0.001	0.004	0.002	0	0	0.002	0	0	0.002	0	0	0	0.003	0.004	0.008
CaO	0.018	0.001	0	0.004	0.001	0.003	0	0.004	0.003	0.001	0.004	0.002	0.005	0.006	0.005	0.003	0.003	0.002
Na_2O	0.018	0	0	0.001	0	0	0.001	0.008	0	0	0	0	0.002	0	0	0	0.001	0.002
K_2O	0.005	0	0.002	0	0	0	0.001	0.002	0.002	0	0.003	0	0	0	0.004	0	0.001	0
total	98.42	97.94	98.10	98.28	97.83	98.62	97.38	97.44	97.26	97.54	98.14	97.49	98.32	98.34	97.97	97.28	97.58	97.28
trace elements (ppm)																		
Ti	<51	<51	<51	<51	<51	<51	<51	<51	<51	<51	<51	<51	<51	<51	<51	<51	<51	<51
Fe	902	910	951	870	5820	5686	5446	5503	4064	2511	2111	1752	1037	994	1175	1354	1249	1218
Mn	<69	<69	<69	<69	<69	<69	<69	<69	<69	<69	<69	<69	<69	<69	<69	<69	<69	<69
Mg	<54	<54	<54	<54	<54	<54	<54	<54	<54	<54	<54	<54	<54	<54	<54	<54	<54	<54
V	139	166	150	135	<48	<48	<48	<48	<48	<48	<48	<48	<48	83	107	148	138	186
Cr	<51	<51	<51	<51	<51	<51	<51	<51	<51	<51	<51	<51	<51	<51	<51	<51	<51	<51
Ca	126	<45	<45	<45	<45	<45	<45	<45	<45	<45	<45	<45	<45	<45	<45	<45	<45	<45
Na	134	<132	<132	<132	<132	<132	<132	<132	<132	<132	<132	<132	<132	<132	<132	<132	<132	<132
K	<57	<57	<57	<57	<57	<57	<57	<57	<57	<57	<57	<57	<57	<57	<57	<57	<57	<57

Appendix B. *Kyanite chemistry determined by electron probe micro analysis. Continued.*

locality	Sormbrua	Sormbrua	Sormbrua	Sormbrua	Sormbrua	Sormbrua	Sormbrua	Sormbrua	Sormbrua
sample nr.	2907406	2907406	2907406	2907406	2907406	2907406	2907406	2907406	2907406
	profile 2	profile 2	profile 2	profile 2	profile 2	profile 2	profile 2	profile 2	profile 2
distance (µm)	420	450	480	510	540	570	600	630	660
major and trace elements (wt%)									
Al_2O_3	62.41	62.88	62.60	63.79	63.51	62.95	62.57	63.05	62.56
SiO_2	34.72	34.51	34.75	35.20	35.24	35.59	35.45	35.75	35.89
TiO_2	0.003	0	0	0.002	0	0	0	0	0.002
FeO	0.144	0.140	0.133	0.144	0.144	0.147	0.149	0.145	0.105
MnO	0.001	0	0	0	0.006	0.001	0.003	0.002	0
MgO	0	0.001	0.002	0.002	0.001	0	0.001	0	0
V_2O_3	0.026	0.022	0.023	0.025	0.023	0.025	0.025	0.025	0.016
Cr_2O_3	0.007	0.003	0.002	0.006	0.003	0.005	0.003	0.003	0.002
CaO	0.004	0	0	0.003	0.001	0.002	0.005	0.004	0.006
Na_2O	0	0	0	0.005	0.004	0	0.004	0.007	0.007
K_2O	0	0.004	0	0.002	0.001	0	0.005	0.002	0.002
total	97.31	97.56	97.51	99.18	98.93	98.72	98.21	98.99	98.59
trace elements (ppm)									
Ti	<51	<51	<51	<51	<51	<51	<51	<51	<51
Fe	1121	1091	1034	1121	1122	1141	1158	1126	819
Mn	<69	<69	<69	<69	<69	<69	<69	<69	<69
Mg	<54	<54	<54	<54	<54	<54	<54	<54	<54
V	173	146	157	170	155	169	171	171	109
Cr	<51	146	<51	<51	<51	<51	<51	<51	<51
Ca	<45	<45	<45	<45	<45	<45	<45	<45	<45
Na	<132	<132	<132	<132	<132	<132	<132	<132	<132
K	<57	<57	<57	<57	<57	<57	<57	<57	<57